

AMINO-TERMINAL SEQUENCES OF THE BACILLUS ANTHRACIS
EXOSPORIUM PROTEINS BCLA AND BCLB IMPORTANT FOR LOCALIZATION
AND ATTACHMENT TO THE SPORE SURFACE

A Thesis

presented to

the Faculty of the Graduate School

at the University of Missouri-Columbia

In Partial Fulfillment

of the Requirements for the Degree

Master of Science

by

BRIAN M. THOMPSON

Dr. George C. Stewart, Thesis Supervisor

August 2008

© Copyright by Brian Thompson 2008

All Rights Reserved

The undersigned, appointed by the dean of the Graduate School, have examined the thesis entitled

AMINO-TERMINAL SEQUENCES OF THE BACILLUS ANTHRACIS
EXOSPORIUM PROTEINS BCLA AND BCLB IMPORTANT FOR LOCALIZATION
AND ATTACHMENT TO THE SPORE SURFACE

presented by Brian M. Thompson,

a candidate for the degree of Master of Science

and hereby certify that, in their opinion, it is worthy of acceptance.

Professor George C. Stewart

Associate Professor Michael Calcutt

Assistant Professor Charles Brown

ACKNOWLEDGEMENTS

I would like to thank Dr. George C. Stewart for the many years of mentoring and support, Dr. Charles Brown and Dr. Michael Calcutt for being on my committee, and Dr. Hsinyeh Hsieh, Krista Spreng, and Kristen Peters for much needed help on the projects contained in this thesis.

TABLE OF CONTENTS

Acknowledgements.....	ii
List of Tables.....	vi
List of Figures.....	vii-viii

Literature Review

Introduction.....	1
General Phenotype/Genotype.....	4
Differentiation of Strains.....	5
Virulence Factors.....	6
The pX01 Plasmid.....	6
Lethal Toxin.....	8
Edema Toxin.....	9
The pX02 Plasmid.....	10
Virulence Regulation.....	11
S-layer and Capsule.....	12
Other Virulence Factors.....	14
Diseases.....	17
Treatment.....	19
Disease Progression.....	19
Disease in Animals.....	26
Germination.....	27
Vaccination.....	29
Sporulation.....	32
Regulation of Sporulation and Sigma Factors.....	34
Spore Structures.....	40
The Spore Coat.....	42
Exosporium.....	46
Formation.....	51

Nap.....	52
The Cap and ExsY.....	54
BclA.....	55
BclB.....	59

Materials and Methods

Bacterial Strains.....	62
DNA Manipulations.....	65
Transformation of <i>E. coli</i>	66
PCR.....	67
Electroporation Conditions.....	69
Isolation of Chromosomal DNA.....	70
Preparation of Competent <i>E. coli</i>	70
Protein Production.....	71
Production of Rabbit Polyclonal Antibodies.....	72
Production of Spores.....	73
Transmission Electron Microscopy.....	74
Epi-fluorescence Microscopy.....	75
Spore Analysis by Flow Cytometry.....	75

Results, Chapter 1

Discovery of Novel Collagen-like Proteins.....	77
Are the N-terminal 19 Amino Acids Required for Exosporium Incorporation?	81
Is Proteolytic Cleavage of the N-terminal 19 Amino Acids Necessary?.....	83
Reporter Oligomerization is Not Required for Exosporium Incorporation.....	85
The Contributions of the Conserved Motif and N-terminal Sequences.....	88
Exosporium Incorporation Utilizing the BclB N-terminal Domain.....	90
Localization of the BclB NTD Under its Native Promoter.....	93
Are the Different Localization Patterns Between BclA and BclB Due to Timing?.....	95
Native BclA is Incorporated Into Spores Expressing the Reporter Proteins.....	98
Are the BclA Fusions Targeted Correctly to the Exosporium.....	98

Results, Chapter 2

The CTL292 Partial <i>bclA</i> Mutant and $\Delta bclA$ Strains.....	100
<i>bclB</i> Mutant Characterization.....	105
Localization of Native BclB.....	108
<i>cotE</i> Mutant Analysis.....	109
Maturation of the Exosporium.....	113
Verification of Potential for Localization of Fusions in Related Bacteria.....	115

Discussion

Identification of Protein Domains Important in Protein Incorporation	116
Exploitation of the Targeting Domains as a BEAD System.....	119

Bibliography	121
---------------------------	-----

List of Tables

Table

1. <i>B. subtilis</i> Sigma Factors.....	40
2. Bacterial Strains.....	63
3. Antibiotic Concentrations.....	64
4. Plasmids.....	64
5. Primers.....	68
6. Fluorescence of Fusion Constructs.....	82

List of Figures

Figure

1. Incidence of <i>B. anthracis</i> Outbreaks.....	2
2. Sporulation.....	37
3. Layers of the <i>B. anthracis</i> Spore.....	42
4. Expression of Late Sporulation Genes.....	47
5. The <i>bclA</i> and Adjacent Operons.....	48
6. Diagram of Fusion Constructs.....	78-79
7. BclA EGFP Fusions Plus Flow Cytometry.....	80
8. Dual Reporter Fusion for Cleavage Assay.....	83
9. Micrographs of Dual Reporter Fusion.....	84
10. Micrographs of BclA Constructs.. ..	86
11. Flow Cytometry on BclA Fusions.....	89
12. Flow Cytometry on BclB Fusions.....	91
13. BclB with the <i>bclA</i> Promoter.....	92
14. BclB EGFP Fusions.....	94
15. Full BclB ORF mCherry Fusions.....	95
16. BclA Fusions with <i>bclB</i> Promoter.....	96
17. Flow Cytometry of BclA Fusion with <i>bclB</i> Promoter.....	97
18. Immunolabeling Fusions for Wildtype BclA.....	98
19. TEM Micrographs with Immunogold Labeling.....	99
20. The CTL292 <i>bclA</i> Partial Mutant.....	101
21. CTL292 BclA Fusions.....	102
22. CTL292 BclA without Motif Fusions.....	102
23. pGS3230.....	103

24. BclA KO Construct Diagram.....	104
25. BclB KO Immunofluorescence.....	106
26. BclB KO BclA Fusions.....	107
27. BclB KO BclA without Motif Fusions.....	108
28. BclB Fusions with <i>bclA</i> Promoter Immunofluorescence.....	109
29. CotE KO Mother Cell BclA Fusions.....	110
30. CotE KO Free Spore BclA Fusions Plus TEM.....	111
31. CotE KO BclB Fusions.....	112
32. TEM and Epi-fluorescence of Exosporium Maturation.....	113
33. TEM and Epi-fluorescence of Exosporium Defects.....	114
34. Expression in Other <i>Bacillus</i> spp.....	115

Literature Review

Introduction

“For neither might the hides be used, nor could one cleanse the flesh by water or master it by fire. They could not even shear the fleeces, eaten up with sores and filth, nor touch the rotten web. Nay, if any man donned the loathsome garb, feverish blisters and foul sweat would run along his fetid limbs, and not long had he to wait ere the accursed fire was feeding on his stricken limbs.”

Virgil: The Georgics III, 30 B.C.

Bacillus anthracis, a spore-forming Gram-positive bacterium, is the etiological agent of anthrax. The anthrax disease has been described in history as early as the book of Genesis in the 15th century B.C. as the 5th plague that killed the cattle of the Egyptians (160). Greek, Roman, Hindu, and European literature all contain reports of anthrax outbreaks. Major outbreaks occurred in Germany in the 14th century and in Russia during the 17th century. The diseased animals were buried in deep pits to avoid spreading of the contagion to the human populations and other cattle in the area. Centuries later the spore-ridden pit could be unearthed by an unsuspecting farmer plowing a field and exposing his whole herd to the ages-old anthrax spores. Most of the more modern outbreaks occurred among those with occupations related to livestock and livestock byproducts. Wool workers were very susceptible to the disease due to the large numbers of spores inhaled

each day from the contaminated wool, and in many areas the disease became known as “wool sorter’s disease.”

Anthrax, although uncommon in developed countries, is still a threat among developing countries. Anthrax is endemic in Central America, the Caribbean, Spain, Greece, the Middle East, and much of Africa. West Africa is the most affected region in the world with continuous outbreaks among both wildlife and humans, with the largest reported outbreak in 1979-1980 consisting of 10,000 cutaneous anthrax infections. Annually there are approximately 20,000 to 100,000 cases of anthrax worldwide (161).

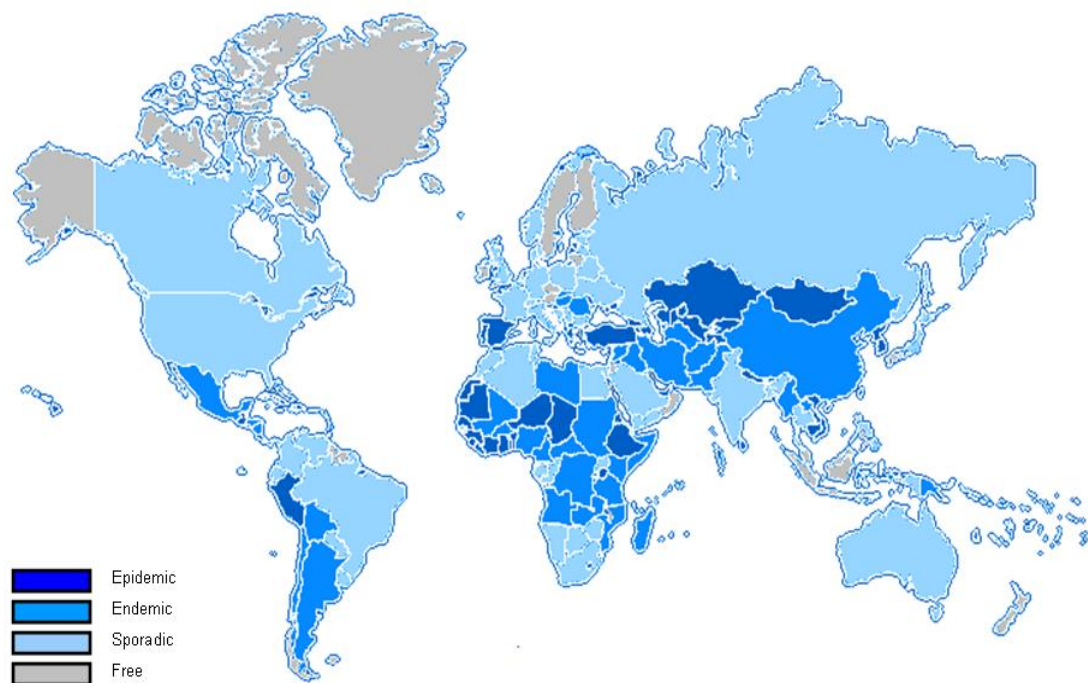


Figure 1: Incidence of *Bacillus anthracis* outbreaks. Adapted from the History Magazine, 2002

Bacillus anthracis was first described by Davaine, a French parasitologist in 1850.

Robert Koch and Louis Pasteur, two founding fathers of modern medical microbiology, both studied this pathogen. In 1888, Koch first described the complete sporulation to germination life-cycle of *B. anthracis* and other spore-formers (1). Pasteur observed that leaving cultures of *B. anthracis* in the sun caused them to become avirulent. The cultures lost their virulence plasmids due to the increased temperature, leading Pasteur to develop the concept of attenuation and the creation of vaccines designed from weakened bacterial strains. These discoveries led to the concepts and vaccine design strategies which have saved millions of lives over the years.

Although most human cases of anthrax are among people who come in contact with animals and animal byproducts, recently some new cases were due to the development of anthrax as a biological weapon. It is an ideal bioterrorism agent, able to be produced in mass quantities and covered in a resistant coat which allows it to remain stable without refrigeration and maintain virulence for hundreds of years. Aerosolization of the spores as a means of dissemination would have dire consequences, infecting unknown thousands with flu-like symptoms and leading to a heavy mortality rate. The World Health Organization estimates that 50 kg of weapons grade anthrax released by an aircraft over an urban population of 5 million would result in 250,000 cases of predominantly inhalation anthrax and an economic impact of 26.2 billion dollars per 100,000 exposed (125).

Anthrax has been listed as a category A select agent by the CDC and WHO, along with tularemia, smallpox, plague, and other pathogens. The USA, USSR, France, and England have all developed anthrax as a weapon of war. In 1937, the Japanese used *B. anthracis* spores as a weapon against the Chinese, and did extensive testing of the bacterium on Chinese prisoners. Recently, Iraq has also admitted to having an active biological warfare program including anthrax. The tragic release of huge stockpiles of biological weapons grade spores at the Russian town of Sverdlovsk in 1979 led to 64 deaths in the surrounding populace. The recent Amerithrax letters in the US lead to 18 cases of anthrax, 11 inhalational cases of which 5 died, and 7 cutaneous cases. The development of better vaccines against anthrax has been a top priority in many countries over the last few years.

General Phenotype/Genotype

Bacillus anthracis is a Gram-positive, non-motile, aerobic spore former. It is primarily a pathogen of ruminants, but occasionally infects humans. When nutrients are scarce, the bacterium produces a centrally located, hardy spore that can resist many environmental insults and survive until the environment is again suitable for stable growth. The bacterium contains a unique amino acid-based capsule. *Bacillus anthracis* is one of the few bacteria that contain group II introns; novel genetic elements that have properties of both catalytic RNAs and retroelements. They encode reverse transcriptase and are either active retroelements, or are derivatives of retroelements, and are able to self-splice (60). Whether the *B. anthracis* spore is able to germinate and subsequently thrive in the soil is

still under debate, but a recent study has shown that it can germinate and grow in the rhizosphere of some grassy plants (68).

Many advances have occurred in the last 30 years in the study of the *Bacillus* pathogens. Although there are numerous *Bacillus* species, only three have been identified as major pathogens. *Bacillus anthracis* is primarily a pathogen of ruminants, and infection is initiated upon access of the spores into the body. *Bacillus cereus*, genetically related to *B. anthracis*, is a major food poisoning agent and causal agent of endophthalmitis. *Bacillus thuringiensis* is a major pathogen of insects with its insecticidal toxins and is currently used as an insect control agent. The major difference between *B. anthracis* and *B. cereus* remains the presence of two virulence plasmids in the *B. anthracis* strains. Other than the presence of the two virulence plasmids, there are about 150 genes that have been shown to differ between *B. cereus* and *B. anthracis*.

Differentiation of Strains

The *Bacillus cereus* group is one of the most taxonomically similar groups of eubacteria (147). In fact, DNA-DNA hybridization and pulse field electrophoresis have shown great homology among *B. anthracis*, *B. thuringiensis*, and *B. cereus* (33). A recent multilocus enzyme electrophoresis study has concluded that the members of this group belong to one species (51). Although traditionally the presence of the *B. anthracis* plasmids pX01 and pX02 were enough to differentiate the species from others of the *B.*

cereus family, recent reports of pX01 and pX02-like plasmids in *B. cereus* have led these plasmids to not be reliable in differentiation studies (126). Analysis of the RNA polymerase B' subunit genes can partially differentiate *B. anthracis* from its sister species (50). Differentiation between *B. cereus* and *B. anthracis* has also been attempted by searching for gamma phage specific for one species of the *B. cereus* family. The presence of the crystal insecticidal toxins helps differentiate *B. thuringiensis* from the others strains. Some strains of *Bacillus cereus* and *Bacillus thuringiensis* spores have filamentous appendages (48, 57). Differentiation between strains has also been tried using variability in optical chromatographic readings, although this may be due to some of the differences in exosporium filaments which are not present in all the species and strains of the various members of the *Bacillus cereus* family (59). Polymorphism in the BclA exosporium gene has also led to the development of a PCR-based test to differentiate *Bacillus cereus* family members (99).

Virulence Factors

The pX01 plasmid

The first discovered of the two virulence plasmids in *B. anthracis* is pX01. This 181 kb plasmid encodes approximately 143 ORFs, including the genes for the production of the three toxin components that make up the two anthrax toxins. The genes responsible for the production of the anthrax toxins are *pagA* (encoding protective antigen), *lef* (containing lethal factor), and *cya* (encoding edema factor) genes. Although the GC

content of 33% would suggest that it is a natural *Bacillus* plasmid the pX01 plasmid contains a pathogenicity island of 44 kb which is surrounded by two insertion elements and several genes predicted to be the result of horizontal transfer. pX01 also encodes *gerX*, a germination locus that is essential for virulence in mice (40, 45). The anthrax toxin genes have also been found, albeit rarely, in *B. cereus* respiratory infection isolates that contain pX01-like plasmids (126). These strains have also been found to contain polysaccharide capsule gene clusters on a separate virulence plasmid.

B. anthracis produces two binary toxin combinations, consisting of a binding component and a effector component. The first aspect of the toxin entry into host cells is the binding of protective antigen (PA) to a receptor. It is known as protective antigen because antibodies produced against PA protect the animal during experimental infection by blocking access of toxins into the host cells. There are actually two anthrax toxin receptors, ANT XR1 and ANT XR2 (32). ANT XR1 corresponds to anthrax receptor/tumor endothelial marker 8, and ANT XR2 corresponds to capillary morphogenesis protein 2. After the PA binds to one of the receptors on susceptible cells it combines into a heptamer in lipid rafts upon the cell membrane (132). The PA precursor is a protein of 83,000 daltons (PA83). After insertion into the target cell membrane the heptamer of PA83 is cleaved by furin or other furin-like proteases to produce a 63,000 dalton protein (PA63) (162). The PA63 heptamer contains a binding domain to facilitate the binding of lethal factor and edema factor. Both lethal factor (LF), the product of the *lef* gene, and edema factor (EF), product of the *cya* gene, have a common N-terminal domain that binds to the cleaved PA63 heptamer. The binding of

the PA63 heptamer to the lethal or edema factor leads to the complex being brought into the cell by receptor-mediated endocytosis by a clathrin-dependent process (133). As the pH of the endocytic vesicle decreases, this acidic environment leads a change in conformation and formation of a pore by the heptamer, releasing the edema factor and lethal factors into the cell cytoplasm. The combination of PA and LF, called lethal toxin (LT), leads to death in high doses in experimental animals (56). The combination of PA and EF, called edema toxin (ET), leads to production of edema in the skin of animals (56). None of the components alone are toxic, as lethal factor and edema factor can not access the cell without PA, which by itself causes no pathology.

Lethal Toxin

Lethal Toxin is a zinc metalloprotease whose target is the N-terminal region of MAPKKs, MEK1, and MEK2 (196). It is capable of cleaving all of the various MAPKKs except MEK5, and these cleavage events lead to rapid cell lysis by apoptosis in murine macrophages. It is believed that the majority of cellular toxicity associated with anthrax infection is due to this intracellular hydrolysis of important host protein substrates (163). Lethal Factor can also lead to the collapse of vasculature and hypoxia. The characteristic pleural effusions and necrosis of the liver, spleen, and bone have all been attributed to the hypoxia-mediated damage due to LT (56).

Edema Toxin

The action of the edema toxin (ET) is dependent upon the host calcium-binding protein calmodulin. ET efficiently converts intracellular ATP into cAMP. The edema factor adenylate cyclase is at least 1,000 fold more active than any of the host adenylate cyclases in cAMP production, and leads to large amounts of secreted fluid in cells (56, 112, 164). Purified ET has been shown to inhibit the chemotactic response of polymorphonuclear leukocytes and also their subsequent phagocytosis (165, 166).

Highly-purified ET can cause death in a BALB/c mouse at very low doses and is more lethal than LT. Purified ET leads to accumulation of fluid in the intestines, hemorrhaging of the ileum and adrenal glands, lesions in the lymphoid organs, bone, bone marrow, GI mucosa, heart and kidneys; and multiorgan failure (56). *In vitro*, ET inhibits adhesion of neutrophils, stimulates their apoptosis, and blocks proliferation of lymphocytes (112).

In the mammalian host it is likely that the two toxins act in synergy to produce all the symptoms of anthrax infection. Both are produced by 3 hrs after germination and suppress superoxide and NO production by phagocytes (118). In later stages of the disease, lethal levels of toxins induce the development of the cytokine-independent shock-like death associated with anthrax (56, 112, 136). EF and LF deficient strains are greatly attenuated in mouse infection models. The cleavage of MEK 1, 2, and 3 *in vitro* by LF leads to activation of macrophages and related signaling would produce cytokines such as TNF α , IL-1, and IL-6 (163). ET inhibits not only induced TNF α secretion but

also inhibits phagocytosis and oxidative burst activities. The two toxins function together to induce shock in a rat model (112). Mice deficient in macrophages are resistant to LF challenge (124). Both toxins cause hypotension (112). LT leads to high extravasation of fluid and ET leads to increased cAMP levels in cardiac pacemaker cells and decreased heart rate (112). More on the actions of the two toxins, as well as their role in modification of the immune system can be found in the **Disease Progression** section below.

The pX02 plasmid

The second discovered virulence plasmid in *B. anthracis* is the 96 kb plasmid pX02, which contains the *capA*, *capC*, *capB*, and *capD* genes responsible for the production of the characteristic poly-D-glutamic acid capsule. This capsule is produced and surrounds the cell after outgrowth *in vivo*, or *in vitro* in the presence of bicarbonate, hindering phagocytosis and perhaps playing a role in adherence to host cells. The weakly antigenic capsule may act to hide the cells from the adaptive immune system. In addition to the capsule genes, pX02 encodes Dep and several global regulators of virulence. CapD (Dep) is a degradative enzyme which can break down the capsule into small D-glutamic acid fragments that are secreted from the cell. The first of these regulators is AcpA, which interacts with and turns on the capsule biosynthesis genes (129). The second, AcpB, also turns on the capsule biosynthesis genes. Both the AcpA and AcpB regulators are turned on by the master regulator, AtxA. AtxA is encoded on pX01, and *atxA* mutants are avirulent (127). The pX02 plasmid is often spontaneously lost, especially

during growth at elevated temperatures, such as 42°C (30). Removal of the pX02 plasmids results in a great attenuation in a mouse infection model (30.)

Virulence Regulation

Control of virulence gene expression in *B. anthracis* is highly dependent upon *atxA*, a global virulence regulatory gene located on the virulence plasmid pX01. In fully virulent strains, containing both the pX01 and pX02 plasmids, AtxA acts as a global regulator controlling expression of the pX02-encoded capsule biosynthesis genes, *capBCAD*; as well as the toxin structural genes *pagA*, *lef*, and *cya* on the pX01 plasmid (127, 128). The AtxA regulator also controls expression of a number of other genes on the chromosome (131). The PagR protein is a major repressor of the *pagA*, *cya*, and *lef* genes. PagR has also been found to affect transcription of the S-layer genes and biases the cells in the presence of CO₂ to produce the Ea1 S-layer protein over the Sap S-layer protein during infection (130). Regulation of PagR is controlled by AtxA (130, 127). This effect may not be direct and is likely the result of intermediate factors (67). AtxA, in the current Koehler model, regulates the capsule genes through the pX02 encoded genes *acpA* and *acpB* (131). *acpA* and *acpB* isogenic mutants have no effect on capsule production, but an *acpA/acpB* double mutant is completely devoid of capsule (129). AcpA and AcpB share substantial amino acid and functional similarities. For many AtxA-regulated genes, including *acpA*, *acpB*, and the toxin genes, expression is greatly induced under conditions of high CO₂ or bicarbonate. This effect (*acpA*, 23-fold and *acpB*, 59-fold) is greater than can be explained by the bicarbonate induction of *atxA* alone (2.5-fold), suggesting that

another regulator or bicarbonate itself upregulates the *acpB* and *acpA* promoters (66, 131, 129).

This reason for bicarbonate and temperature induction of toxin and capsule genes may be from recognition of host surroundings and the necessary induction of toxin production to survive and thrive in the host environment. The concentration of bicarbonate for optimal expression is the same concentration that is found in the bloodstream, 48 mM. Toxin production is also regulated by the sporulation regulator Spo0A, which exerts its effect through the regulator AbrB; and recently been reported to be regulated by GerH, potentially through Spo0A (155).

S-layer and Capsule

In addition to the usual peptidoglycan and cytoplasmic membrane of most Gram-positive bacteria, *B. anthracis* encodes two other surface layers. The first layer is formed at the outermost point of the cell wall. A single protein polymer is assembled in a large crystalline sheath that surrounds the entire bacterium (7). The S-layer may play a role in involvement of cell shape maintenance, protection from complement, interactions with host macrophages, and in molecular sieving (5). The S-layer is comprised of one of two proteins depending on the growth phase of the bacterium. The protein Sap (surface array protein) is first assembled into the S-layer during growth, and is slowly replaced during stationary phase with the Ea1 protein (Extractable antigen 1) (6). The S-layer proteins

can comprise 5-10% of the total cell protein (5). S-layer proteins have not been found to be important in virulence, as the LD₅₀ in mice does not change in the absence of the S-layer, however, they may confer increased resistance to complement pathway-mediated defenses. Along with the EA1 and Sap S-layer proteins, other putative S-layer proteins have recently been found (61). These S-layer proteins are able to be recognized by the immune system as potential vaccine candidates (61).

Surrounding the entire bacterium is the capsule, composed of polymers of poly-D-glutamic acid (5, 154). An amino-acid composed capsule is rare, but it is also found on the related species *Bacillus licheniformis*. The two most important virulence factors are considered to be the capsule and toxins.. The capsule is encoded on the pX02 plasmid by the *capB*, *capC*, and *capA* genes. The role of the capsule in pathogenesis is to interfere with phagocytosis of the bacterium and to surround the bacterium in a poorly immunogenic polymer to help hide the bacterium cell membranes from the immune system (5). Both survival of the bacterium in the blood stream and progression to septicemia are also enhanced by the presence of the capsule. During germination and outgrowth in the presence of serum and elevated levels of CO₂, the capsule is released through openings on the vegetative cell surface. The formation of the capsule is exterior to the S-layer, but does not require the S-layer for its attachment to the cell surface (5, 6, 7). The capsule genes are essential for virulence in a mouse model of inhalational anthrax (119).

Other Virulence Factors

Bacillus anthracis encodes for a number of other virulence factors. Recently it has been found that if *B. anthracis* is grown under anaerobic conditions, it can induce production of the anthrolysins (62). The anthrolysins consist of Anthrolysin O and three phospholipase Cs. These four anthrolysins have overlapping function, but each are essential for virulence in an inhalational model of anthrax in mice (35, 36). Expression of the anthrolysins occurs in the early stages of infection, as they are turned on when the spores are engulfed by macrophages (62). In fact, mutations in the phospholipase Cs lead to the inability of spores to grow in association within macrophages. The hemolysin Anthrolysin O is secreted by vegetative cells and is lethal to human leukocytes, monocytes, and lymphocytes *in vitro*, in addition to lysing erythrocytes (148). Activity of Anthrolysin O is hindered by the presence of cholesterol, as minute quantities of cholesterol or sera leads to binding to and inactivation of the hemolysin (148).

Bacillus cereus and *Bacillus thuringiensis* control a number of secreted hemolysins by the regulator PlcR (63). The PlcR regulon in *B. anthracis* has been reported to be silent due to a *plcR* gene truncation (63). But under strict anaerobic conditions the anthrolysins are active, suggesting that the truncated PlcR upregulator of *B. anthracis* is active under these conditions (62). The PlcR regulon has been reported to inhibit sporulation and is incompatible with the AtxA-controlled virulence regulon (64). It was originally predicted to have been evolutionarily silenced due to this incompatibility (64). All the anthrolysin determinants in *B. anthracis* have PlcR binding sites. Transcription of *plcR* is activated during stationary phase in *B. cereus* and is autoregulated. PlcR activates at

least 15 genes encoding proteases, phospholipases, and two enterotoxin complexes (65, 63).

Other virulence factors include the sortase genes, *srtA* and *srtB*, which play a role in the interaction of the vegetative bacterial cells and the macrophages. This role may be indirect, as the sortase mutants are not able to fully localize bacterial proteins to the exterior layers of the cells. These mistranslocated proteins are likely the effector molecules that allow the bacterium to survive inside the host cells (37). *Bacillus anthracis* also requires the presence of siderophores for growth in macrophages and for virulence, and like other pathogens, need this continual uptake of iron to be able to replicate efficiently enough to maintain an infection (38, 46). *B. anthracis* has two distinct siderophore gene clusters (38). Due to the dramatic growth of *B. anthracis* in the host, it is understandable that *B. anthracis* would need siderophores to obtain sufficient iron at an optimal rate for maximal growth. This increased growth is essential for virulence as the bacteria overruns the host immune system.

Two putative collagen binding adhesions have been identified and are expressed on the surface of *B. anthracis* vegetative cells (52). These adhesins may help the bacterium bind to the extracellular matrix and help protect them from attack by the immune system. The Gram-positive cell surface is composed of many macromolecules, including peptidoglycan, teichoic and lipoteichoic acids (LTAs), S-layer, and cell surface proteins. The teichoic and lipoteichoic acids give the bacterium an overall negative charge. This negative charge on the teichoic acids becomes a major attractant for positively charged antibacterial compounds (93). Many Gram-positive organisms have developed the

means of coating the negative charges on the LTA with D-alanine. In *B. anthracis* this is accomplished by the products of the *dltABCD* operon. *dltA* encodes a D-alanine:D-alanyl carrier protein ligase which covalently attaches D-alanine to the 4' phosphopantetheine prosthetic group found on the D-alanyl carrier protein Dcp encoded by *dltC* (93). DltB is a transmembrane channel and DltD is a chaperone protein ensuring the fidelity of the D-alanine ligation to Dcp. Loss of function of any of the four *dlt* genes is sufficient to terminate the entire pathway (93). Addition of D-alanine to LTA in outgrown *B. anthracis* led to complete resistance to lysozyme and β -defensin-1 (produced by endothelial cells), and moderate resistance to sPLA₂, HNP-1, and HNP-2 (defensins produced by phagocytic cells) (93). Addition of D-alanine to the LTA also allowed the vegetative cells to better survive engulfment by macrophages and afforded better resistance to positively-charged antibiotics (93). *Staphylococcus aureus* and *Listeria monocytogenes* strains lacking the *dltABCD* operon are less virulent in their respective mouse models (73, 90).

The exosporium of the endospore of *B. anthracis* contains an arginase (141). Many bacterial pathogens are killed by efficient production of NO and other free radicals by macrophages. The arginase in spores of *B. anthracis* can compete with the macrophage for arginine, inhibiting its ability to be modified into NO (141).

Diseases

The symptoms and outcomes of persons infected with *B. anthracis* differ based upon the route of infection. Spores gain entry into the body either via open wounds in the skin, by ingestion of spores, or by inhalation of the spores into the lungs. Infection by all three routes can lead to serious and lethal systemic infection.

One of the most common routes of infection in humans is entry of spores into abrasions in the skin. The incubation period ranges from 1-12 days. The cutaneous form is first characterized by the formation of a black pustule at the site of entry as the bacteria produces edema and lethal factors. This painless eschar leads to significant edema of the surrounding areas, and in some cases the bacterium can gain access to the bloodstream, leading to systemic anthrax (29). The mortality rate of cutaneous anthrax infections is about 20% without antibiotic treatment, but cases of progression to systemic anthrax can have a mortality rate of up to 95%.

The second route of infection, although fairly rare, is gastrointestinal anthrax. This is usually caused by ingestion of undercooked meat from an infected animal, and this was last reported in the USA in Minnesota in 2000 (30). The incubation period is 1-7 days. Symptoms include bloody diaherria, severe abdominal pain, fever, and nausea. This can be a common route of infection in herbivores, as the spores can be ingested along with associated plant matter. This is predicted to be the main lifecycle of *B. anthracis*, as some experts point out that *B. anthracis* probably does not maintain a full

lifecycle in the soil. In humans the mortality rate of ingestional anthrax is about 25-60%, despite antibiotic therapy (29).

The last, and by far the most lethal route of infection, is inhalational anthrax. This is the most serious concern regarding anthrax, as an aerosolized attack using *Bacillus* spores could be potentially devastating if unleashed on a naïve population. Infection is rarely recognized before bacteremia and toxemia develop. It is difficult to diagnose, as it produces non-descript flu-like symptoms early in the course of infection. The Department of Defense estimates the LD₅₀ of anthrax spores to be 8-10,000 spores in humans, although that number varies greatly from report to report. After a short time, the bacteria flood the bloodstream and the patient becomes septic, leading to shock, fever, and respiratory failure. The patient usually succumbs within 24 hours of the beginning of sepsis. At this late stage the bacteria are very resistant to treatment, and the mortality rate is as high as 95% (29). It is important that antibiotic therapy in cases of inhalational anthrax be continued for up to 60 days, as spores can persist in the lungs and cause repeat infection after the usual 14 day antibiotic therapy (167, 170).

Very rare reports of meningitis due to *B. anthracis* are usually a complication that arises from infection elsewhere in the body and dissemination after bacteremia and is has a high mortality rate (approaching 100%) (29). Renal anthrax and ophthalmic anthrax have also been described, but are extremely rare.

Treatment

Treatment of cutaneous anthrax is intramuscular administration of 1 million units of procaine penicillin every 12-24 hours for 5-7 days (26). In serious illness, usually septic or pulmonary anthrax, 2 million units of penicillin G per day are administered intravenously or 500,000 units administered intravenously through a slow drip every 4-6 hours. Streptomycin, in conjunction with penicillin, has a synergistic effect at 1-2 g doses per day. Some penicillin-resistant strains of *B. anthracis* have been reported (168). Unfortunately, the strain used in the Amerithrax letters and in many historic outbreaks produces an inducible β -lactamase (169). It appears to be highly sensitive to penicillin *in vitro*, but in patients with high bacterial loads the bacteria may induce β -lactamase production and penicillin resistance. There are published reports of strains resistant to penicillin *in vitro* and *in vivo* (29). Ciprofloxacin at 400 mg intravenously twice daily is the current recommended treatment for those infected with anthrax (26). The recommended regimen for inhalational anthrax is ciprofloxacin plus 1-2 additional antibiotics (26). The duration of treatment should be 60 days for inhalational anthrax, as ungerminated spores may germinate after prolonged stay in the lungs post-treatment and emerge into fatal infection (170).

Disease Progression

Inhalational anthrax always initiates with the entry of spores into the pulmonary cavity and spore uptake by resident alveolar macrophages and lung dendritic cells

(LDCs) (39, 41, 42, 92, 116, 122, 134). Alveolar macrophages represent the major phagocytic population in the lungs, although LDCs are more efficient at phagocytosis of spores than alveolar macrophages. Spores and germinated vegetative cells are able to be internalized by fibroblasts and epithelial cell lines *in vitro* as well (34). Alveolar macrophages are the primary site of spore germination *in vivo* in inhalational anthrax infections (22, 40, 41). Spores germinate in the phagolysosome of the macrophages or LDCs while in the lungs or en route to the mediastinal lymph nodes (39). Germination within macrophages is dependent on the *gerH* germination operon and the presence of germinants L-alanine and adenosine found inside the macrophages (22). There is little if any germination inside the lung mucosa itself (77). Alveolar macrophages are thought to act as a “Trojan horse,” delivering the bacteria to the unsuspecting lymph nodes. LDCs also sample lung environments and could potentially deliver the spores to the mediastinal lymph nodes as well. Both macrophages and LDCs express sporocidal activities *in vitro* (2, 28, 49, 92, 115, 122, 171). There is an approximate 10-fold decrease in CFU of engulfed spores in the first 2.5 hours *in vitro*. The 10% that do persist begin to multiply and overtake the macrophages. Macrophages play a critical role in the mouse model of infection, whereas PMNs play a minor secondary role (124, 138). A macrophage-deficient mouse model was more susceptible to infection, showing a role of the macrophage in resisting infection and not just as a “Trojan horse” (124).

Many spore and vegetative cell motifs are recognized by host pattern recognition receptors through MyD88-dependent and –independent processes. Vegetative cells signal through TLR2, most likely due to the presence of lipoteichoic and teichoic acids in

the cell wall, and Anthrolysin O signals through TLR4 (27). NOD protein signaling, which recognizes bacterial peptidoglycan components, leads to upregulation of inflammatory cytokines and activation of macrophages. *Bacillus* spp. have been found to be the most stimulatory of all bacteria tested in their ability to activate NOD1 (27). *Bacillus* spp also activate NOD2, but these cell wall recognition receptors are not species specific (2). NOD1 recognizes iE-DAP dipeptide and related structures found in all Gram-negative and some Gram-positive bacteria and NOD2 recognizes muramyl dipeptide (MDP). Most of the stimulatory activity towards these receptors is found in the supernatant of growing cultures, suggesting that released modified pieces of peptidoglycan are the actual stimulants (2).

Bacillus anthracis can induce an immunostimulatory response to both spores and vegetative cells during *in vitro* and *in vivo* mouse infections. Alveolar macrophages and LDCs coming into contact with spores produce $\text{TNF}\alpha$, IL-1 β , IL-6, and IL-8 (2, 28, 116). The IL-1 β response can be induced *in vivo* with as little as 100 spores (116). IL-1 β production leads to macrophage expression of NO. The NO spore-killing response of macrophages is critically dependent on the internalization of spores, presumably due to internal recognition receptors (28, 141). IL-1 β and $\text{TNF}\alpha$ indirectly activate and recruit phagocytes, promoting clearance and destruction of ungerminated spores in the lungs (28). Mouse strain susceptibility to *B. anthracis* spores was due to the presence of a gene locus involved in inflammation that leads to the production of IL-1 β and IL-18 (107, 175). Spores themselves induce the production of IFN- β and activation of alveolar macrophages (2, 28, 116). IL-6 induces B-cell antibody formation and recruitment (28,

116). Although many studies have shown the immunostimulatory effects of spores and vegetative cells of *B. anthracis*, in the context of host infection in a fully virulent strain, the host defenses begin to be shut down by the bacteria as soon as outgrowth and induction of virulence factor gene expression begins.

Human dendritic cells exposed to *B. anthracis* spores trigger reprogramming of their chemokine expression from the tissue homing receptors CCR2 and CCR5 to the lymph node receptor CCR7 (115). This reprogramming would greatly help the spores by directing them to the regional lymph nodes more efficiently. The engulfed spores germinate, multiply, escape the phagolysosome, and are released *en route* and during arrival of the macrophages and LDCs to the mediastinal lymph nodes (39, 49). During this process *B. anthracis* upregulates and produces many of its virulence factors, including the toxins, capsule, and other virulence factors mentioned above. PA and other toxin genes are produced in the germinating cells in as little as 1 hour after infection, concurrently with spore-laden macrophage arrival in the perivascular and peribronchiolar lymph node channels in a guinea pig model of infection (43, 114). Lysis of the macrophages and the release of the bacteria are dependent on an *atxA*-regulated gene or genes that is not a toxin gene, but another gene product encoded on the pX01 plasmid (39). The escape of the bacterial cells from the macrophages has also been linked to toxin secretion and InhA1 (140).

At 4 hours post-infection in a guinea pig model, spores and vegetative cells were found in and around phagocytes in the peristial lymph nodes (114). In rhesus monkey and

chimpanzee models of inhalation anthrax, infectious spores were taken up and delivered to the mediastinal lymph nodes within 6-18 hours post-infection (114). Once in the lymph nodes, the bacteria multiply rapidly and produce copious amounts of the toxins. These toxins offset any immunostimulatory effects described earlier and lead to local immunosuppression within the infected lymph nodes.

Initial immunosuppression by the *B. anthracis* toxins begins soon after germination of the spores in the alveolar macrophages and LDCs. LT has been reported to abolish the secretion of proinflammatory cytokines by macrophages (118, 134) and LDCs (115, 120, 172). LT can induce apoptosis of macrophages *in vitro* through the inhibition of p38 MAPK and its anti-apoptotic signals (135, 138). ET cooperates with LT in the suppression of early cytokine expression and inhibition of other phagocytic cell types. The combination of ET and LT inhibits priming and activation of PMNs and their ability to produce sporocidal NO. It also inhibits chemotaxis of PMNs to the lymph nodes and inhibits interferon production (139). Exogenous interferon therapy blocks the apoptosis of macrophages, promotes activation, and leads to more effective spore killing (139). LT disrupts the production of PLA₂ in pulmonary phagocytes, which was found to be critical in anthrax spore killing (173). After inhibition of PMNs and alveolar macrophages, monocytes remain the sole defender left in the fight against *B. anthracis*, but to no avail, as LT inhibits the differentiation of monocytes into macrophages *in vitro* and therefore inhibits their ability to fight off invaders (174, 175). Cholesterol-dependent anthrolysin O is lethal to human PMNs, monocytes, lymphocytes, and lytic to RBCs (148).

Although the association of *B. anthracis* with antigen presenting cells such as alveolar macrophages and LDCs in the lymph nodes would suggest a potential for activation of an adaptive immune response, this is unlikely due to the short time course of infection owing to the rapid replication and toxin production by *B. anthracis* in inhalational cases. In other forms of anthrax, the adaptive immune system may have time to be mobilized, but the adaptive immune response is also inhibited by the anthrax toxins. LT has been shown to inhibit the expression of co-stimulatory molecules, which in the presence of bacterial antigen presentation may lead to not only the inability to mount a response to the antigens but likely the induction of tolerance (120). Tolerance to bacterial antigens may lead to the development of protective T regulatory cells to hinder future adaptive immune responses to *B. anthracis* epitopes and lead to a poor response to future infections. Additionally, LT and ET abolish T-cell activation and cytokine secretion including IL-2 induction of T-cell proliferation (177, 178). LT also acts as an inhibitor of the humoral response through cleavage of MKKs important in B-cell proliferation and IgM production (120, 137). ET induces a Th2 shift and diverts the immune system into a poor anti-bacterial response (114, 176, 179). Major players in the adaptive immune response are inhibited by the *B. anthracis* duo of toxins, and phagocytes are killed or deactivated leading to the unchecked proliferation of the bacteria in the lymph nodes.

After a series of multiplications, immune cell death, and recruitment in the lymph nodes; the lymph node begins to swell. As the mediastinal lymph node expands, the bacteria soon gain access to the bloodstream and begin to stream out. The bacteria will also spread

to adjacent lymph nodes through the lymphatics. Massive bacteremia ensues, followed shortly by toxemia as the cells secrete the toxins. Some phagocytic cells have toxin-induced resistance to the circulating toxins, but the presence of the capsule protects the bacteria from the resistant macrophages and complement and is essential for dissemination throughout the body (119, 121).

The last stage of the disease is characterized by the distant actions of the toxins at sites throughout the body, and usually begins at 24 hours post-infection in a guinea pig model. The toxins lead to vascular injury with edema, hemorrhages, and thrombosis, through several mechanisms that lead to the death of the host. LT acts on the major endothelial barrier by action on the central actin fibers and modification of endothelial cell distribution (112, 114, 163, 182). LT's actions on the VE-cadherins and induction of endothelial cell apoptosis induce bleeding, hypotension, and cardiac distress (123, 180, 181). ET causes necrosis throughout the body in zebrafish, and rapidly kills mice (56, 112, 114, 183). ET also leads to hypotension by action on cardiac pacemaker cells (112, 114, 183). The two toxins' attack on the circulatory system leads to hypotension, vascular collapse, and hypoxia throughout the body. The lack of adequate blood flow and hypoxia plus action of ET and LT leads to massive damage of the internal organs (136). The PA subunit and Anthrolysin O activity together lead to hemolysis of the remaining RBCs (138). LT and ET are linked to disruption of platelet function and aggregation, leading to worsening of the leakage in the blood vessels (182, 183). The massive vascular leakage leads to pleural effusion and this fluid buildup is usually the cause of death by asphyxiation. As the host dies and nutrients become limited the bacteria

becomes dormant. Once the bacilli become exposed to oxygen by opening of the remains by bloating gases, trauma, or autopsy, the bacilli quickly sporulate and can spread to the surrounding environment, starting the infection cycle anew.

Disease in Animals

Endemic anthrax cases usually begin by ingestion of food or water that is contaminated with anthrax spores. An animal dying of anthrax produces an enormous amount of spores, and when the carcass is exposed to air by escape of bloated gases the bacilli sporulate rapidly. The majority of outbreaks occur after heavy rains following a period of drought, as spores from the environment become distributed in the water.

The disease in animals usually takes one of 3 forms: peracute, acute, and chronic. The peracute form is most often seen in cattle and other ruminants (26). Disease onset is rapid and death ensues quickly due to cerebral hypoxia. The subacute and acute forms are frequent in cattle, horses, and sheep. Symptoms of the subacute/acute phases consist of fever, a stop in rumination, periodic depression, respiratory difficulty, convulsions, and eventually death. Bloody discharges from the natural orifices as well as edemas in various parts of the body are sometimes observed (26).

Outbreaks in less susceptible species like pigs, and sometimes cattle, horses, and dogs are usually of the chronic form, although some animals will succumb to the acute form. The main symptom of the chronic form is pharyngeal edema. Frequently, a foamy bloody

discharge can be seen coming from the sides of the mouth. The animals die from asphyxiation. The chronic form can also present itself as intestinal anthrax (26). Under necropsy, the acute animals will display rapid decomposition and bloated carcasses. Hemorrhaging and splenomegaly, as well as enlarged kidneys, liver, and lymph nodes are often seen.

Germination

In order to initiate germination and restore vegetative growth when conditions favor outgrowth, the spore must be able to monitor the outside environment. The germination receptors, located in the spore cytoplasmic membrane, encounter the germination signals as they pass through the external spore coat layer. Early events in germination begin as the spore membrane increases in fluidity (184, 185). Cations from the spore coat are released into the environment, including H^+ , K^+ , and Ca^{2+} . One of the major releases of cations is dipicolinic acid (DPA). DPA release leads to degradation of the spore's peptidoglycan cortex (17). This is followed by release of Ca^{2+} ions and activation of lytic enzymes, like CwlJ and SleB. These lytic enzymes start the degradation of the peptidoglycan and spore coat layers, leading to water uptake and the start of metabolism and increase in ATP synthesis (9, 11). The SASPs (small acid soluble proteins) that coat and protect the spore DNA are degraded by germination proteases and any damaged DNA is repaired. Degraded SASPs proteins are used as a nutrient source for the emerging spore (8). The current dogma is that different germinants bind to tricistronic

encoded germination receptors on the inner membrane, like the well characterized GerA receptor of *B. subtilis* (16).

The GerA family of germination receptors react to different stimuli (21). High concentrations of alanine (100 mM), or low concentrations (1 mM) with the presence of His, Pro, Trp, or Tyr can induce significant germination in 1 hour (16). D-alanine can inhibit germination by L-alanine (187). The GerS germinant receptor family recognizes aromatic ring structures. The presence of purines (inosine, adenosine, or guanosine [weaker]) with many amino acids (Ala, Cys, His, Met, Phe, Pro, Ser, Try, Tyr, Val) can induce germination (16). This induction was inhibited in the *gerS* mutant spores, which were unreactive to the strong germinants inosine and alanine (16). No purine alone will cause germination in *B. anthracis*, but can in *B. cereus* (186).

The gene for GerX, another of the GerA family of receptors, is located on the pX01 plasmid of *B. anthracis*. *gerX* mutants are attenuated for virulence in a mouse model (41). GerH also plays a role in germination of endospores in macrophages *in vitro* (22). Different *Bacillus* species react to differing germination stimuli (11). *B. cereus* and *B. anthracis* germinate most efficiently in the presence of alanine or inosine and cofactors. The presence of other cofactors greatly increases the ability of the germination receptors to signal. Anti-spore polyclonal antibodies significantly hinder the ability of spores of *B. anthracis* to germinate, potentially by blockage of access of germinants to germination receptors or by blocking lytic digestion of the spore coat layers (20).

Vaccination

Anthrax was the first disease in which the principle of vaccination was found to be effective. 1881, in Pouilly Le Fort, the Pasteur strain of *B. anthracis* was the first attenuated bacterium used successfully as a vaccine. In 1937 the Sterne strain of *B. anthracis* was isolated. It is cured of the pX02 plasmid, rendering it unable to produce the antiphagocytic capsule. The Sterne strain is used as a live vaccine to this day, but only in a veterinary capacity. It induces great protection in many studies and is utilized as a livestock vaccine in anthrax-endemic regions (30, 105). Since it is a live vaccine and has potential to harm the animal with its other virulence factors, it has not been considered safe for use in humans. However, it was utilized as a human vaccine during the cold war years in the former Soviet Union. Several new vaccine candidates have been proposed and/or tried in animals over the last half-decade.

Human vaccines based on cell-free filtrates of nonencapsulated strains of *B. anthracis* were developed in several Western countries in the 1950s. PA and other secreted proteins were absorbed from cell supernatants using aluminum hydroxide gel (Alum), and this cell-free cocktail was given to humans. This newer vaccine, named AVA for Anthrax Vaccine Adsorbed requires doses at 0, 2, and 4 weeks as well as at 6, 12, and 18 months, followed by annual boosters. Annual booster shots are necessary, since vaccine is only protective for one year (105). The vaccine confers poor protection from challenge with aerosolized spores in a number of animal models (106, 108). AVA vaccines also provide less protection than the live spore Sterne strain vaccine and have a number of side effects

(105, 189). Reaction to the AVA vaccine is not just to PA, although it is the major factor responsible for protection. Approximately 69 proteins of *B. anthracis* react to antiserum generated by the AVA vaccine, which may not constitute the full gambit of protective antigens (31, 104). Full protection against anthrax infections may require the use of multiple immunogens.

A laboratory study has shown that inclusion of formaldehyde-inactivated spores to AVA or other PA-based vaccines results in total protection in both mice and guinea pigs (3). Even the newer recombinant PA-based vaccines provide less protection than the live Sterne spore vaccines, but have fewer side effects than AVA (30). The addition of better adjuvants to the AVA vaccine has been shown to increase its efficacy (101). A recombinant PA vaccine bound to alhydrogel has been found to protect rhesus monkeys from an aerosolized dose of virulent *B. anthracis* spores (98). Production of antibodies by other more efficient vaccine delivery methods may also be helpful in future vaccine strategies (102).

Ideally a vaccine could be developed necessitating fewer doses and conferring better protection than the currently used AVA vaccine, and with the potency of the Sterne vaccine but without the hazards. PA is the basis for many of the new vaccine designs. Other immunogens, for instance the capsule (103), could be beneficial additions to the AVA or other recombinant PA vaccine strategies. Antibodies to PA offer protection by neutralization of the LT and ET toxins (98). High-affinity monoclonal antibodies produced against PA protect animals during *B. anthracis* infections (100). Laboratory

animals used in the development of vaccines include mice, guinea pigs, and rabbits, with the use of rhesus monkeys as a non-human primate model. Mice are very susceptible to anthrax, with the presence of only either the capsule or the toxins being necessary to produce lethal infections (107).

Production of anti-spore antibodies and anti-spore IgG inhibits the germination of *B. anthracis*. Antibodies against both germinated and ungerminated spores have the same neutralizing effect (20). Anti-PA antibodies have the ability to stimulate phagocytosis of spores by macrophages and inhibit some spore germination *in vitro* (43). The ability of anti-spore antibodies to inhibit germination is not a consequence of overall binding, but correlates to which epitopes are bound. There is no association between agglutination and ability to inhibit germination (20). One proposed mode of action is the blocking of the pores that allow germinants to enter the spore by the anti-spore antibodies (20). GerH is necessary for the germination of spores in macrophages (22). The use of *gerH* mutant spores may allow the use of a spore vaccine to illicit an anti-spore response without the fear of germination and infection. Some protection afforded by spore vaccines is accomplished by stimulation of IFN γ producing CD4⁺ T lymphocytes (197).

The addition of BclA, a potent immunogen in the exosporium of the spore, to a recombinant PA DNA vaccine leads to better protection than PA alone (53). Other spore antigens may increase the protection as well (198). Antibodies to recombinant PA lead to delayed germination of spore and a modest increase in uptake by macrophages and spore

killing. (43) The tetrasaccharide of the BclA glycoprotein may also be an effective vaccine addition that can illicit a response and be added to future vaccines (82).

Sporulation

Most of the literature on sporulation has been derived from studies of *B. subtilis*.

Bacillus subtilis is the best characterized member of the genus *Bacillus* genetically.

Sporulation of *B. anthracis* has not been studied in detail and general extrapolations can be dangerous, as *B. anthracis* has over 1000 genes with no homology to *B. subtilis* (168). *B. anthracis* also contains an extra spore layer (the exosporium) and some homologs of *B. subtilis* sporulation genes have been shown to play different roles in *B. anthracis* (47).

Under conditions of nutrient starvation and in the presence of oxygen, cells of the *Bacillus* spp. undergo the process of sporulation. Sporulation allows production of a dormant spore which can survive adverse conditions and allows the bacteria to reemerge when the environment is more suitable to sustained growth. The production of endospores allows *Bacillus* spp. to become resistant to UV rays, ionizing radiation, pressure, heat, desiccation, high salinity levels, pH, and chemical agents. This dormant and highly resistant endospore allows the survival of the bacteria in contaminated soil for many years. Many researchers have argued that *B. anthracis* does not grow in the soil and persists only as endospores. The presence of nitrate in the soil leads to sporulation and killing of any vegetative cells (4). In a more recent study, *B. anthracis* spores were found to germinate and multiply in the rhizospheres of several grass species (68). The

spore has no detectable levels of metabolism, little to no ATP and NADH, and no enzyme activity (192). Cells remain in this metabolically inactive form until the presence of inosine and/or alanine and other co-factors leads to initiation of germination and outgrowth.

During the process of sporulation, groups of genes are sequentially activated and silenced in an 8-10 hour period that leads the nutrient-deprived cell through a series of developmental stages (110). This process is broken down into a series of time points denoted using the Roman numerals 0-VII (47). Each Roman numeral signifies the hour in which each event occurs. Gene mutations at each timepoint are denoted by the addition of the respective Roman numeral and order that they are important, i.e., the sporulation mutant Spo0A is active during the 0 hour time point (end of exponential growth). Sporulation is initiated at Stage 0 with the master sporulation regulator Spo0A. During Stage I DNA replication initiates at an axial filament in the center of the vegetative cell. Stage II denotes the time point where the spore septum begins to be formed to initiate the unequal cell division and formation of two compartments, the larger *mother cell* compartment and the much smaller *forespore* compartment.

The forespore is engulfed by the mother cell membrane, leading to the forespore being encased by two bilipid membranes. This is the hallmark of the third stage of sporulation (Stage III). During Stage IV, a thick layer of carbohydrate and spore-specific peptidoglycan is layered between the two forespore membranes. This layer is known as the cortex. The outer membrane of the forespore is layered with sequential layers of

spore coat proteins and calcium dipiconate during Stage V of sporulation. Addition of the final spore coat layers, which provide several of the inherent resistance properties that protect the endospores, and the final exosporium formation are accomplished during Stage VI. The outermost exosporium layer is synthesized during Stage VI in *Bacillus anthracis*, *cereus*, and *thuringiensis* (18, 191). The final stage of sporulation, Stage VII, is marked by the lysis of the mother cell and release of the mature spore into the environment (47). Figure 2 outlines the general process.

Sporulation gene transcription in *B. anthracis* has been found to occur in 5 semi-distinct waves (54, 88). Interestingly, the spore-associated proteins are produced much earlier than they are incorporated, and these proteins are predicted to be inherently more stable than their vegetative cell counterparts, leading to increased concentration of spore related proteins and a decrease in shorter lived vegetative cell proteins (54, 88). Sporulation-specific sigma factors are transcribed in a defined series that has been well characterized in *B. subtilis*, and lead to the waves of sporulation gene transcription (146).

Regulation of Sporulation and Sigma factors

Regulation of gene expression in bacteria occurs primarily at the level of transcription. DNA-binding proteins can significantly affect the efficiency of transcription, but the specificity of the transcription reaction depends on the interactions between the RNA polymerase (RNAP) and the promoter sites. RNAP is most commonly found in two parts, the core RNAP, which catalyzes the polymerization of ribonucleotides into a RNA

complementary copy of a DNA template, and the holoenzyme complex, which contains subunits of the RNAP core complex (β , β' , and two α) plus an additional protein subunit called the sigma factor. The sigma factor determines the specificity of the RNAP for target gene promoters and dissociates from the core RNAP when transcription from the sigma-specific promoter is initiated.

During the life cycle of many bacterium, different sigma factors are turned on and off to modify their gene expression to best suit their current environment and stresses. The cascade of sigma factors in *Bacillus subtilis* has been well characterized. Alternative sigma factor usage in *B. subtilis* can be used as a model for alternate sigma usage in *B. anthracis*, but some care must be taken, as sporulation target genes and recognition sequences are not identical between the two species.

σ^A is the primary sigma factor in the vegetative cell. It is responsible for transcription of the housekeeping genes and genes involved in very early sporulation. It is by far the most abundantly utilized sigma factor, involved in expression of most genes utilized during growth in rich media (110). The σ^A -dependent transcripts include DNA damage response genes, heat shock response genes, genes responsible for stationary phase degradative enzyme synthesis, and the development of bacterial competence. The sigma factor (σ^A) is critical for the initiation of sporulation and directs the transcription of several of the *spo0* genes, most notably Spo0A. Spo0A is a DNA binding protein that acts as the transcriptional activator/repressor that initiates a cascade of events leading to

sporulation. σ^A has been found to act on sporulation-related genes through at least Stage II of sporulation (activation of SpoIIG and SpoIIE; 110).

The sigma factor (σ^B) regulates the expression of stress responses, including responses to heat shock, O₂ limitation, and exposure to high salt or ethanol (110). It is also activated when *Bacillus* enters into the stationary phase of growth. Although σ^B plays a role in the response to these stresses, it is not essential, as a σ^B -null mutant is not more susceptible to environmental stressors (110). σ^B plays no significant role in transcription of sporulation-related genes.

The extremely low abundance of σ^C has limited its study, and it has no known effects of regulation of transcription of genes to date (110). σ^D is involved in expression of genes for flagellum, secretion machinery, and chemotactic protein sensors (110, 113). Both σ^C and σ^D play no major roles in sporulation, despite the timing of σ^D 's upregulation during the exponential and stationary phase of growth. σ^L likewise does not play a role in sporulation, with just a minor role in expression of amino acid degradative enzymes (110, 113).

σ^H expression is controlled by early stage sporulation factors. σ^H is essential for sporulation, but it is also present during exponential vegetative growth, where it may play a role in transcription of vegetative genes (110, 113). Most sporulation gene transcripts are also enhanced by the activity of Spo0A-related enhancers of transcription. σ^H also

plays roles in competence, TCA cycle enzyme synthesis, and DNA repair enzymes (110). σ^H has been recently found to be involved in toxin gene expression in *B. anthracis* (113).

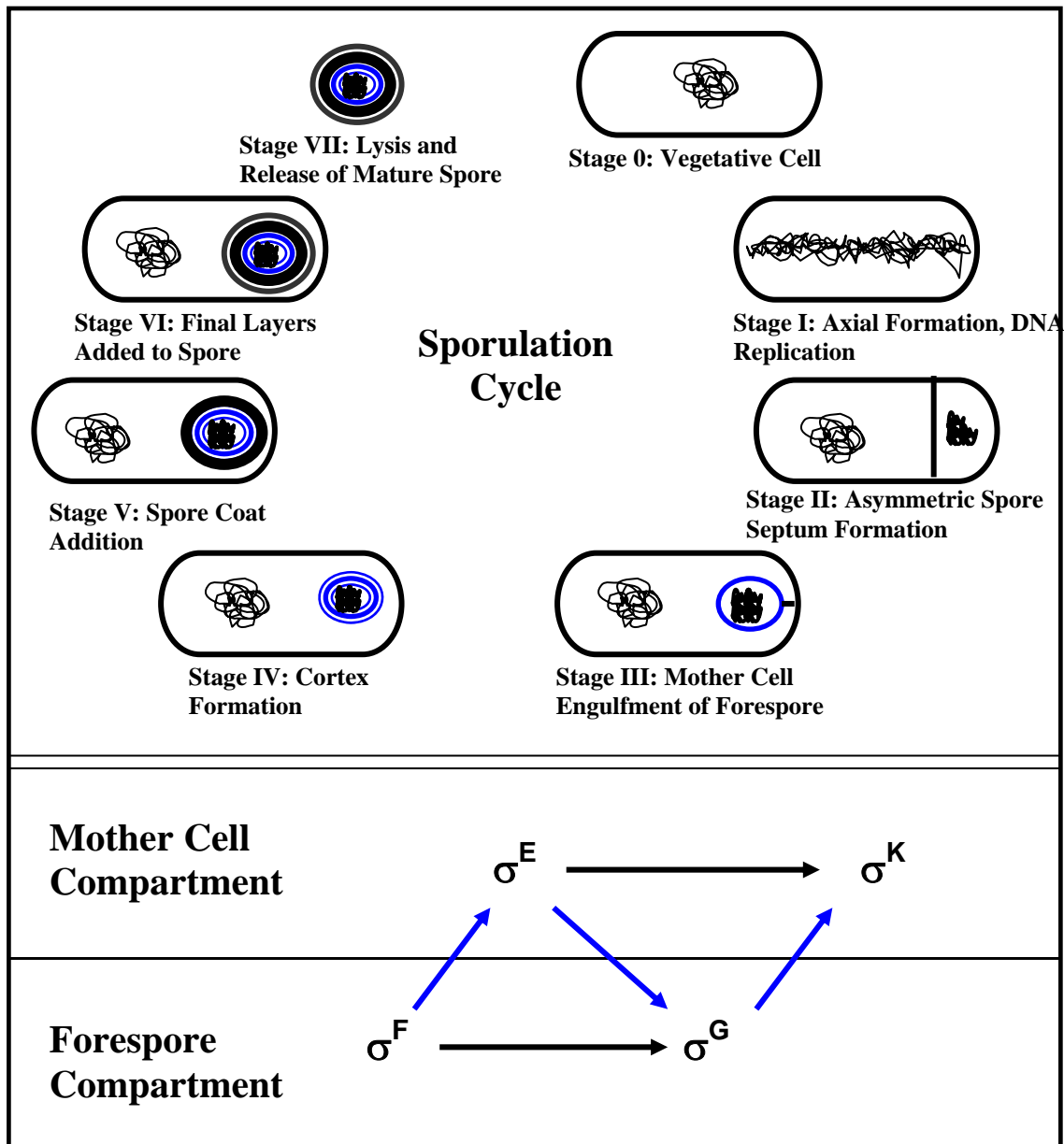


Figure 2. Top panel denotes a representation of the sporulation cycle of *B. subtilis*. The bottom panel demonstrates the interactions between sporulation specific sigma factors,

with direct effects denoted by black arrows and indirect effects denoted by blue arrows.

Adapted from Hilbert *et al.* (111)

Both σ^E and σ^K are mother cell-specific transcription factors. They direct early and late phase transcription of genes, respectively, and transcribe genes essential to addition of spore coat and exosporium proteins. The σ^E sigma factor becomes active during Stage II of sporulation and into later stages. Seventeen known genes in *B. subtilis* are under the regulation of the σ^E (110, 113). σ^E -dependent transcripts are responsible for spore septum formation, forespore engulfment, peptidoglycan and cortex formation, and layering of some of the early spore coat proteins, including CotE. σ^E -dependent products are also involved in the cleavage of pro- σ^K into active σ^K (110). This cleavage is tightly regulated, and delays production of active σ^K until its products are ready to be assembled into the spore over the initial layering of the σ^E transcribed products. σ^K expression initiates between the third and fourth stage of sporulation, and the pro- σ^K is cleaved to its active form during late stage IV. This may rely on processing by a protein that is dependent on σ^G expression in the forespore (110, 113). σ^K -controlled genes include germination receptors, genes involved in DPA accumulation and synthesis, and most of the genes that encode proteins in the spore coat and exosporium. σ^K , by virtue of its replacement of other sigma factors, also acts to inhibit production of early stage sporulation genes (111).

The sporulation genes that are transcribed in the forespore compartment utilize σ^F - and σ^G -specific promoters. *SigF* is transcribed during stage II of growth. σ^F activation in the

forespore compartment is due to cleavage of the pro- σ^F into the active form (110). σ^F is activated after production of the spore septum between the mother cell and the forespore. σ^F transcribed genes include those encoding the enzymes and other products necessary for protein cleavage and efficient nutrient acquisition in the germinating spores. σ^F also plays a role in the cleavage of the pro- σ^E protein into its active form by an unknown mechanism. σ^G is a forespore specific sigma factor. It is active during the third and fourth stages of sporulation. σ^G transcribed genes include those encoding the SASP proteins, which are involved in protection and packaging of the spore DNA. A σ^G -encoded protein acts by an unknown mechanism to cleave pro- σ^K into σ^K (111). These sporulation-specific sigma factors are sequentially linked and act upon one another to precisely regulate the assembly of the spore in different compartments in a phase-dependent manner (109). This ensures an ordered, complete structure is constructed, leading to the ability of the spore to survive many environmental challenges. The interactions between the spore-specific sigma factors are demonstrated in **Figure 2**. **Table 1** summarizes the sigma factors expressed in *B. subtilis*, their roles, and their putative binding sites.

Sigma Factor	Genes	Function	Promoters		
			-35	Spacer	-10
Vegetative Sigmas					
σ^A	<i>sigA, rpoD</i>	Housekeeping/early sporulation	TTGACA	17	TATAAT
σ^B	<i>sigB</i>	General stress response	RGGXTTRA	14	GGGTAT
σ^C	Unknown	Postexponential gene expression	AAATC	15	TAXTGYTTZTA
σ^D	<i>sigD, flaB</i>	Chemotaxis/flagellar gene expression	TAAA	15	GCCGATAT
σ^H	<i>sigH, spoOH</i>	Postexponential gene expression, Competence and early sporulation	RWAGGAXXT	14	HGAAT
σ^L	<i>sigL</i>	Degradative enzyme gene expression	TGGCAC	5	TTGCANNN
Sporulation Sigmas					
σ^E	<i>sigE, spoIIGB</i>	Early mother cell gene expression	ZHATAXX	14	CATACAHT
σ^F	<i>sigF, spoIIAC</i>	Early forespore gene expression	GCATR	15	GGHRARHTX
σ^G	<i>sigG, spoIIIG</i>	Late forespore gene expression	GHATR	18	CATXHTA
σ^K	<i>sigK, spoIVCB:spoIIIC</i>	Late mother cell gene expression	AC	17	CATANNTA

Table 1: Summary table of sigma factor target genes, sequences, and role in sporulation.

H=A or C, N= A,G,T,or C, R=A or G, W=A, G, or C, X= A or T, Y=C or T, and Z= A or G. Adapted from Haldenwang *et al.* 1995 (110)

Spore Structures

The spore is the infectious agent of *B. anthracis*. The *B. anthracis* endospore is formed in several steps. Asymmetric septation of the nutrient-starved vegetative cell produces the large mother cell and small forespore compartments. The mother cell then engulfs the forespore, encasing it with two distinct membranes. The first step in assembly of the spore is the packaging of the DNA, ribosomes, tRNAs, and other cellular components into the core of the forespore. Newly-packaged DNA and enzymes are protected by the production of the thick layer of modified spore-specific peptidoglycan, called the spore cortex, between the two forespore membranes (11). DNA is condensed by small acid-

soluble proteins (SASPs), low molecular weight proteins that surround the DNA and protect them from UV, radiation, heat, and other chemicals (58). SASPs are synthesized late in sporulation. They bind and alter the DNA structure and properties dramatically. The low water content of the core inactivates the enzymes present in the core and helps induce dormancy.

This low percentage of water in the core (27-55% in spore versus 75-80% in growing cells) and the low amount of free water in the core restricts the flow of macromolecules and enhances the resistance properties of the spore due to freezing and desiccation. Also in great abundance in the spore core is pyridine-2,6-dipicolinic acid (DPA). DPA consists of 5-15% of the spore dry weight and is chelated mostly by Ca^{2+} . This molecule is secreted in the first moments of spore germination in conjunction with the influx of large amounts of water. DPA plays a large role in the reduction of the water content of the spore core (58).

External to the cortex is found a series of proteins that form a lattice called the spore coat. The spore coat is made up of proteins synthesized in the mother cell and layered onto the outermost of the two forespore membranes. The spore coat consists of greater than 50 proteins in *B. subtilis* (10). Surrounding the spore coat, and presumably the last layer placed on the outside of the spore, is the loose balloon-like structure known as the exosporium. The exosporium is also synthesized within the mother cell. After a final stage of maturation the mother cell lyses to release the mature spore. See Figure 3.

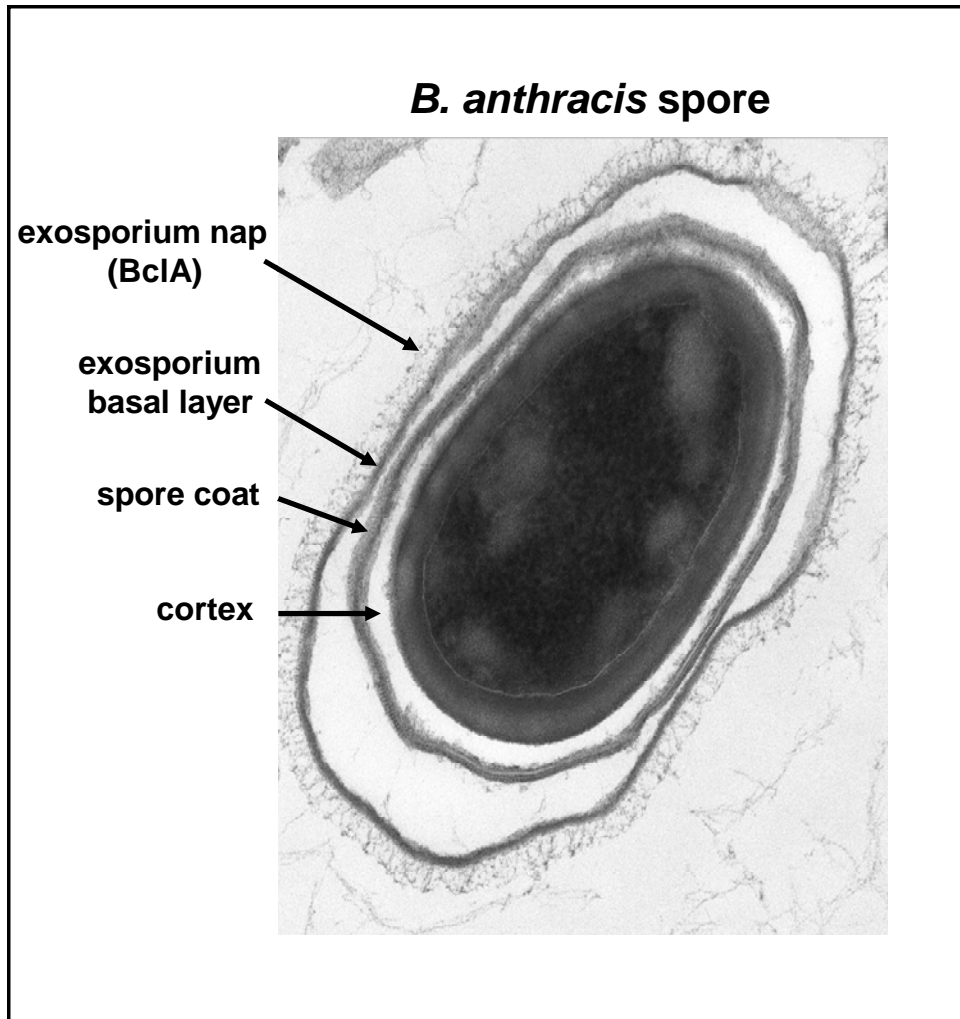


Figure 3: Layers of the *B. anthracis* spore

The Spore Coat

In the well characterized *B. subtilis*, the spore coat contains a complex mixture of at least 24 proteins which can be resolved into two or three morphological layers (55, 87). Coat assembly requires regulatory proteins and key morphogenetic factors. The coat also plays a role in germination, perhaps by providing access for germinants to the germinant receptor proteins located in the cytoplasmic membrane (24). Lytic peptidoglycan

hydrolase enzymes may also be located in the spore coat, which are involved in lysis of the spore cortex during germination (188). The spore coat proteins undergo extensive crosslinking, with many of the spore coat proteins containing multiple cysteine residues. The crosslinked spore coat is involved in some spore resistances: exogenous lytic enzymes that can degrade the spore cortex, UV light, hydrogen peroxide, and can protect the spore from predation from protozoa, but has little to no role in spore resistance to heat, radiation, and other chemicals (58, 158).

Although *B. anthracis* and *B. subtilis* have similar numbers of predicted spore coat proteins and a few common coat proteins, the outer coat layers vary significantly (55). The *B. subtilis* spore coat is a relatively thick structure with a distinctly light inner layer and a darker outer layer (87). In contrast, the *B. anthracis* spore coat, appears thin and compact (87). It is also separated by a gap, sometimes called an interspace, from the exosporium, not present in *B. subtilis*. In most cases, the precise function of various spore coat proteins has been difficult to determine, since gene disruptions had no measurable phenotypic effects.

Coat assembly in *B. subtilis* is a complex multistep process. One early event in coat assembly is the essential localization of SpoIVA to the outer membrane of the forespore on the mother cell side (110, 113). SpoIVA marks the exterior of the outer membrane as the site of all future coat protein assembly and directs the layering of the initial spore coat layers. A layer of coat proteins is assembled around SpoIVA. A *spoIVA* mutant in *B. anthracis* failed to progress past the early stages of sporulation and never

produced mature spores (87). These mutant spores lacked the cortex, and the mother cells were filled with swirls of electron dense coat material (87). SpoIVA appears to have a role in *B. anthracis* similar to that in *B. subtilis*, namely marking and directing assembly of the spore coat layers on the outside of the forespore. The outermost part of the initial coat layer contains the coat protein CotE (87). In the final stage of coat assembly, the inner and outer coat layer appears between the CotE and the SpoIVA layers (87). The CotH protein, directed by the CotE protein in *B. subtilis*, directs deposition of several other coat proteins.

The *B. anthracis cotE* mutant was found to lack attachment of the exosporium, and also had detached spore coat layers (87). Examination of the *cotE* mutant spores under atomic force microscopy (AFM) revealed a loss of the typical pole to pole ridges found in *B. anthracis* spores (12). These data show that the CotE protein is essential for anchoring the coat layers and exosporium to the core and that it also plays a role in the proper construction of the spore coat. Proteomic studies did not find CotE in the exosporium, so its role in anchoring of the exosporium occurs within the spore coat, or it plays an indirect role (87). CotE may play a role in stability of the exosporium, as it may control ExsY and CotY assembly, since these genes are homologs of the CotZ protein of *B. subtilis*, which is controlled by CotE (87).

The ExsA proteins of *B. cereus* and *B. anthracis* have been found to be vital in proper assembly of the spore coat and the exosporium (81). Obvious defects in the spores were evident under transmission electron microscopy (TEM). Mutant spores became

extremely sensitive to lysozyme, were unstable, and tended to lyse when subjected to freezing and thawing. The spore coat layers and exosporium were misformed, and remained free and unattached to the spore core (81).

A *cotY* mutation in conjunction with an *exsY* mutation leads to spore coats that are very thin, with a decrease in resistance to lysozyme, phenol, chloroform, and toluene (86). The double mutant has difficulty constructing an attached exosporium, and CotY as well as CotE may play a role in maintaining an ordered structure upon which an exosporium can be constructed (86, 87).

A major coat protein has been identified in all of the *B. cereus* family members, and it has been named CotA. This 13-kDa protein has 6 cysteine residues and is likely to crosslink with many other coat proteins (24). CotA confers resistance to lysozyme. The *cotA* determinant has a consensus σ^K promoter element, consistent with the appearance of the CotA antigen at stage IV of sporulation. TEM studies revealed that a *cotA* mutant lacked the majority of the spore coat as well as had an increased sensitivity to chloroform, phenol, and bleach. AFM studies show the *B. anthracis* and *B. cereus* spore coats are covered in ridges that run along the long axis of the spore, and that presence of the exosporium hides these features (12). These ridges may be reflective of the dehydration state of the spore core at the time of imaging (14).

Exosporium

The outermost layer of the *B. anthracis* spores is the exosporium. *Bacillus subtilis*, the best characterized spore-former, does not possess a defined exosporium, consequently, many of the mechanisms involved in exosporium construction are unknown and currently under investigation. Scanning electron microscopy has revealed the exosporium contains a paracrystalline basal layer and a hair-like outer layer called the nap (142, 143). Several proteins of the exosporium are related to the morphogenetic and outer spore coat proteins of *B. subtilis*, but many of them have no known homology to any known proteins outside the *B. cereus* family. A proteomic analysis of exosporium proteins revealed the presence of 137 exosporium-predicted proteins, but the extract used in this study was not pure exosporium, and contained contaminating spore coat and other proteins (88).

The primary permeability barrier and source of spore antigens is the exosporium (15, 23). The exosporium may also play a role in interactions with the soil environment, binding to immune cells in the mammalian host, and evasion of host defenses. It helps protect underlying epitopes from recognition by the innate immune system and also allows the spores to be more resistant to killing by host macrophages *in vitro* (28, 39). This exosporium layer is chemically complex, consisting of protein, amino and neutral polysaccharides, and lipids (190). Exosporium antigens first appear at stage III of sporulation. The exosporium has been speculated to be the reason for the extreme hydrophobicity of the spore, and therefore might play a role in adhesion (78).

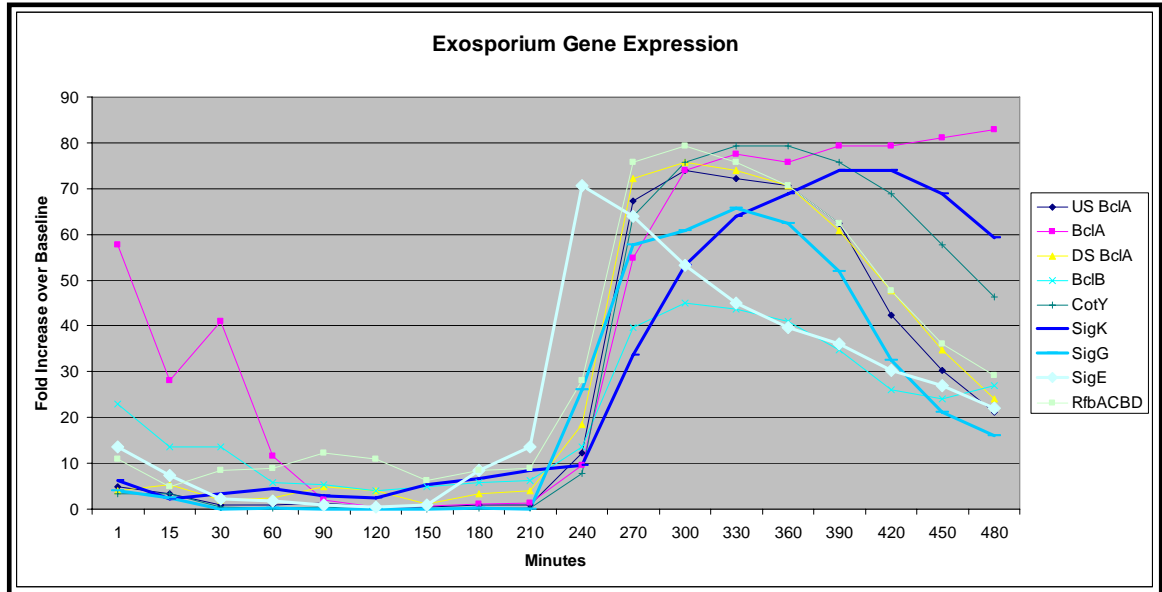


Figure 4: Expression of late sporulation genes, adapted from Bergman *et al.* (54)

Characterization of exosporium proteins extracted from *B. cereus* has recently identified more than 10 proteins (79). These included ExsB, ExsC (not expressed in *B. anthracis*), ExsD, ExsE, BxpB/ExsF, ExsG and ExsJ. Only the *exsJ* and *bxpB* genes have been further characterized to date. ExsJ is a glycoprotein that migrates at a mass of 72 kDa and 205 kDa. This most likely represents the monomer and trimer versions of the protein, as is found in the similar BclA and BclB proteins of *B. anthracis* (79). The *exsJ* gene has high homology (>88%) to the *exsH* gene found elsewhere in the chromosome, and the major differences between the two proteins are found in the N-terminal regions of the two proteins. In both *B. anthracis* and *B. cereus*, the presence of an exosporium biosynthesis operon is apparent. Following the *bclA* determinant is a series of glycosylation biosynthesis genes (glycosyltransferases and methyltransferases) followed

by a rhamnose biosynthesis gene cluster. The spore carbohydrate glycosylation machinery is predicted to place the sugar residues on the BclA and BclB proteins. The glycosylation machinery determinants are transcribed concurrently with *bclB*, *bclA*, and other σ^K -directed genes, consistent with late sporulation mother cell expression. Beyond the rhamnose determinants is a series of genes with sequences similar to *B. subtilis* coat genes. Among this group of genes is the gene encoding the basal layer protein BxpB/ExsF, ExsY (a CotY homolog), and CotY proteins. This region is conserved among the *B. cereus* family members, but only parts of the operon are present in the *B. subtilis* chromosome (79). See **Figure 5**.

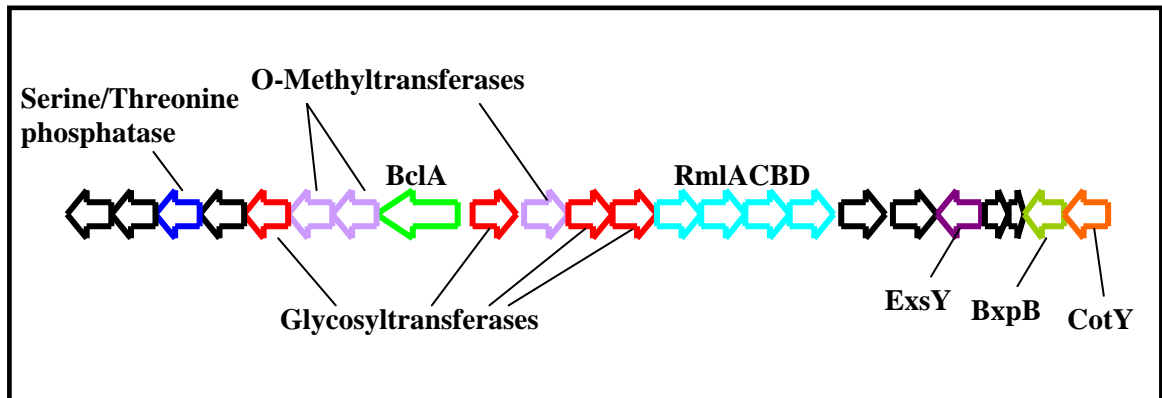


Figure 5. The *bclA* operon and adjacent spore-associated operons.

Several proteins have been isolated from the exosporium of *B. anthracis*. Alanine racemase and nucleoside hydrolase were isolated and identified, as well as the CotY and ExsY components (13). S-layer proteins were also found, but these are likely contaminant (13). The BxpB protein was identified in the *B. anthracis* exosporium (13). BxpB/ExsF, ExsY, and BclA were all found in a high molecular weight grouping of proteins migrating at greater than 250 kDa (13). A novel protein, ExsK, was also found in the *B. anthracis* exosporium, but has not been identified as an exosporium protein yet in *B. cereus* (13). The *B. anthracis* exosporium contains an arginase which may compete with macrophages for free arginine, limiting their ability to produce NO and other free radicals to attack the germinating cells (141).

The basal layer consists of four paracrystalline sheets, each exhibiting a hexagonal perforate lattice structure (142, 143, 159). BxpB, along with BxpA, BxpC, and ExsK; are all currently predicted to be basal layer proteins (25). The *bxpB* determinant encodes a 17-kDa protein found to be located in the basal layer by immunogold labeling. This protein forms strong covalent complexes with BclA and other basal layer/nap proteins, including ExsY and CotY. ExsY and CotY are homologues of CotZ and are CotE-controlled spore coat proteins of *B. subtilis* (87).

When BxpB is extracted by SDS from spores, it is isolated as both a monomer and in high molecular weight complexes with BclA and possibly ExsY and CotY. *bxpB* mutants cannot assemble a hairlike nap, although BclA is still synthesized at normal levels (25).

The lack of BxpB leads to expedited spore germination and outgrowth, potentially due to easy access of germinants into the spore (25). CotY, ExsY, CotB-1, and CotB-2 may be associated with the basal layer or outer coat protein layers (25). Also incorporated into either the basal layer or the nap is alanine racemase, superoxide dismutase, and inosine-uridine-preferring nucleoside hydrolase. These enzymes could protect the spore from reactive oxygen species during infection, and suppress premature germination by less than optimal levels of germinants (13, 79, 187). The major germinants of *B. cereus* spores are alanine and inosine (9, 11, 16). Alanine racemase converts L-alanine to D-alanine, a competitive inhibitor of germination. A nucleoside hydrolase would degrade inosine, preventing germination by minute quantities of inosine.

The immune inhibitor A protein (InhA) protein has been found in all three species of the *B. cereus* family in various degraded and native forms (18). This protein, best characterized in *B. thuringiensis*, is a zinc metalloprotease and degrades proteins of the immune system (18). It is highly toxic to *Drosophila*. It migrates as a band of 72-kDa and as several smaller bands of 46, 22, and 18 kDa (18). The protein is secreted throughout the life cycle of the vegetative cell, but a homolog is found associated with, or is a contaminant of, exosporium preparations. InhA is a major component of the exosporium of *B. cereus* and *B. thuringiensis*, but is only found in minor quantities in *B. anthracis* (13, 79, 140). The InhA metalloprotease allows *B. cereus* spores to escape from macrophages and may play a small role in macrophage escape by *B. anthracis* as well (140).

Formation

Exosporium antigens appear as early as stage III of sporulation (191). *B. cereus*, *B. anthracis*, and *B. thuringiensis* all contain specific glycoproteins on the surface layer of the exosporium (18, 99, 19). The major glycoprotein in *B. anthracis* is BclA which is highly immunogenic (19). It is the major component of the hair-like nap that forms the outermost layer of the exosporium. Many proteins of the exosporium have recently been described, but the overall function of the exosporium has yet to be determined (13). This loose balloon-like structure is made up of at least 20 proteins (13, 18, 79). Most of this layer is made up of protein, but many of these proteins are glycosylated and potentially lipidated. The exosporium can bind to lectins, which may bind to the many glycosylated proteins found in the exosporium (193). The exosporium is 2% of the mass of the spore and is about 50% protein, 20% lipid, 20% neutral polysaccharides, and 10% other components (190).

The BxpA and BxpB/ExsF proteins have been isolated from the exosporium (15). The Gln-rich BxpA protein is predicted to form sheaths, as it shares homology with filarial sheath proteins (15). A *bclA* mutant allows antibody access to basal layer proteins, suggesting that the BclA protein inhibits the ability of antibodies to access the basal layer. The sugarless *rmID* mutant, responsible for glycosylation of BclA, also allows access of antibodies to the basal layer. This suggests that the glycosylation of BclA leads to inhibition of antibody entry (15). Anti-BxpA antibodies bind BxpA more efficiently in the glycosylation-deficient $\Delta bclA$ and $\Delta rmID$ strains (84). The BxpB protein

does not contain a repeat region and is associated with BclA and other high molecular weight exosporium proteins. The *exsFA* and *exsFB* genes map to different parts of the *B. anthracis* chromosome, but are homologs of each other. They share 78% identity to each other, with the majority of the differences occurring at the N-termini. ExsFA and ExsFB (BxpB and homolog) proteins are also involved in exosporium integrity and the incorporation of BclA into the nap (80). Loss of ExsFA leads to a decrease in BclA incorporation in the nap, and a double knockout of *exsFA* and *exsFB* leads to no incorporation of BclA in the nap (80). ExsFA and ExsFB are found in high molecular weight complexes co-migrating with BclA, BxpB, ExsY, and CotY (80).

Nap

A major component of the exosporium is the hair-like nap, which is mostly comprised of BclA (15, 19). The nap and the associated hair-like filaments were first described on the exosporium of *B. anthracis* in 1966 (144). Truncations of the BclA collagen-like region (CLR) also lead to a decrease in the size of the hair-like filaments on the outer surface of the spore; further evidence that this protein is BclA (75, 83). Proteins of the nap are likely to be the first proteins seen by the innate immune system in interactions with the spores (83, 19). The hair-like nap differs in length from species to species, and even from strain to strain (15, 83). The nap does not play a role in the resistance of the spore to various insults (19).

BclA also comprises the major protein species seen on western blots of exosporium extracts when using a polyclonal anti-spore antibody (15, 19). Antibodies both to the BclA protein or the carbohydrate portion of BclA have been produced (15). Ruthenium red allows the visualization of the nap under TEM by binding to the glycoprotein moieties (156). A 715-Da tetrasaccharide and a 324-Da disaccharide are linked to BclA by GalNAC (19, 23). Many copies of the tetrasaccharide are linked to the collagen-like region of BclA, but the disaccharide most likely is attached outside the collagen-like region (CLR) (23). The nap extends from the exosporium for 600Å^o (15, 83). Deletions in the CLR lead to a decrease in the glycosylation with the tetrasaccharide, but not the disaccharide. This was discovered by hydrazinolysis and led to the discovery of a *B. anthracis* specific sugar identified as anthrose (23). The BxpB protein plays a role in incorporation of the BclA glycoprotein into the exosporium (25).

Also reported to be in the exosporium and likely the nap is the protein InhA (immune inhibitor A). It is reported to be the major antigen on the outside of *B. cereus* spores. The BclA protein is coated with sugars, a major portion comes from the *rmlACBD* operon adjacent to the *bclA* operon on the chromosome (92). The *rmlACBD* operon encodes enzymes necessary for rhamnose biosynthesis. Although spores from a *rmlD* mutant were more efficiently taken up by macrophages and bound more efficiently to macrophages, they were not more virulent in a guinea pig model (92). Interestingly, macrophages can recognize and internalize collagen via the mannose receptor, and this may recognize the collagen-like proteins of the nap (145).

The Cap and ExsY

ExsY is required for complete formation of the exosporium of *B. anthracis* (85). Assembly of the exosporium in an *exsY* mutant is halted after partial formation of a polar exosporium-like structure termed the “cap” (85). The exosporium cap produced could readily be stripped off under growth in liquid media (85). The *exsY* mutant grown on solid media retained the cap structure. An *exsY* mutant also appears to lack BxpB, showing a relationship between the two proteins. The mutant spores ruptured a novel sac-like structure in the exosporium during germination and outgrowth (85, 86). This sac was still evident when $\Delta exsY$ spores were grown in solid media. ExsY is found not only incorporated into high molecular weight complexes with the BclA protein, but also found in monomers, dimers, and trimers (85, 86). BclA is not assembled into the exosporium but rather is secreted into the supernatant in an *exsY cotY* double mutant, further suggesting an interaction between the two proteins. ExsY has a consensus σ^K promoter, consistent with its expression during the spore coat/exosporium assembly phase of sporulation.

The presence of the cap has led to the development of the bottle cap model for spore germination (97). According to this model, ExsY plays a role in the development of the exosporium beyond the cap. This cap may be the first structure of the exosporium to be assembled, since it appears first under TEM analysis. Alanine racemase, an enzyme commonly found in the exosporium, was shown to only be localized in the three quarters of the exosporium that is not part of the cap (97). This suggests that the assembly of the

cap and the assembly of the rest of the exosporium are sequential and separate, and their formation discontinuous. During germination and outgrowth, the emerging cell bursts through the exosporium and underlying layers, and this always appears to be at the end of the spore that corresponds to the cap (97). This led to the prediction that the cap is designed to facilitate the emergence of the outgrowing cell.

BclA

BclA (*Bacillus* collagen-like protein of *anthracis*) has been found in all the *B. cereus* family members. The BclA protein is comprised of distinct N-terminal and C-terminal domains, with a series of collagen-like glycine, proline, and threonine (GPT) repeats comprising the extensive middle portion of the protein. Several aspects of the BclA protein are similar to collagen, and lead to the prediction that BclA can form a triple helical structure. A glycine residue occupies every first amino acid in the repeating GXX triplet sequence. 39% of the non-glycine residues in the repeat are prolines, which are essential for triple helix stabilization by limiting rotation of the polypeptide chains (69, 94, 194). Computer modeling predicts that BclA exists in a coiled conformation (19). Recombinant BclA naturally forms a triple helical structure upon heating and cooling the protein (75). The native BclA protein is exceptionally stable, and may act as a protective shield to the spore. BxpB, ExsFA, and ExsFB play a role in BclA being incorporated into the nap layer of the exosporium (80).

The 35 amino acid BclA N-terminal domain is similar in structure to members of the TNF family, and its role is currently unknown. N-terminal sequencing of the protein extracted from spores has shown that the first 19 residues of the protein are processed to remove 19 aa from the N-terminus (15, 19). The N-terminus also faces towards the basal layer in the orientation of the exosporium (19).

The internal repeat region is hydrophobic with 70 collagen-like triplet repeats (GXX) and 54 GPT triplets (19). The hydrophobic nature of BclA may explain the general hydrophobicity of the entire spore (78). Between residues 41-232 is the repeat of $((\text{GPT})_5\text{GDTGTT})_2$ known as the BclA repeat (15). Variations in the BclA repeat, as well as parts of the N and C termini displaying sequence polymorphisms, allow species and strain discrimination (99, 83). Differences in the number of repeats also correspond to the length of the hair-like nap on the exosporium (83). Mutants of *bclA* are apparently devoid of a visible nap on the outer surface of the exosporium (19).

The 134 aa C-terminal domain (CTD) is essential for forming the triple helical structure of the BclA protein. The CTD itself can naturally form a heat stable triple helix (75).

This domain also faces away from the spore in the exosporium, and is the most external part of BclA. Recombinant BclA is resistant to many proteases, but is highly susceptible to collagenases, whereas the native glycosylated BclA is resistant to both (75, 72).

Collagenase treatment of the rBclA leads to digestion of the amino terminal portion of the collagen like region, but the CTD remains resistant (72). BclA complexes also have a dissociation constant equivalent to a triple helix when examined by circular dichroism

(75). This CTD most likely acts as the stabilizing point, to which the rest of the BclA protein is folded. rBclA will spontaneously refold into a triple helix, starting with the CTD (75). BclA is predicted to have a lollipop structure, with the collagen-like region containing the stalk and the CTD forming a triple helical head of the globular protein (69). The globular CTD domain is strikingly similar to the C1q protein of complement and tumor necrosis factor. Both BclA and C1q have been shown to be capable of interacting with the lung surfactant component C (SP-C), a major part of the lung alveolar surfactant layer (69).

The structure and role of BclA in the pathogenesis of *B. anthracis* are just now being elucidated. BclA electrophoretically migrates at >70 kDa, which is much greater than the 34 kDa expected from its amino acid sequence. This is potentially due to the large content of prolines, which have been shown to modify the migration of collagen-like proteins (15, 194). These collagen-like proteins are extremely rare in prokaryotes (19, 94). The repeated threonine residues throughout the repeat may serve as multiple sites of O-linked glycosylation (83). These proteins can form triple helical structures, without the need for hydroxyprolines that eukaryotes use in their collagen triple helices. Threonines can substitute by making direct hydrogen bonds to neighboring carbonyls to stabilize the structure (195). This stabilization can be enhanced by glycosylation of the threonines. Glycosylation of threonine residues in worm collagen greatly stabilize the triple helices (195). The glycosylation of BclA may lead to resistance to protease activity. The ability of bacterial collagen-like proteins to form triple helices *in vitro* has

been recently shown with the streptococcal collagen-like proteins (95, 96). They contain a long collagen-like internal region and may be involved in adhesion.

Two O-linked oligosaccharides, a 715-kDa tetrasaccharide and a 324-kDa disaccharide are released from spore- and exosporium-associated BclA after hydrazinolysis treatment (19, 23). Each oligosaccharide is probably attached to BclA by a GalNAc linker (19, 23). The tetrasaccharide is found in multiple copies in the collagen-like region of BclA, and the disaccharide is most likely attached outside this region (74). The disaccharide is composed of a rhamnose residue and a component identified as 3-O-methyl-rhamnose. The tetrasaccharide is 2-O-methyl-4-(3-hydroxy-3-methyl-butamido)-4,6-dideoxy- β -D-glucopyranosyl-(1 \rightarrow 3)- α -L-rhamnopyransol-(1 \rightarrow 3)- α -L-rhamnopyranosyl-(1 \rightarrow 2)-L-rhamnopyranose. The terminal end sugar is 2-O-methyl-4-(3-hydroxy-3-methylbutamido)-4,6-dideoxy-D-glucose. This terminal sugar has been named anthrose. The anthrose sugar moiety of BclA is not found in the other members of the *B. cereus* family, although they all contain the BclA protein. This sugar could be exploited as a novel target of diagnostic kits (74). These sugars have been synthesized *in vitro* (70, 71).

Synthetic GPT repeats also are stabilized by glycosylation (69). Recombinant BclA expressed in *E. coli* hosts is not glycosylated. BclA is rarely found without being glycosylated, hinting at a linked production/glycosylation pathway (19). When the native protein in the spore is extracted and treated with trifluoromethanesulfonic acid (TFMS) to remove the glycosylation, the protein still retains a small portion of the sugar moieties

(15, 19). A *bclA* mutant sporulates and germinates with kinetics similar to wild-type strains (19). The *bclA* gene has a putative σ^K promoter upstream of the open reading frame, consistent with sporulation stage expression of proteins produced in the mother cell. This open reading frame is followed by two inverted repeats after the termination codon.

The highly glycosylated nature of BclA may play a role in binding of the spores by carbohydrate recognition molecules of antigen-presenting cells (APCs, 19). This glycosylation also may protect the protein coat and spore from enzymatic cleavage and help exclude some molecules from gaining access to the spore. It may also play a role in adherence, as several other collagen-like proteins in prokaryotes have been predicted to be adhesins (95, 96, 152). *bclA* mutant spores presented no significant change in virulence in a mouse model of infection (77), but the time course of disease was modified. BclA is a major immunodominant antigen of the spore. This response is not to the extensive glycosylation of the spore, which can elicit an immune response, but is to the protein component (15). Using a live or irradiated spore vaccine, an immune response to the tetrasaccharide itself can be made, and is another potential target for future vaccines (82, 76).

BclB

Recently, a second collagen-like spore glycoprotein of *B. anthracis* was identified (89). This new glycoprotein was named BclB for *Bacillus* collagen-like protein B. Other

exosporium glycoproteins, ExsJ and ExsH, have been identified in *B. cereus* and *B. thuringiensis*, but have not been found in *B. anthracis*. Both ExsJ and ExsH have been found to migrate during electrophoresis as a >205 kDa species. ExsJ has been found to contain rhamnose, galactosamine, and a third unidentified sugar. ExsH has a region of collagen-like repeats, like ExsJ, but the carbohydrate composition has not been identified (89). The *bclB* determinant was predicted to have been formed from a unique crossover event between ExsH-like or ExsJ-like genes derived from *B. cereus* or *B. thuringiensis* (89).

Upon urea extraction of spores of *B. anthracis*, two high molecular weight glycoproteins were identified (89). One was the well characterized BclA protein, and the second, migrating at 205-kDa, was the newly identified BclB protein. When deglycosylated, BclB migrated as a band of about 83-kDa, suggesting that it has a collagen-like triple helix structure similar to BclA or is an extensively glycosylated protein. Using GC-MS analysis, 3-O-methyl rhamnose, rhamnose, and galactosamine were found to be part of the BclB glycoprotein, all three of which are also present in BclA (89). BclB contains a repeated GXX motif, GITGVTGAT, which has been named the BclB repeat.

We have recently identified motifs of the BclA and BclB proteins. These surface-exposed proteins are external to all other exosporium proteins known to date and may play a role in the interactions of the spore with the immune system of the host (199.) The N-terminal regions of BclA and BclB have not been characterized to date, and we hypothesize that they are involved in the localization and attachment and of these

proteins. This study was undertaken to analyze these motifs, and the overall role of these proteins in exosporium assembly.

Materials and Methods

Bacterial Strains

The bacterial strains used in this study are listed in Table 2. All *E. coli* strains were cultivated in L Broth or Tryptic Soy Broth (TSB, Oxoid). All *Bacillus anthracis*, *Bacillus subtilis*, *B. cereus*, and *B. thuringiensis* strains were grown in Brain Heart Infusion broth (BHI, Difco), with or without 0.5% (w/v) glycerol, or L Broth, unless otherwise noted. Agar plates were made by mixing the above broths with 1.5% (w/v) agar prior to autoclaving. Antibiotic selection was used for the maintenance and selection of plasmids and recombination events, and was used at the concentrations noted in Table 3.

Table 4 contains a table of the plasmids used in this study. Frozen stocks of all clones and constructs was made by heavily inoculation of freshly grown cultures into BHI broth containing 20% (w/v) glycerol and placed on dry ice. After quick freezing on dry ice, the cryo-tubes were placed at -80°C for long term storage and recorded in the Stewart Laboratory stockbook.

Table 2: Bacterial strains used in this study.

<u>Strain</u>	<u>Genotype</u>
<i>E. coli</i>	
DH5 α	<i>F- ϕ80lacZΔM15 Δ(lacZYA-argF)U169 deoR recA1 endA1 hsdR17(rk-, mk+) phoA supE44 thi-1 gyrA96 relA1 λ-</i>
GM48	<i>F- λ- dam-3 dcm-6 thr-1 leuB6 ara-14 tonA31 lacY1 tsx-78 glnV44(Am) galK2(Oc) galT22 thi-1</i>
M15	See Qiagen manufacturer's specifications
Able K	<i>lac(LacZω-) [KanR McrA- McrCB- McrF- Mrr- HsdR(rK-)] [F' proAB lacIqZΔM15 Tn10 (Tetr)]</i>
<i>B. anthracis</i>	
Δ Sterne	7702 pX01- pX02-
CLT292	Δ Sterne <i>BclA</i> Δ 63:1130 KanR pX01- pX02- (C. L. Turnbough)
MUS1691	Δ Sterne <i>BclB</i> ::Kan pX01- pX02-
MUS1758	Δ Sterne <i>BclA</i> ::Kan pX01- pX02-
MUS1759	Δ Sterne <i>BclA</i> ::SpcR pX01- pX02-
<i>B. subtilis</i>	
MO1099	<i>amyE</i> ::erm
<i>B. cereus</i>	
6S1	from Bacillus Genetic Strain Collection
14579	ATCC strain 14579
<i>B. thuringiensis</i>	
kurstaki	Cry-
israelensis	plasmidless

Table 3: Antibiotic Concentrations

	<u>Chloramphenicol</u>	<u>Kanamycin</u>	<u>Erythromycin</u>	<u>Neomycin</u>	<u>Ampicillin</u>
<i>E. coli</i>	10 µg/ml	25 µg/ml	250 µg/ml	N/A	100 µg/ml
<i>B. anthracis</i>					
<i>B. cereus</i>	10 µg/ml	50 µg/ml	5 µg/ml	25 µg/ml	N/A
<i>B. thuringiensis</i>					
<i>B. subtilis</i>					

Table 4: Plasmids used in this study

<u>Plasmids</u>	<u>Description</u>	<u>Markers</u>
pBT1742	pMK4 with Full BclA ORF EGFP	AmpR, CmR
pBT1744	pMK4 with BclA NTD EGFP	AmpR, CmR
pBT1750	pMK4 with BclA NTD -19 aas EGFP	AmpR, CmR
pBT1693	pMK4 with BclA NTD GFPuv	AmpR, CmR
pBT1694	pMK4 with BclA NTD DsRed	AmpR, CmR
pBT1701	pMK4 with BclA NTD no motif DsRed	AmpR, CmR
pBT1720	pMK4 with BclA NTD motif only DsRed	AmpR, CmR
pBT1729	pMK4 with <i>bclA</i> promoter only DsRed	AmpR, CmR
pBT1747	pMK4 with BclB NTD DsRed	AmpR, CmR
pBT1746	pMK4 with <i>bclA</i> promoter BclB NTD DsRed	AmpR, CmR
pBT1758	pMK4 with <i>bclA</i> promoter mCherry BclA NTD EGFP	AmpR, CmR
pBT3919	pMK4 with BclB NTD plus IHIP EGFP	AmpR, CmR
pBT3861	pMK4 with <i>bclB</i> promoter only GFPuv	AmpR, CmR
pBT3864	pMK4 with BclB NTD GFPuv	AmpR, CmR
pBT3862	pMK4 with BclB NTD motif only GFPuv	AmpR, CmR
pBT3859	pMK4 with BclB NTD no motif GFPuv	AmpR, CmR
pBT3952	pMK4 with BclB NTD EGFP	AmpR, CmR
pBT3955	pMK4 with Full BclB ORF mCherry	AmpR, CmR
pBT3927	pMK4 with <i>bclB</i> promoter BclA NTD DsRed	AmpR, CmR
pGS3630	pUCpE BclA::Kan KO shuttle vector	AmpR, EryR, KanR

DNA Manipulations

Plasmid DNA from *E. coli* was isolated by following the Wizard Plus SV Plasmid DNA purification system (Promega) protocol or by the procedure of Birnboim and Doly (149). Quantification of the purified plasmid DNA was spectrophotometrically determined using the Nano-Drop ND-1000 spectrophotometer. Restriction endonuclease digestions were performed under the conditions set forth by the manufacturers. A characteristic digestion would be 10 μ l of plasmid DNA at a concentration of 150 ng/ μ l; combined with 17 μ l ddH₂O, 3 μ l of the corresponding restriction digestion buffer, and 1 μ l of the restriction enzyme.

Clean up of plasmid and chromosomal DNA, ligation reactions, and PCR products was accomplished by extraction with an equal volume of TE-saturated phenol (pH 8.0) followed by extraction with an equal volume of chloroform. One final centrifugation (30s, 10,000 g) was performed to fully remove any residual phenol/chloroform from the samples. A 0.1 volume of 3M Na acetate (pH 5.0) was added to the DNA, followed by 2.5 volumes of 95% chilled ethanol. The mixture was incubated on ice for 10 minutes, followed by a final spin of 10 minutes in a Marathon 16Km microcentrifuge (Fisher Scientific). The ethanol supernatant was decanted, and the remaining DNA pellet was placed in a Centrivap Concentrator (Labconco) for 20 minutes to remove any residual ethanol from the samples. The dried DNA pellet was resuspended in 20 μ l of ddH₂O. If

the product was to be ligated post-precipitation, the two digested products would be mixed at the appropriate ratio prior to precipitation with ethanol.

Screening of isolated plasmid DNA or digested restriction products was accomplished by electrophoresis in a 1% (w/v) agarose gel containing ethidium bromide (EtBr, 0.5 µg/ml) in Tris-acetate electrophoresis buffer. The DNA was premixed with 3 µl DNA loading buffer (Promega) and loaded into individual wells of the gel.

Gel purification of DNA was accomplished using the procedure provided by the Quantum Prep Freeze N' Squeeze DNA gel purification kit (BioRad) or the Qiaquick Gel Extraction Kit (Qiagen). DNA ligations were performed at 16°C using T4 DNA ligase in a 20 µl volume. When the DNA recovery rates were especially low due to low-copy plasmids or loss of samples, DNA pellets after ethanol precipitation were resuspended in 9 µl of dH₂O and added to 1µl 10x T4 DNA ligase buffer and 0.5 µl T4 DNA ligase. Ligations were usually performed with a ratio of insert to vector of 3:1. Ligation was allowed to continue overnight (14-20 hours) at 16°C in a Microcooler II constant temperature chamber (Boekel Scientific).

Transformation of *E. coli*

Frozen competent cells were thawed on ice. 5-10 µl of ligated DNA or 1-2 µl of pure plasmid DNA was added to 50 µl of cells and allowed to sit on ice for 10 minutes. The cell-DNA mixture was heat-shocked by incubation of the mixture in a 37°C water bath for 5 minutes. Immediately after heat shocking, 250 µl of L broth was added to the mixture, and the cells were incubated for 60 min. at 37°C with shaking at 250 rpm. After

a hour of incubation the broth was plated in 100 µl aliquots on plates containing the appropriate antibiotic, or resuspended in 5 ml of L broth with antibiotics and incubated overnight at 37°C.

PCR

All primers were obtained from IDT technologies (Coralville, IA). Primers were resuspended in 1 ml ddH₂O. Aliquots of primers diluted to 25 ng/µl were prepared and stored frozen at -20°C. PCR reactions were performed using Ex-Taq polymerase as outlined by the manufacturer (Takara). A typical reaction would be: 10 µl 10X reaction buffer, 8 µl d[NTP]s, 3 µl primer 1 (25 ng/µl), 3 µl primer 2 (25 ng/µl), template DNA (2 µl of chromosomal miniprep DNA, 0.2 µl if plasmid DNA), 0.5 µl Ex-Taq enzyme, 73.5 µl ddH₂O for a total of 100 µl per reaction. Reactions were allowed to continue for 35 cycles, at T_Ms appropriate for the primers used. Extension times were set conservatively, corresponding to approximately 1 minute per Kb of expected PCR product size.

Table 5: Primers used in this study

<u>Number</u>	<u>Name</u>	<u>Sequence</u>
36.00	qBclA5pB	cgggatccatgtcaataataattatt.....
37.00	qBclA3pS	agcgtcgacttaagcaacttttcaat.....
64.00	GFPuv 5p BclB Soe	ttcccgggtcttcccccaatgagtaaaaggagaagaacttttc
65.00	GFPuv 5p BclA Soe	ccaccgataccaccaatgagtaaaaggagaagaacttttcac
66.00	RFP 5p BclA Soe	ttaccaccgataccaccaatgaccatgattacgccaagcttg
67.00	RFP 5p BclB Soe	accttcccgggtcttcccccaatgaccatgattacgccaagcttg
80.00	5p GFP/Ch SOE BclB Ex	gttcttcccccaattcatattccaatggtagcaaggcgagg
85.00	3p BclA Pro Soe BclA Motif	tggtatcgggtggaatgtaggtcctacaagcataaattcacctcataaagcg
88.00	3p BclB pro Soe GFP	agtgaaggttcttctcttactcaatfaaatccccctcattccac
92.00	5p DsRed Soe BclA Motif	atgcttgtaggacctacattaccaccgataccaatgaccatgattacgccaagcttgc
95.00	3p BclA No Motif Soe DsRed	gctgataaagattcatcggggttaattcatttgaataattattttgacataaattcacctcataaagcg
96.00	5p GFP Soe BclB Motif	aataatggacctacttcccgggttcttcccccaatgagtaaaaggagaagaacttttc
98.00	3p BclB No Motif Soe GFP	gaaaagtgtgtgtgttactcatttctggcctattatgctttatccaacc
99.00	3p BclB Motif Soe GFP	tgggggaagaaccggggaaggtaggtccaattcaatfaaatccccctcattccac
100.00	BclA 3p GFPuv Soe	ttctctttactcattgggtatcgggtggaatgtaggtcc
101.00	BclA 3p RFP Soe	tggcgtaatcatgggtcattgggtggtatcgggtggaatgtaggtcc
103.00	GFPuv 3p Xh	ctcgagttattttagagctcatccatgcc
104.00	RFP 3p Xh	ctcgagtaaaaggaacagatgggtggcgtccctcg
106.00	BclA 5p Promoter Xh	ctcgagtaatcacctcttccaatc
107.00	BclB 3p GFPuv Soe	ttcttctcttactcattgggggaagaaccgggaaggtagg
109.00	BclB 3p ProtA Soe	aatgtttttttttcaatgggggaagaaccgggaagg
110.00	BclB promoter Xh	ctcgagattagaacgtaaccaatttag
129.00	5pbcla xh	aactcgagctgaaggcaatgtatc
130.00	3pbcla xh	aactcgagcaattctctctctag
142.00	5p BclB-DsRed SOE BclA Pro	acgttttatggagggtgaatttatgaacagaatgacaaattatgg
143.00	3p BclA Pro SOE BclB-DsRed	ccataatttgcattctgtttcataaattcacctcataaagcgt
144.00	5p BclA-DsRed SOE BclB Pro	atgtggaatgaggggatttaaatgtcaataataattatc
145.00	3p BclB Pro SOE BclA-DsRed	gaataattattatttgcatttaaatccccctcattccacat
157.00	3p GFP/Ch Xh	gcctcgagttactgtacagctcgtccatgc
158.00	5p GFP/Ch SOE A Full	ccattattattgaaaaagttgctatggtagcaaggcgagg
159.00	3p Full A SOE GFP/Ch	cctcgcccttgctcaccatagcaactttttcaataaatgg
160.00	5p GFP/Ch SOE B Full	gtaagcgagggtcttaatacgtcatggtagcaaggcgagg
161.00	3p B Full SOE GFP/Ch	cctcgcccttgctcaccatgacgatattaagacctgcgttac
177.00	5p GFP/Ch SOE BclA	ttaccaccgataccaccaatggtagcaaggcgagg
178.00	3p BclA SOE GFP/Ch	cctcgcccttgctcaccatgggtggtatcgggtgtaa
179.00	5p GFP/Ch SOE BclB	accttcccgggttcttcccccaatggtagcaaggcgagg
180.00	3p BclB SOE GFP/Ch	cctcgcccttgctcaccatgggggaagaaccgggaagg

PCR products were cloned into either the Invitrogen pCR Topo 2.1 TA or the Stratagene pSC α -1 cloning vectors in accordance with the supplier's protocol. DNA inserts were sequenced using the M13 upstream and downstream primers on an Applied Biosystems 3730 DNA Analyzer using Applied Biosystems Prism BigDye Terminator cycle sequencing chemistry, and the sequences compared to the TIGR-sequenced genome of the *Bacillus anthracis* Sterne strain.

Electroporation conditions

An overnight culture of *Bacillus anthracis* was grown in BHI broth with 0.5% (w/v) glycerol with appropriate antibiotics. 0.5 ml of this overnight culture was used to inoculate 100 ml of BHI + 0.5% (w/v) glycerol in a 500 ml Erlenmeyer flask. The culture was allowed to incubate at 37°C with shaking until the OD₆₀₀ reached 0.6. The culture was then passed through a disposable Analytical Test Filter Funnel apparatus with a pore size of 0.45 μ m (Nalgene). The cells were then washed with 25 ml of ice cold Electroporation buffer (199), and this step was repeated three times. After the third wash, the filtered cells were recovered in 5 ml of ice cold Electroporation buffer and placed on ice.

1 mm gap electroporation cuvettes were loaded with 100 μ l of cells and 1 μ g of high quality plasmid DNA obtained from a *dam*⁻ host. After loading, the cuvettes were pulsed at 25 μ Fd, 100 Ohms, at 2.5 kV. Immediately after pulsing, the cell/DNA mixture was resuspended in 1 ml of BGGM (199). After incubation at 37°C for 1 hour,

aliquots were plated onto BHIA plates with the appropriate antibiotics and allowed to incubate overnight at 37°C.

Isolation of Chromosomal DNA

B. anthracis strains were cultured in 10 ml TSB with appropriate antibiotic selection at 37°C. The cells were harvested by centrifugation, washed with 10 ml TE buffer (0.01 mM Tris-HCl, 0.001 mM EDTA, pH 8.0), and the cell pellets frozen at -25°C for several hours to overnight and then thawed, resuspended with 0.1 ml TE, and incubated at 37°C for 30 minutes to induce autolysis. The cell lysate was treated with RNaseA (25 µg) and N-lauryl sarcosine (0.8% w/v). Proteinase K (25 µg) was then added and the sample incubated at 60°C for 1 hr. The sample was then cooled on ice and sequentially extracted with TE-saturated phenol and chloroform. The DNA was either dialyzed against distilled water at 4°C overnight or precipitated with ethanol as described above, and then resuspended in sterile distilled water.

Preparation of Competent *E. coli*

Cells from an *E. coli* competent cell stock were streaked onto a prewarmed L agar plate and incubated overnight at 37°C. One colony was picked and inoculated into 5 ml L broth in a 15 ml polypropylene conical centrifuge tube (Fisher Scientific) and incubated overnight with shaking at 37°C. 1L of prewarmed L broth (with appropriate antibiotics) was inoculated with 1 ml of the overnight culture and incubated at 37°C with

shaking. Growth was allowed to continue until absorbance at 600 nm reached 0.2 for *recA*⁺ strains or 0.6 for *recA*-negative strains. The culture was then chilled on ice for 10 minutes. The culture was dispensed into 6-250 ml centrifuge bottles, and centrifuged at 3,000 g for 10 minutes. After discarding the supernatant the pellets were resuspended in 50 ml of 0.1 M CaCl₂ (4°C). The bottles were placed in an ice bath for 10 minutes, followed by another spin at 3,000 g for 10 minutes. The supernatant was again decanted and the pellets were resuspended in 10 ml of 0.1 M CaCl₂ and pooled. The pooled competent cells were kept on ice for 20 hours. After 20 hours, 2.5 ml of sterile glycerol were added, and the competent cells were aliquoted into sterile microcentrifuge tubes, quick-frozen on dry ice, and then stored at -80°C for future use.

Protein Production

The ORFs of selected genes were PCR amplified and cloned into the plasmid pQE30 (Qiagen), to allow for inducible expression in *E. coli* by the addition of IPTG. These plasmid constructs were transformed into either GM48 or Able K strains of *E. coli* bearing the pREP4 plasmid that encodes the LacI repressor, to minimize basal transcription of the cloned ORF. A 5 ml overnight culture of the plasmid-containing bacteria was inoculated into 1 liter of prewarmed LB broth containing antibiotics and incubated with shaking for several hours at 37°C. When the O.D.₆₀₀ reached 0.6, 2 ml of 0.5 M IPTG was added to the flask to induce expression of the His-tagged protein. After 1 hour of induction, the culture was centrifuged for 10 minutes at 5,000 rpm using

centrifuge bottles in a GSA rotor in a Sorvall RC5B Plus centrifuge. Cell pellets were frozen at -80°C until the protein purification procedure was carried out.

Purification of proteins was done using a His-Spin Protein Miniprep purification kit (Zymo Research). Each cell pellet was resuspended with 1 ml of Zymo His-Binding Buffer, for a total of 2-3 ml per culture. 1g of 0.1 mm glass beads (Biospec) was added into bead-beating tubes along with 1 ml of the resuspended cell pellet. The bead-beating tubes were bead-beat for 4-1 minute pulses, and centrifuged for 5 minutes in a microcentrifuge at 10,000 g to remove the beads and cell debris. The supernatant was removed and the His-tagged proteins purified over the His-purification columns as per the manufacturer's suggested protocol. The eluted fractions were pooled and then dialyzed twice against PBS or distilled water at 4°C overnight. Protein concentrations were determined using a Nano-Drop ND-1000 spectrophotometer and protein stored at -80°C until use. Purity of the protein was assessed by SDS-PAGE.

Production of Rabbit Polyclonal Antibodies

A vial of Ribi adjuvant plus MPL + TDM + CWS Emulsion (Corixa) was warmed up to 42°C for 10 minutes. 1 ml of sterile saline was added to the emulsion with a 21 gauge needle and vortexed vigorously for 3-4 minutes. 250 µg of purified protein was mixed with saline to a volume of 500 µl. This mixture was added to 500 µl of the adjuvant emulsion for a final volume of 1 ml. This immunogen sample was mixed vigorously by vortexing. Six subcutaneous injections were given and the rabbit was boosted after 3, 6 and 9 weeks. Prior to each boost, a bleed of 10 ml was performed. The

resulting serum was tested for reactivity to recombinant protein by Western Blot analysis. When the desired antibody titer was reached, the rabbit was sacrificed and a terminal bleed was obtained.

The collected blood was allowed to clot at 4°C for 1 hour. A swab was used to remove adherent material from the top of the tube. Tubes were centrifuged for 10 minutes at 5,000 rpm in a SM-24 rotor (Sorval). Clear sera were removed and aliquoted into labeled cryo-freeze tubes (Corning). These were then frozen and stored at -80°C until use.

Production of Spores

To obtain large quantities of spores, a 5-ml exponential phase culture was grown under antibiotic selection. Swabs of the culture were then inoculated evenly and heavily onto nutrient agar plates and incubated at 30°C for 5 days. Samples were taken and examined under phase contrast microscopy to assay the ratio of spores:vegetative cells. When greater than 95% of the samples were released spores, sterile swabs dipped in PBS were used to gently harvest the spores off the surface of the nutrient agar plates. The collected spores were pelleted in a microcentrifuge by centrifugation, and the supernatant discarded. The spore pellet was washed 3x in PBS to remove residual cell debris. Storage of the spores was accomplished at room temperature or at 4°C.

Transmission Electron Microscopy

To the buffer-washed spores, 1 ml of a 2% (w/v) glutaraldehyde, 0.1 M sodium cacodylate solution containing 0.1% (w/v) ruthenium red (Electron Microscopy Sciences, Fort Washington, PA) was added and incubated for 1 hour at 37°C. Each pellet was then washed in cacodylate buffer and fixed for 3 h at room temperature in a 1% (w/v) osmium tetroxide (Electron Microscopy Sciences), 0.1 M sodium cacodylate solution containing 0.1% (w/v) ruthenium red. A negative control was treated identically, but ruthenium red was omitted from these two steps. Spores were washed in buffer and embedded in 3% (w/v) agar (EM Science, Gibbstown, NJ). Dehydration involved sequential treatment with 25, 50, 75, 95, and 100% acetone. Polymerization was carried out at 60°C in Epon/araldite resin. Electron microscopy sections were cut at 85 nm thickness and put on 200 mesh carbon-coated copper grids and then stained with a 2% (w/v) uranyl acetate solution (Electron Microscopy Sciences) for 40 min at 37°C. The sections were then treated with Sato's Triple Lead for 3 minutes, washed in ultrapure water, and stained again for 18 minutes in 5% (w/v) uranyl acetate, followed by one final wash and were observed by transmission electron microscopy with a JEOL 1200EX electron microscope.

Immunogold labeling of embedded spores was performed after fixation of spores in a 2% glutaraldehyde (w/v) and 2% (w/v) formaldehyde PBS solution. After dehydration and embedding as listed above, the cut grid sections were blocked in a 1% (w/v) BSA solution for 30 minutes. The grids were thrice washed in PBS, and the primary antiserum was added to the grids at a concentration of 1:25 in Incubation buffer

(Aurion). Following an one hour incubation at room temperature, the grids were washed 6X in Incubation buffer, and were incubated with 1:25 goat anti-rabbit secondary conjugate with 15 nm colloidal gold (Aurion) and incubated for two hours (199). After a series of washes in PBS, the grids were post-fixed in 2% (w/v) gluteraldehyde on 0.1 M PBS for 5 minutes followed by washes in PBS and distilled water.

Epi-fluorescence Microscopy

5 mg of spores (wet wt.) were resuspended in blocking solution (StartingBlock, Pierce) and incubated at room temperature for 45 minutes with occasional mixing. The spores were then pelleted and resuspended in StartingBlock. Rabbit anti-BclA or anti-BclB polyclonal antiserum (1:250 dilution) was then added and incubated at room temperature for 45 minutes with occasional mixing. The spores were washed 3X in StartingBlock and then incubated with (amount) FITC-Protein A conjugate (Sigma Chemical Co.) and incubated for 45 minutes at room temperature with occasional mixing. The spores were subsequently washed 3X with StartingBlock, resuspended in PBS, and then examined by epi-fluorescence microscopy using a Nikon E600 microscope.

Spore Analysis by Flow Cytometry

10 mg of spores were resuspended in 500 µl of 4% (w/v) paraformaldehyde in PBS and incubated for 2 hours at room temperature. The spores were then washed 4X with PBS and then resuspended in StartingBlock and incubated with mixing at room temperature

for 45 minutes. The spores were then pelleted and resuspended in StartingBlock. Rabbit polyclonal antiserum (1:250 dilution) against BclA or BclB was then added and incubated with mixing at room temperature for 45 minutes. The spores were then washed 3X in StartingBlock PBS and then incubated with mixing with FITC-Protein A conjugate (Sigma Chemical Co.) and incubated for 45 minutes at room temperature. The spores were subsequently washed 3X with StartingBlock, followed by 2X with PBS and then processed on a FACScan flow cytometer using a 488 nm argon laser (Beckton Dickinson Biosciences). Data were analyzed using Cell Quest analysis software (Beckton Dickinson).

Results, Chapter 1

Discovery of novel collagen-like proteins

BclA and BclB are collagen-like proteins that have been shown to be glycosylated and are found in the exosporium layer of *B. anthracis* spores (19, 89, 199). Additional proteins are encoded in the *B. anthracis* genome with collagen-like triplet amino acid repeats. These determinants possess sequences resembling σ^K promoter elements and each is expressed during the sporulation phase of the *B. anthracis* life cycle (54, 110). The N-terminal portion of these proteins possess interesting sequence similarities (Fig. 6A). Given that the BclA protein associates with the exosporium via its N-terminus (75), we investigated whether this N-terminal conserved sequence (as marked in Fig. 6A) is responsible for targeting BclA and other collagen-like proteins to the exosporium.

A

MSNNYSNGLNPDESLSASAFDPNLVGPTLPPIPPFTLPTG	BclA
MSEKYIILHGTALEPNLIGPTLPPIPPFTFPNG	BAS3290
MVKVVEGGGKSKIKSPLNSNFKILSDLVGPTTFPPVPTGMTGIT	BAS4623
MKQNDKLWLDKGIIGPENIGPTTFVLPPIHPTG	BclB
LI/vGPTL/FPPIPP	Consensus

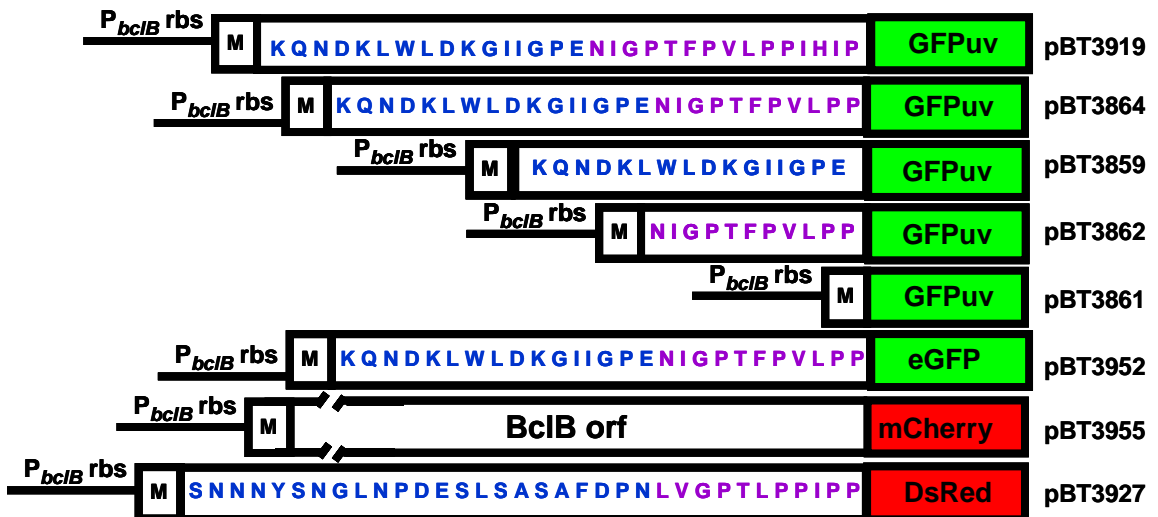
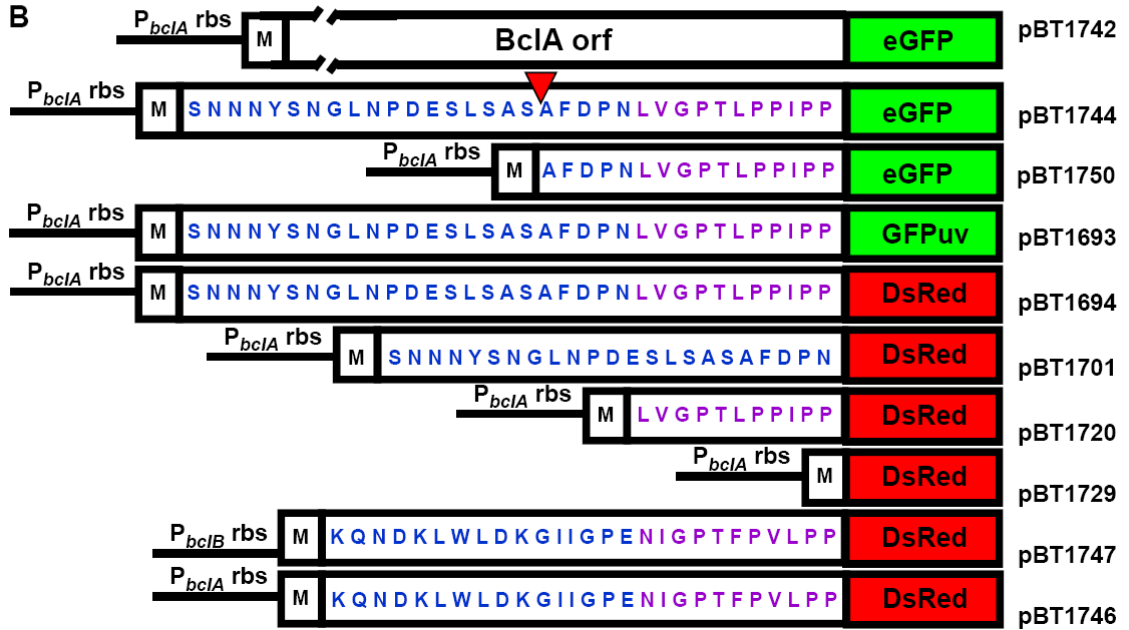


Fig. 6. A). N-terminal sequence alignments of four *B. anthracis* collagen-like proteins. Each protein sequence is displayed beginning with the N-terminal methionine residue. The conserved region is marked in red in each sequence. A consensus sequence is presented in blue below the alignments. Gene designations in Δ Sterne are indicated to the right of the sequences. **B).** Diagram of the constructs included in the thesis. Conserved regions are marked in purple. The red arrow corresponds to the site of a previously described cleavage event (15, 17). The names of the corresponding fusion-encoding plasmids are indicated to the right of the constructs.

To determine if the N-terminal domain of BclA is sufficient to target the native protein to the exosporium, two gene fusions were generated to the eGFP fluorescent reporter. PCR amplification of the upstream promoter/regulatory sequences of *bclA* through the conserved motif or the entire *bclA* coding sequence was performed. These PCR products were then spliced with the eGFP reporter gene to produce in-frame fusions (Fig. 6B). The DNA constructs were subcloned into the pMK4 shuttle plasmid (200) and introduced into the plasmid-free Δ Sterne strain of *B. anthracis* by electroporation. Transformants were grown in brain heart infusion broth and induced to sporulate by culturing on nutrient agar plates at 30°C for 3 days. Expression of the reporters was examined by epi-fluorescence microscopy. The transformed cells containing the *bclA* ORF fusion (pBT1742) or N-terminal domain fusion (pBT1744) did not express the eGFP reporters during exponential growth, consistent with the known expression pattern shown by gene array analysis (54). As the cells expressing the fusions transitioned into stationary phase with the concomitant physiological shift to the sporulation process, fluorescence appeared throughout the mother cell cytoplasm (Fig. 7A-B).

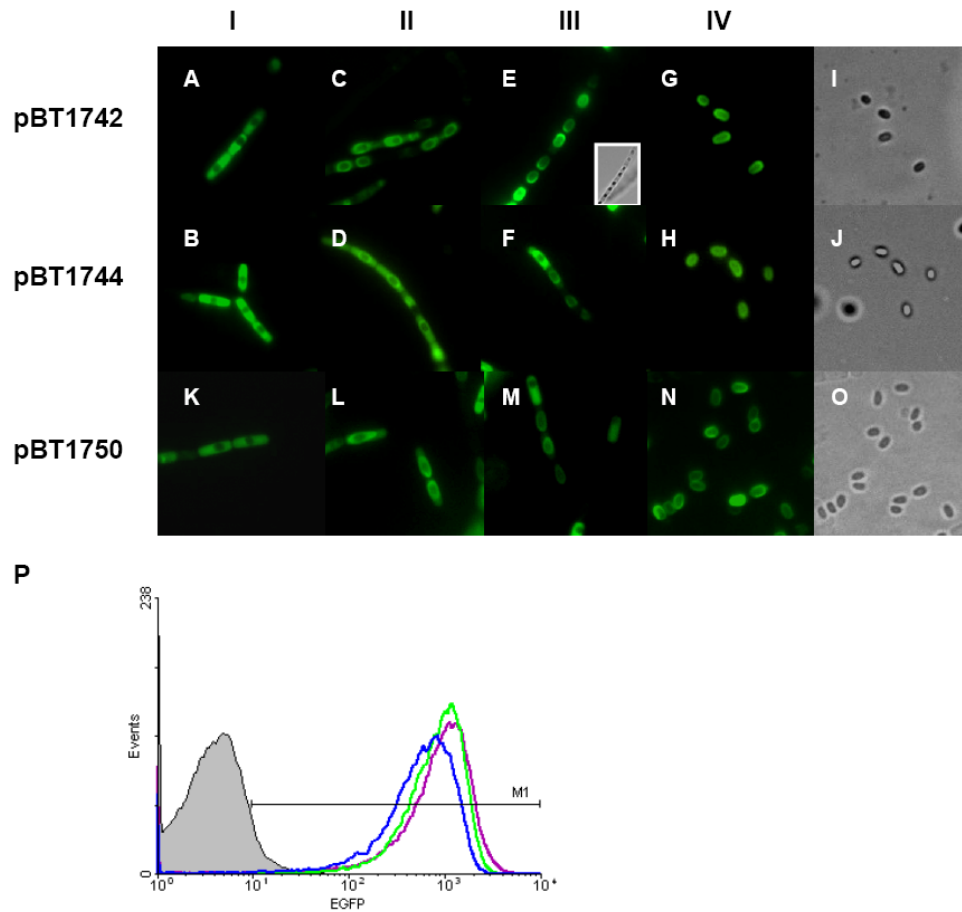


Fig. 7A-O). Micrographs of sporulating cells and spores from strains expressing the entire BclA ORF (pBT1742), the N-terminal domain (pBT1744), and the N-terminal truncation pBT1750 fusion constructs. Roman numerals at the top of the figure correspond to spore developmental stages of cells bearing the BclA N-terminal domain fusions: I, appearance of the fusion protein in the mother cell cytoplasm; II, concentration of the protein around the spore periphery; III, loss of fluorescence from the mother cell cytoplasm; and IV, released spores. Panels I, J, and O are brightfield images of the free spores whose fluorescence is shown in Panels G, H, and N, respectively. **P).** Histogram of the flow cytometry results for spores containing the pBT1744, pBT1742, and pBT1750 fusions. The gray area is the Δ Sterne (pMK4) control spores. The green and purple lines correspond to the pBT1744 and pBT1742 fusions, respectively. The blue line represents the pBT1750 fusion.

The developing spore surface does not appear to be initially enriched for these reporters during the early phases of spore development, with the emergent spore evident as a darkened area in the sporulating cell and with no enhanced fluorescence around the spore periphery. At a later time in the sporulation process, an enhanced fluorescence became evident at the spore periphery. This was accompanied by a corresponding decrease in cytoplasmic fluorescence, presumably marking the incorporation of the fusion constructs into the exosporium (Fig. 7C-D). Synthesis of the fusion protein thus appears to be temporally distinct from incorporation into the exosporium. Later, the cytoplasm of the mother cell lost fluorescence while the surface of the spore remained fluorescent (Fig. 7E-F and inset). This loss of cytoplasmic fluorescence presumably resulted from deposition of the protein on the spore surface, leakage of the protein from the cell, breakdown of the fusion protein, or a combination of these events. Examination of the spores at later times revealed the presence of released, highly fluorescent spores (Fig 7G-J).

Are the N-terminal 19 amino acids required for exosporium incorporation?

BclA released from spores lack the N-terminal 19 amino acids (15, 19). It is unknown whether the proteolytic event was part of the incorporation process or occurred when the BclA was released from the spores. To determine whether the N-terminal amino acids are required for efficient incorporation into the exosporium, a third fusion (pBT1750) was constructed, containing the *bclA* promoter, RBS, and initiation codon; followed by the the

coding sequence for amino acids 20-35 of BclA (Figure 6B). This construct mimics the spore-extracted form of BclA (differing only by the N-terminal methionine residue), and allows for examination of the role of the truncated N-terminus in incorporation of BclA (Figure 7K-O). The pBT1750-expressing cells mirrored the pBT1742 and pBT1744 fusions, suggesting that the initial 19 amino acids were not important for localization of BclA to the exosporium.

To quantify the reporter expression levels, a direct comparison of the fluorescence associated with each spore type was undertaken by flow cytometry. All three fusions, (spores containing pBT1744, pBT1742, and pBT1750) localized to the spore surface with similar kinetics (Fig. 7P). Greater than 97% of the spores for all three fusions were positive for fluorescence (Table 6).

Designation	% Positive Spores	PMF	PMF Fold Increase Over Background
ΔSterne pMK4	6.75	17.25	1.0
pBT1742	97.18	817.25	47.4
pBT1744	99.14	766.84	44.5
pBT1750	97.4	527.57	30.6
ΔSterne pMK4	3.9	5.5	1.0
pBT1694	96.6	94.6	17.2
pBT1729	3.8	5.7	1.0
pBT1701	73.2	15.2	2.8
pBT1720	11.4	6	1.1
pBT1747	4.2	5.9	1.1
pBT1746	72.5	16	2.9

Table 6) Quantification of flow cytometry results of fusions

The positive mean fluorescence (PMF) for the purified, paraformaldehyde-fixed spores was 767 for pBT1744, 817 for pBT1742, and 528 for pBT1750. These data suggest that the N-terminal domain of mature BclA is not only sufficient, but as efficient as the intact BclA protein in targeting the reporter protein to the spore surface. The loss of the N-

terminal 19 amino acids did not greatly affect the incorporation of BclA, with only a modest decrease in the amount of fluorescence seen in the pBT1750 containing spores.

Is proteolytic cleavage of the N-terminal 19 amino acids necessary for attachment of native BclA?

Although the initial 19 amino acids were not essential for efficient targeting and incorporation of the BclA protein into the exosporium, it was unknown whether the proteolytic event was necessary for incorporation of the NTD fusions, or occurred when the BclA fusion was released from the spores. To address this question, another fusion was constructed, with the *bclA* promoter followed by the mCherry reporter gene fused to the BclA NTD fused to GFPuv (Figure 8.)



Figure 8. Representation of construct pBT1758, with cleavage site indicated by the red arrow. The internal region is the NTD of BclA, with the conserved motif labeled in purple.

Separation of the two reporters would signify a cleavage event. As seen in Figure 9, the pBT1758 fusion is produced in the mother cell of sporulating cells, emitting an orange

appearance (Fig 9A.) The orange appearance rather than the typical yellow is due to the higher fluorescence of mCherry versus GFPuv (202).

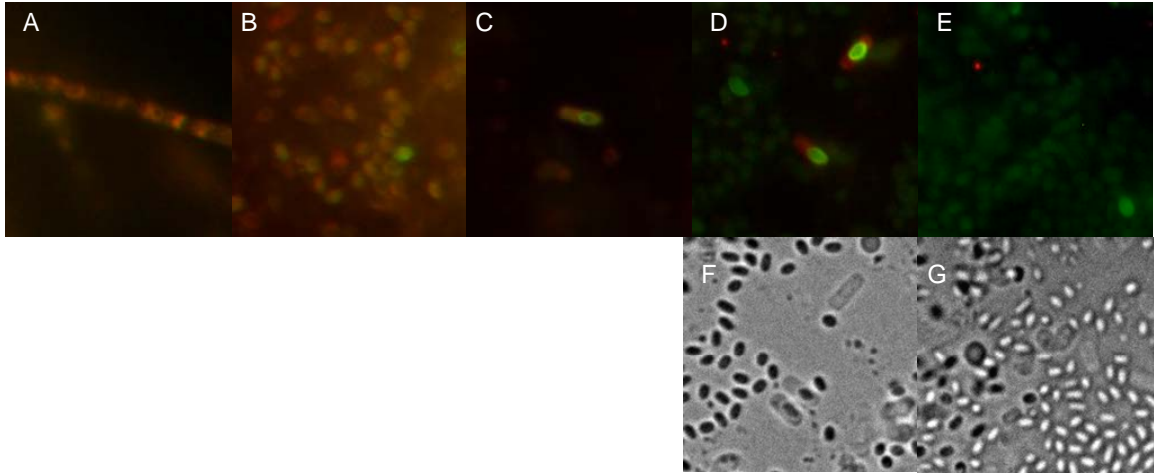


Figure 9. Production and Incorporation of the pBT1758 construct, in the progressive time points indicated in Figure 7.(A-E) **F, G)** Corresponding brightfield images of D, E respectively.

After the dual reporter fusion was made, it localized to the area adjacent to the newly emerging spore (Fig. 9B.) As the spore matured, the pBT1758 fusion began to be cleaved, releasing the mCherry reporter to the cytoplasm while the remaining BclA GFPuv reporter fusion is incorporated into the exosporium (Fig. 9C-D, F). Further processing lead to the localization of the GFP fusion to the spore, and the free mCherry remained in the mother cell (Fig. 9D). As the spores were near the point of release, the mCherry fusion fades away due to either protease digestion or release into the surrounding environment, and the resultant spore was green (Fig. 9D, E). The final product was a released GFPuv tagged spore (Fig. 9E, G). This demonstrates that the

cleavage event occurred at the developing spore, and not in the mother cell cytoplasm. Transport of the fusion to the spore occurred initially, followed by cleavage at the spore and subsequent attachment to the exosporium. Cleavage and incorporation are not necessarily dependent on one another, as the pBT1750 fusion with the initial 19 N-terminal amino acids removed is incorporated without the cleavage event.

Reporter oligomerization is not required for exosporium incorporation

The interwinding of the individual native BclA molecules to form a triple helix in wild-type spores is made possible by interactions among the C-terminal domains of the BclA monomers (75). The ability of pBT1744 and pBT1750 fusions, lacking both the C-terminal domain of BclA and the collagen-like region (CLR) with its associated glycosylation sites (23), to localize to the exosporium suggests that neither oligomerization of proteins nor glycosylation of the CLR are essential for incorporation of proteins into the exosporium of *B. anthracis*. Although not essential, oligomerization of proteins may be beneficial in localization to the exosporium. We constructed two additional constructs that contained the BclA protein sequence from pBT1744, but fused to the GFPuv reporter (pBT1693) or DsRed (pBT1694). The GFPuv reporter has a natural propensity to dimerize under physiological conditions, and the DsRed reporter protein obligately tetramerizes (201, 202). The pBT1693 and pBT1694 constructs displayed expression kinetics and fluorescent distribution profiles similar to the eGFP fusions. In all cases, fluorescence appeared initially after sporulation had commenced

followed by an increased concentration of the fluorescent reporter around the spore periphery (Fig. 10A-C, F-H).

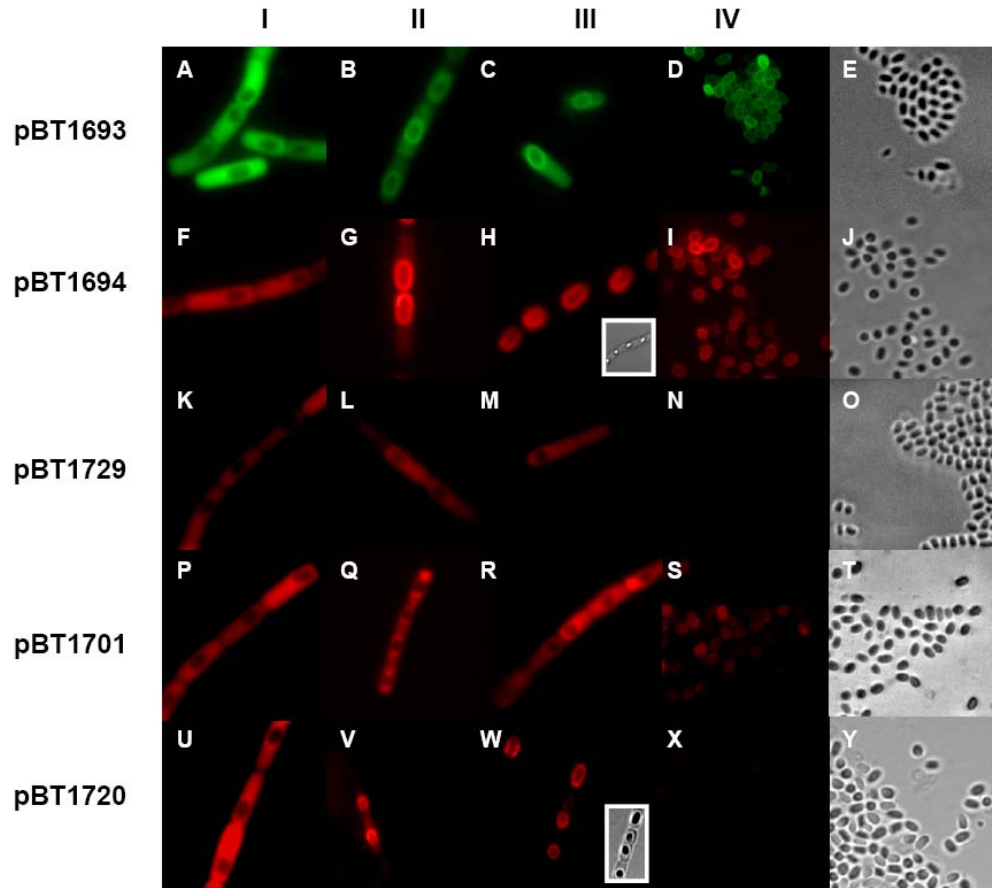


Fig. 10). Micrographs of sporulating cells and spores from strains expressing the BclA N-terminal domain-GFPuv (pBT1693), BclA N-terminal domain-DsRed (pBT1694), DsRed control (pBT1729), the deleted motif (pBT1701), and the conserved motif-only (pBT1720) fusion constructs. Stages indicated at the top of the figure correspond to those described in Fig. 7.

The pBT1694 construct had a complete loss of cytoplasmic fluorescence prior to spore release, as evident by the presence of the filament cell wall (Fig. 10H and inset). Spore

release was concurrent with the loss of cytoplasmic fluorescence in the pBT1693 construct (Fig. 10C). The complete loss of cytoplasmic fluorescence in the pBT1694 prior to the release of the spores may signify either the complete incorporation of the fusion constructs into the exosporium or a delay in the lysis of the mother cells. The DsRed self-association of this tetramerizing protein (202) may form a tight shell around the spores and mask structures on the maturing spores whose appearance trigger autolysis of the mother cells. After lysis of the mother cells, released spores retained surface-associated fluorescence (Fig. 10D, E, I and J).

To eliminate the possibility that the reporter proteins bind non-specifically to the exosporium, a control fusion was constructed. DsRed was expressed under the control of the *bclA* promoter and ribosome binding site but without any of the *bclA* N-terminal coding sequence (pBT1729). Although containing identical promoter and RBS elements as the aforementioned constructs, the pBT1729-containing cells exhibited diminished fluorescence in the cytoplasm, suggesting that the DsRed protein without the N-terminal BclA sequence had a substantially shorter half-life in the sporulating cells. However, the DsRed in the pBT1729-containing cells did not concentrate around the periphery of the spore (Fig. 10K-M) and the released spores were not fluorescent (Fig. 10N and O). Thus the labeling of the spores by the reporter fusions appeared not to be the result of non-specific binding of the reporter proteins to the spore surface.

The contributions of the conserved motif and N-terminal sequences to exosporium incorporation of the reporter proteins

To determine if the conserved motif sequence identified in Fig. 6A was required for attachment of the fusion proteins to the spore surface, fusion constructs were created that either contained the BclA N-terminal sequence lacking the conserved sequence (LVGPTLPPIP; pBT1701), or contained only the conserved motif fused to DsRed (pBT1720). The fusion protein without the conserved motif exhibited a reduced concentration around the spore periphery and cytoplasmic fluorescence was present up to the time of spore release. Only modest levels of fluorescence were detected on released spores (Fig. 10P-T). Thus loss of the conserved N-terminal BclA sequence resulted in a diminished exosporium incorporation of the fusion protein.

The fusion protein, consisting of the conserved motif fused to DsRed, but lacking the rest of the BclA N-terminal residues (pBT1720) concentrated around the spore periphery quickly after being expressed with a corresponding decrease in cytoplasmic fluorescence. However, released spores were devoid of fluorescence (Fig. 10U-Y). Thus the presence of only the conserved motif resulted in the fusion protein being targeted to the spore periphery, but was insufficient to allow attachment of the protein to the exosporium. The BclA N-terminal 24 amino acids missing in this fusion protein contain the site for the proteolytic cleavage event that may be involved in the attachment of BclA to the exosporium (15, 17). Optimal localization and attachment of fusion constructs to the exosporium necessitates the need for both the conserved motif as well as other sequence components contained in the N-terminus of BclA, at least amino acids 20-24.

To quantify the level of incorporation of each of the fusion constructs into the released spores, flow cytometry was performed on purified, paraformaldehyde-fixed spores (Fig. 11 and Table 6). The DsRed fluorescence of the spores bearing the intact BclA N-terminal 35 amino acid sequence (pBT1694) was 6.2-fold greater than all other DsRed-containing fusion constructs (Fig. 11).

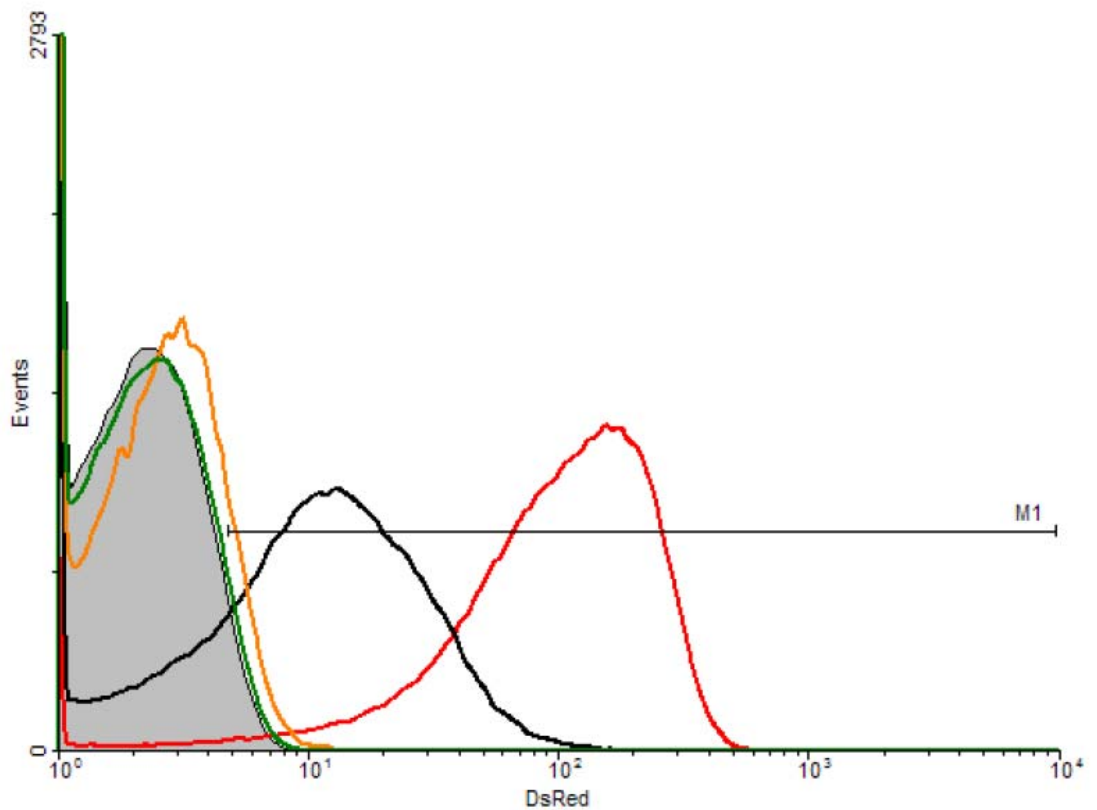


Fig. 11). Flow cytometry histograms of the fusion constructs. The gray area represents Δ Sterne (pMK4) negative control spores. The red and black lines represent spores containing the

pBT1694- and pBT1701-encoded fusions, respectively. The orange and dark green lines represent spores containing the pBT1720- and pBT1729-encoded fusions, respectively.

The fusion lacking the conserved motif (pBT1701) was detectably fluorescent, with greater than 73.2% of the spores positive over background and with a positive mean fluorescence (PMF) of 15.2, but these values were substantially lower than those obtained with pBT1694-bearing spores (96.6%, 94.6 PMF). The pBT1720 conserved motif-only fusion gave little detectable fluorescence above that of the negative control spores (11.4% to 3.9%, PMF 6). Spores from cells expressing DsRed without BclA N-terminal residues (pBT1729) were not detectably fluorescent over background (3.8% vs 3.9%).

Exosporium incorporation utilizing the BclB N-terminal domain
indicates a role for the timing of expression in the efficiency of
exosporium incorporation

After establishing that the BclA N-terminal domain was sufficient to localize proteins to the spore periphery, the ability of the corresponding BclB domain to target proteins to the exosporium was studied. The DsRed reporter was fused to the BclB N-terminus with the coding sequence up to and including the conserved region, with the natural *bclB* promoter and RBS (pBT1747). Previous reports have suggested that *bclB* and *bclA* are transcribed at an identical stage in sporulation, but with *bclB* transcribed at a ~2-fold lower level (54). However, the pBT1747-encoded fusion and corresponding constructs with or without the conserved motif appeared in the cytoplasm earlier in the sporulation process

than the BclA fusions and at a greatly reduced level, lower than the reported 2-fold difference in mRNA (54). Released spores contained barely detectable levels of the fusion protein (Fig. 12, 13G). Constructs are indicated in the Figure 12 legend.

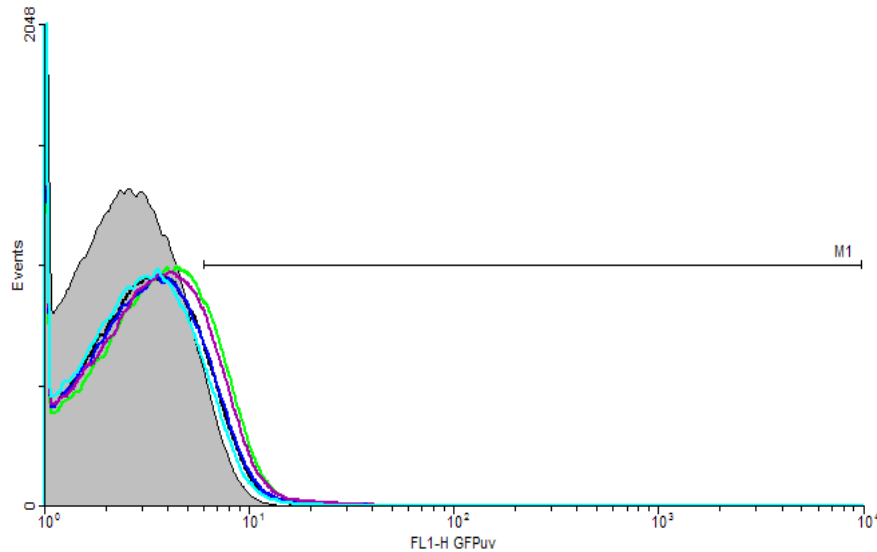


Figure 12.) Flow Cytometry histogram of BclB GFPuv fusions under control of the native *bclB* promoter. The grayed area corresponds to wildtype Δ Sterne spores (5.7% Fluorescent), the green line represents BclB NTD fused to GFPuv (19.2%), the purple line BclB NTD with 4 additional amino acids added (17.4%), the blue line is the BclB conserved motif only fused to GFPuv (13.9%), the teal line is BclB NTD with the conserved motif removed with GFPuv (11%).

Removal of the conserved motif or the conserved motif alone corresponded with a decrease in the overall fluorescence of the released spores containing the native *bclB* promoter. The early production of BclB and its decreased fluorescence over time, the

low basal expression level, and the weaker GFPuv reporter, all make it difficult to decipher the role of the conserved motif in these constructs.

To increase production of the fusion proteins, the BclB N-terminal sequence fused to DsRed was positioned under the control of the more active *bclA* promoter and RBS elements (pBT1746). The pBT1746 reporter was expressed at a level similar to that of the pBT1694 reporter construct and with *bclA* expression kinetics. The pBT1746 construct mimicked the pBT1694 construct, with fluorescent fusions produced and localizing around the spore periphery before release of the fluorescent spores (Fig. 13A-F).

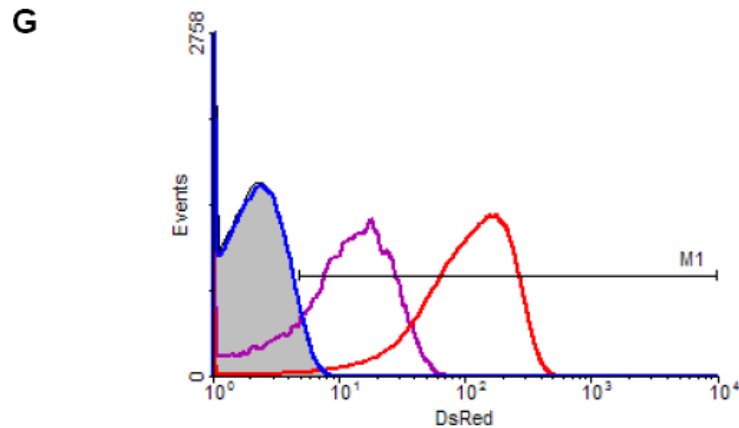
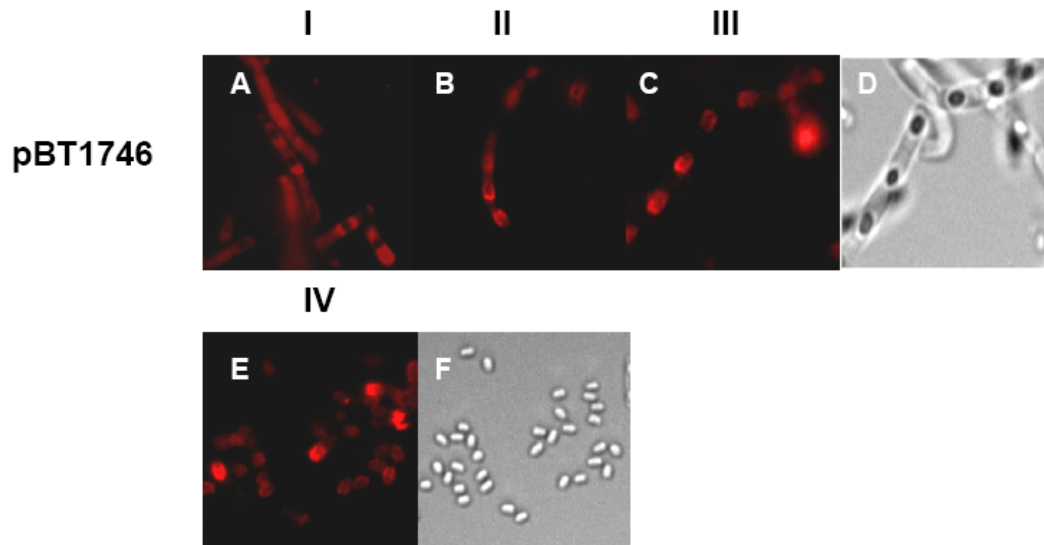


Fig. 13A-F). Micrographs of sporulating cells and spores from strains expressing the the pBT1746-encoded fusion (containing the *bclA* promoter and BclB N-terminal domain) at the developmental stages described in Fig. 3. Panels D and F are brightfield images of the spores or sporulating cells whose fluorescence is shown in Panels C and E, respectively. **G).** Flow cytometry histogram of spores containing constructs pBT1746 (purple), pBT1747 (*bclB* promoter and BclB N-terminal domain; blue), pBT1694 (BclA N-terminal domain-DsRed; red), and control pMK4 in Δ Sterne (gray area).

There appeared to be a difference in the localization pattern on the pBT1746, with the fluorescence spread across the spore in a slightly mottled fashion, not the more uniform distribution seen with the pBT1693 and pBT1694 fusions. Although incorporation was evident, the capacity of the BclB domain to target proteins to the spore surface was reduced when compared to that of the BclA N-terminal fusion (Fig. 13G). The pBT1746 spores were 72.5% positive compared to 96.6% for pBT1694, with a PMF of 16.1 compared to 94.6. This illustrates that the presence of the BclB N-terminus is sufficient to localize foreign proteins to the exosporium, but the degree of incorporation is dependent upon the proper timing of expression of the protein, sequence of the targeting domain, and, perhaps, the level of expression.

Localization of the BclB NTD under its native promoter

To image the localization of the BclB NTD domain under its native promoter, the pBT1747 construct was remade using the enhanced fluorescence of the EGFP reporter gene. Fluorescence appears throughout the mother cell early in the maturation of the spore, with localization of the BclB fusion to the emerging spore soon thereafter (Fig.

14). Fluorescence appears around the entire emerging spore, different than the characteristic ring that is seen with the BclA fusions that presumably correspond to the exosporium layer. Whether the BclB NTD EGFP fusion localizes to both the interspace/spore coat and exosporium layer is still unknown. The fluorescence intensity of the spores diminishes before release of the spore, suggesting coverage by the exosporium or release/digestion of some EGFP fusions (data not shown). Released spores are faintly fluorescent, due either to coverage of the fluorescent BclB fusion by exosporium/other proteins or a small amount of the BclB fusion being attached to the exosporium layer. It appears that timing of the production of the BclB fusions with the *bclA* promoter changes its localization pattern to the exosporium and a characteristic ring pattern of localization.

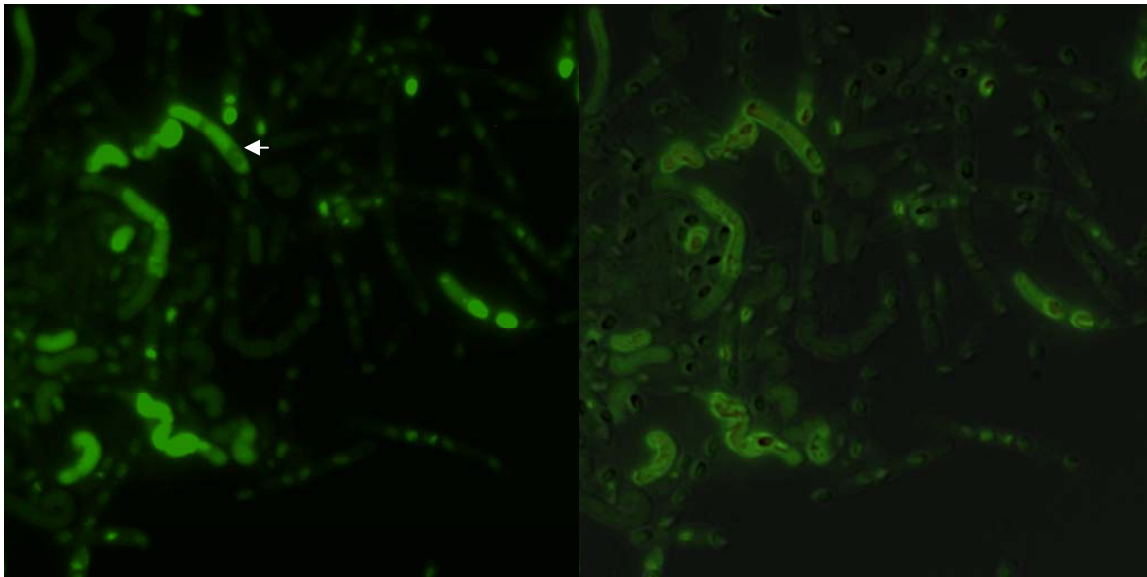


Fig. 14). Localization of the BclB NTD EGFP fusion. Left) Fluorescent micrographs of the sporulating cells. Right) Overlaid brightfield and fluorescent image on the left. The short arrow represents early mother cell production of the BclB fusion

Similar results are seen when the entire BclB ORF is fused to the mCherry reporter. The fusion appears early in the mother cell and quickly localizes to the spore, again without the characteristic ring pattern seen with BclA (Fig. 15). Free spores appear fluorescence as well, but still diminished when compared to the internal localization of the fusion constructs.

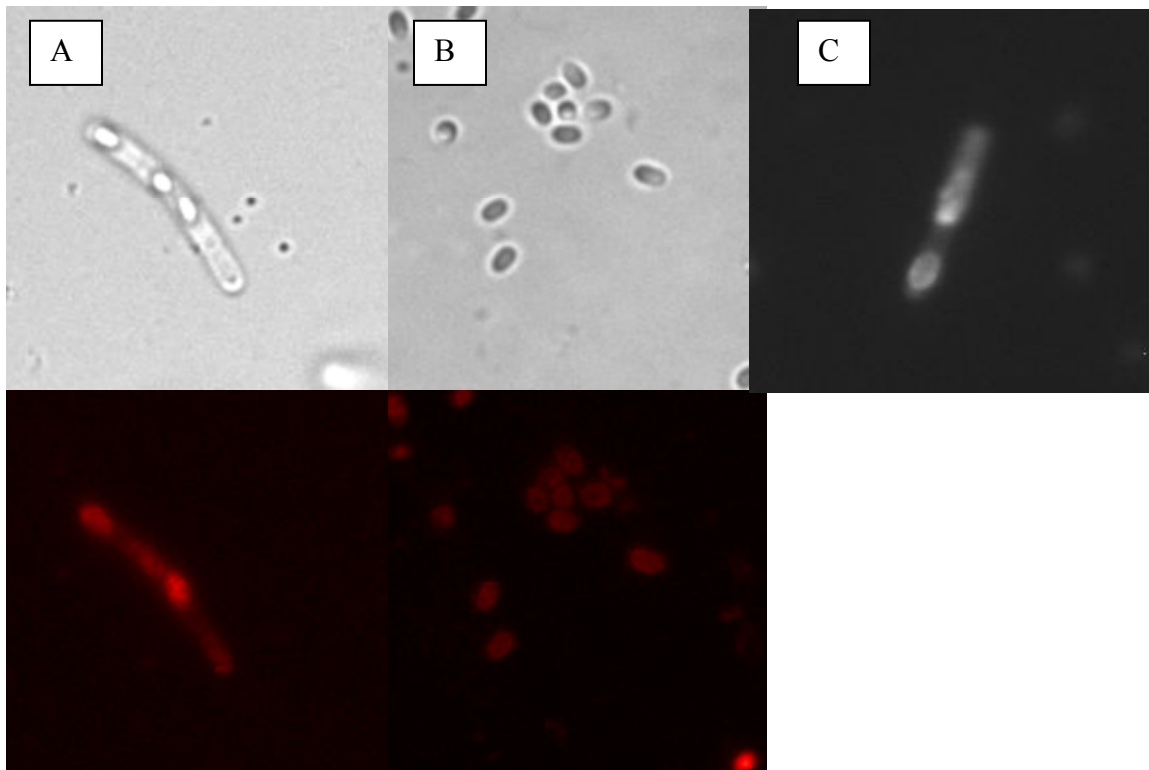


Fig. 15). The BclB ORF fused to mCherry. A) Localization of the fusion to the emerging spore as in Figure 14. B) Fluorescence of released spores. C) Enhanced image of localization of the BclB ORF fusion to emerging spores.

Are the different localization patterns between BclA and BclB due to timing of expression alone?

If BclB fusions localize to an internal site under its native promoter, and localizes to the exosporium under the control of the *bclA* promoter, can the localization of BclA fusions change to an internal site if expressed under the control of the early *bclB* promoter? Expression of the BclA NTD fusion under control of the *bclB* promoter leads to accumulation of the reporter fusion in the mother cell, but no early localization to the spore, and accumulation of the fusion in the polar regions of the cells (Fig. 16 and data not shown). Late in the maturation of the spore, the remaining BclA NTD DsRed fusion can be incorporated into the exosporium, resulting in light red spores, as can be seen by epifluorescence (Fig. 16) and flow cytometry (Fig. 17). The fluorescence of the free spores is similar to the BclB NTD DsRed fusion under control of the *bclA* promoter. Interestingly, there is a noticeable difference in the free spore fluorescence between the BclA NTD DsRed and the BclB NTD DsRed under control of the *bclB* promoter. This suggests either the BclB fusion is less stable than the BclA, or is not incorporated as efficiently, or is buried beneath outer layers of the spore.

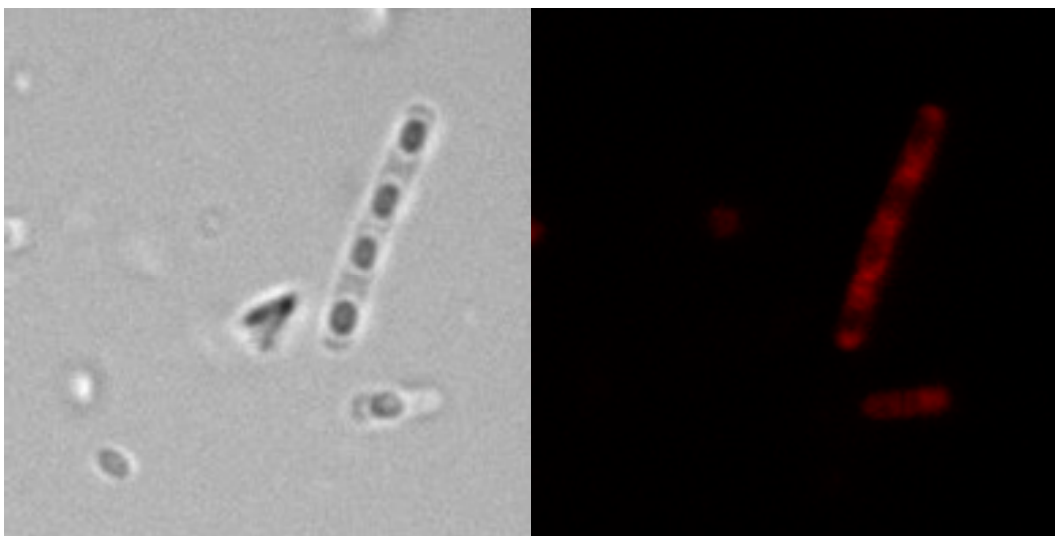


Fig. 16). Micrographs of the BclA NTD DsRed fusion under control of the *bclB* promoter. Short arrow demonstrates emerging spores within a mother cell, noting the lack of localization around the emerging spore. Longer arrows denote free fluorescent spores.

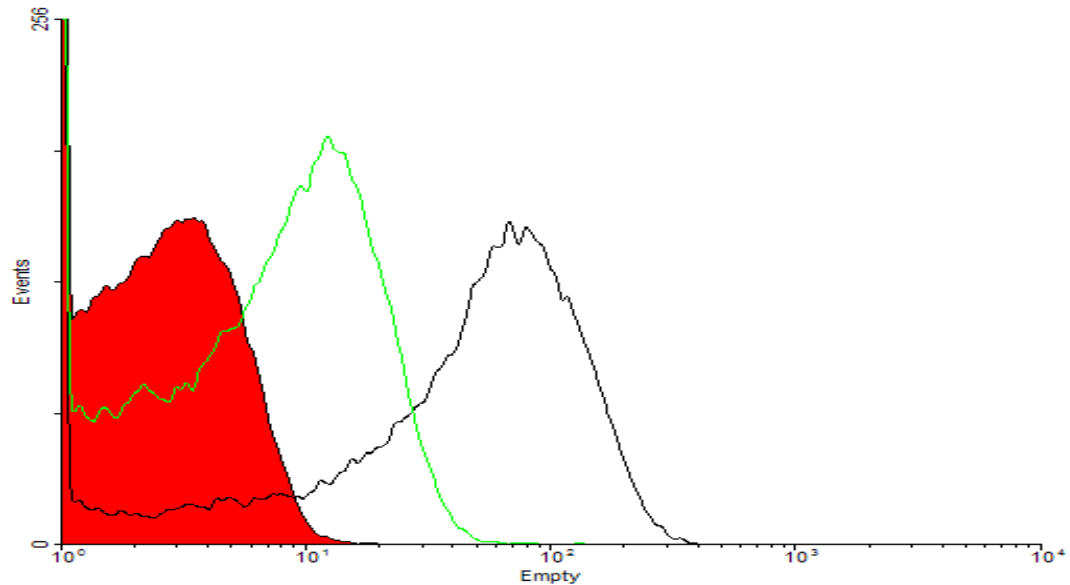


Fig. 17). Flow Cytometry histograms of fluorescence. Red area marks Δ Sterne wildtype spores. Green line represents the BclA NTD DsRed fusion under control of the *bclB* promoter. The black line represents the BclA NTD DsRed under its native promoter.

Native BclA is incorporated into spores expressing the reporter proteins

To determine if native BclA was still incorporated into the exosporium in cells expressing the Bcl-domain-containing fusions, fluorescent purified spores were incubated with rabbit anti-recombinant BclA polyclonal antibodies followed by FITC-Protein A conjugate (Fig. 18). Spores from each of the DsRed fusion constructs retained the ability to bind anti-BclA antibodies, indicating that native BclA was incorporated into the spores. Spores from the promoter-only constructs (pBT1720 and pBT1729) produced spores with wild-type levels of BclA, as expected (Fig. 18D, F). Spores with the fusion protein incorporated into the exosporium demonstrated a pronounced heterogeneity in the amount of fusion protein on the spore surfaces relative to the native BclA levels in individual spores in the population (Fig. 18A-F). This was especially noticeable in the pBT1746 fusion, suggesting that the incorporation of the fusion hinders binding or access of the anti-BclA polyclonal antibodies to the native BclA.

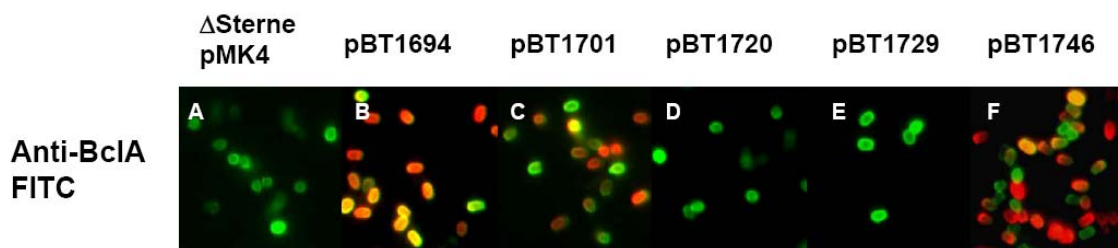


Fig. 18). Micrographs of spores obtained from cells containing DsRed fusion constructs after immunolabeling with polyclonal rabbit anti-rBclA antibodies and FITC-protein A. Native BclA stained areas appear green, fusion proteins appear red, and co-localization results in a yellow color. pBT1694, BclA N-terminal domain fused to DsRed; pBT1701, BclA N-terminal domain

deleted for the conserved domain sequence fused to DsRed; pBT1720, BclA conserved motif only fused to DsRed; pBT1729, DsRed lacking BclA residues; and pBT1746, DsRed bearing the BclB N-terminal domain expressed under the direction of the *bclA* promoter.

Are the BclA fusions targeted correctly to the exosporium?

To determine the exact localization of the BclA NTD fusions, released spores were immunolabeled with gold colloidal particles and imaged under TEM. Both the spores labeled with anti-GFP polyclonal rabbit antibodies and anti-rBclA rabbit polyclonal antibodies localize to the exosporium, both the nap and the basal layer (Fig. 19).

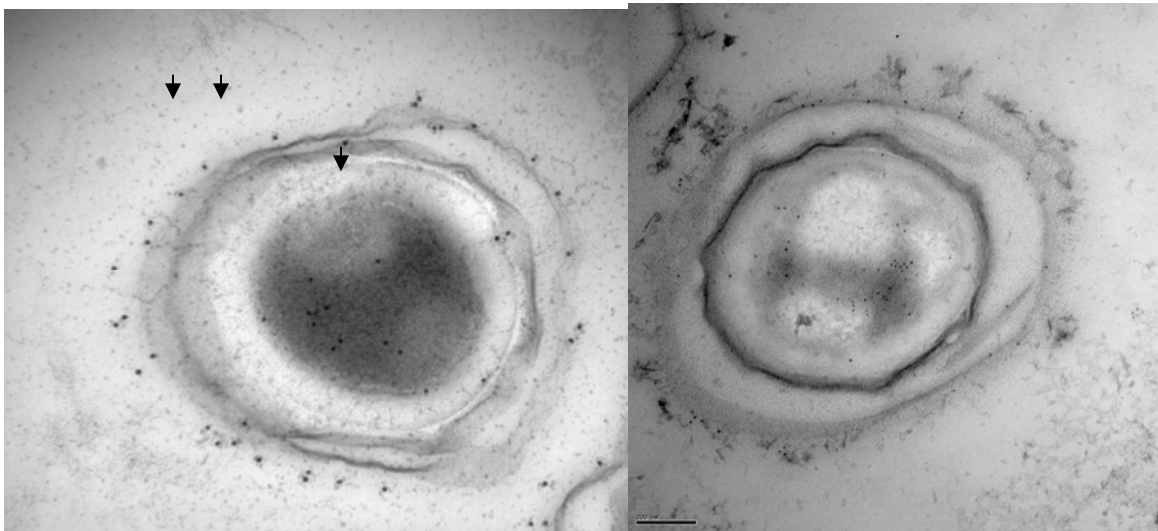


Fig. 19). TEM micrographs of spores expressing the BclA NTD EGFP construct. Left) Immunolabeled spore with anti-GFP antibodies. Right) Immunolabeled spore with anti-BclA antibodies.

Results, Chapter 2

The use of the fusion reporter system has been helpful in determination of the production, cleavage, localization, and attachment of both the BclA and BclB proteins. Use of this reporter system not only allows for characterization of the glycoproteins, but also allows for the characterization of late sporulation-associated mutants and can help in the characterization of the entire exosporium assembly process.

The CTL292 partial *bclA* mutant and $\Delta bclA$ strains

Strain CTL292 is a mutant of *bclA* constructed with bp 63-1130 of the *bclA* ORF deleted with a kanamycin cassette inserted downstream of the *bclA* stop codon. Chromosomal DNA was isolated from the *bclA* mutant strain CTL292 (a gift from Charles Turnbough, Jr., 75) and PCR amplification was carried out with the primer pair 129-130 to amplify a DNA fragment whose ends were external to the deletion, and the primer pair primers 36-37 to amplify internal to the *bclA* open reading frame. The internal deletion and the presence of the kanamycin cassette were verified by PCR and the shift of the amplicon size from 2.8 kb to 3.9 kb in length. The junction of the deletion was also verified by the presence of a 120 bp product versus the 1.1 kb wild-type *bclA* ORF length, demonstrating the deletion of the collagen-like region (CLR) of *bclA*.

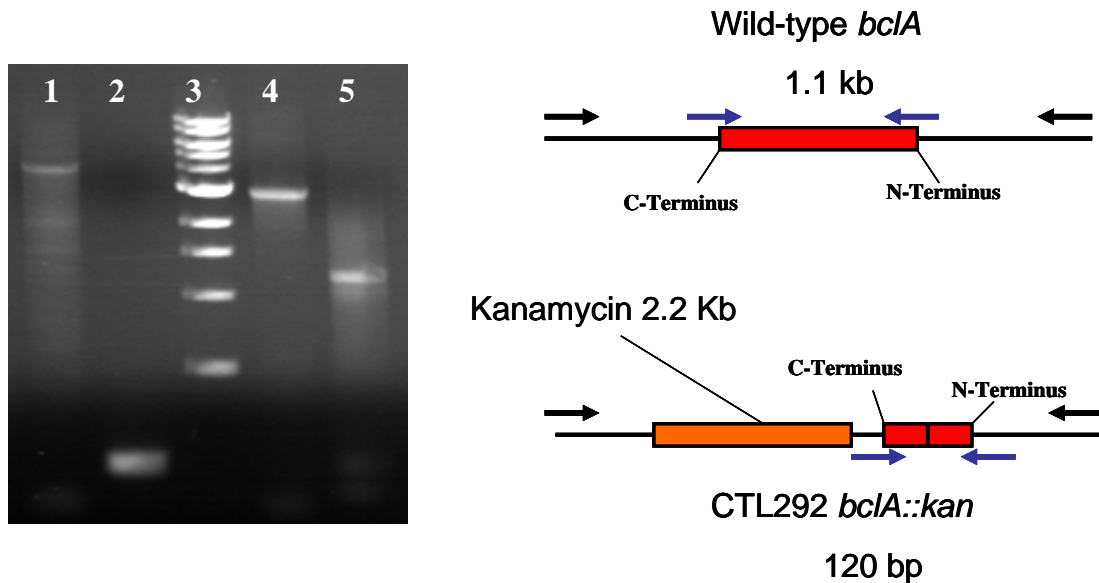


Figure 20 : PCR analysis of the *bclA* mutant CLT292. Left, PCR gel: Lane 1, CTL292 *bclA* flanking regions, Lane 2, CTL292 *bclA*, Lane 3, DNA ladder, Lane 4, ΔSterne *bclA* flanking regions, Lane 5, ΔSterne *bclA*. Right: Representative map of the *bclA* gene in CTL292. Blue arrows denote internal primer locations, Black, primers amplifying flanking regions

Interestingly, this construct still contains the BclA NTD including the cleavage site, but without the localization motif, followed by a truncated C-terminal globular domain. When the BclA NTD DsRed construct is introduced into the CTL292 strain, the initial stages of spore maturation appear normal (Fig. 21A, B). But as the incorporation of the BclA fusion construct begins, a distinct horseshoe pattern emerges in the incorporated fusions (Fig. 21C). When the spores are released from the mother cell, the fluorescence remains behind in strips, leaving free spores devoid of fluorescence (Fig. 21D). This pattern was also observed in the Full BclA ORF DsRed fusion in the CTL292 mutant. This construct can not restore the phenotype in the CTL292 mutant.

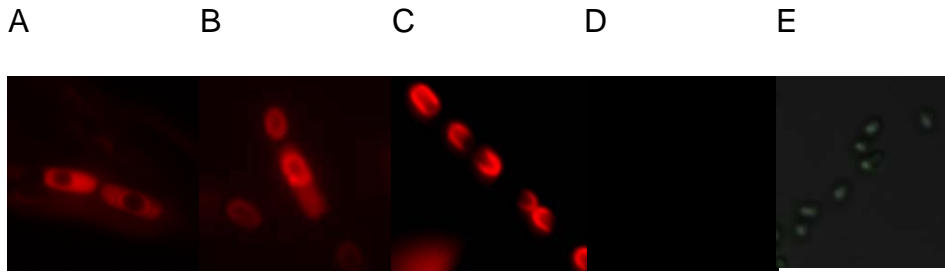


Figure 21) Micrographs of the BclA NTD DsRed fusion in the CTL292 *bclA* mutant.

Stages in A-D correspond to stages I-IV explained in the figure legend of Fig. 7.

This horseshoe pattern is not seen with the fusion of BclA without a conserved motif fused to DsRed (Fig. 22). Without wildtype BclA, the BclA NTD DsRed fusion needs the motif to localize normally.

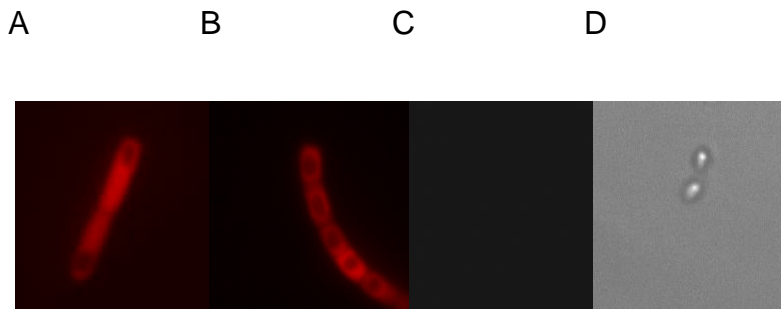


Fig. 22). Micrographs of the BclA NTD without the conserved motif fused to DsRed fusion in the CTL292 *bclA* mutant. Stages in A-C correspond to stages I, II, and IV explained in the figure legend of Fig. 7.

To analyze the role of the native BclA in the localization and incorporation of the reporter fusions, a precise deletion of the entire *bclA* ORF was made. The pUCpE BclA:Kan plasmid (pGS3630, Figure 23) was constructed with flanking 1 kb regions of

homology upstream and downstream of the BclA ORF. This was cloned into the shuttle vector pUCpE, with both Gram-positive and Gram-negative origins of replication.

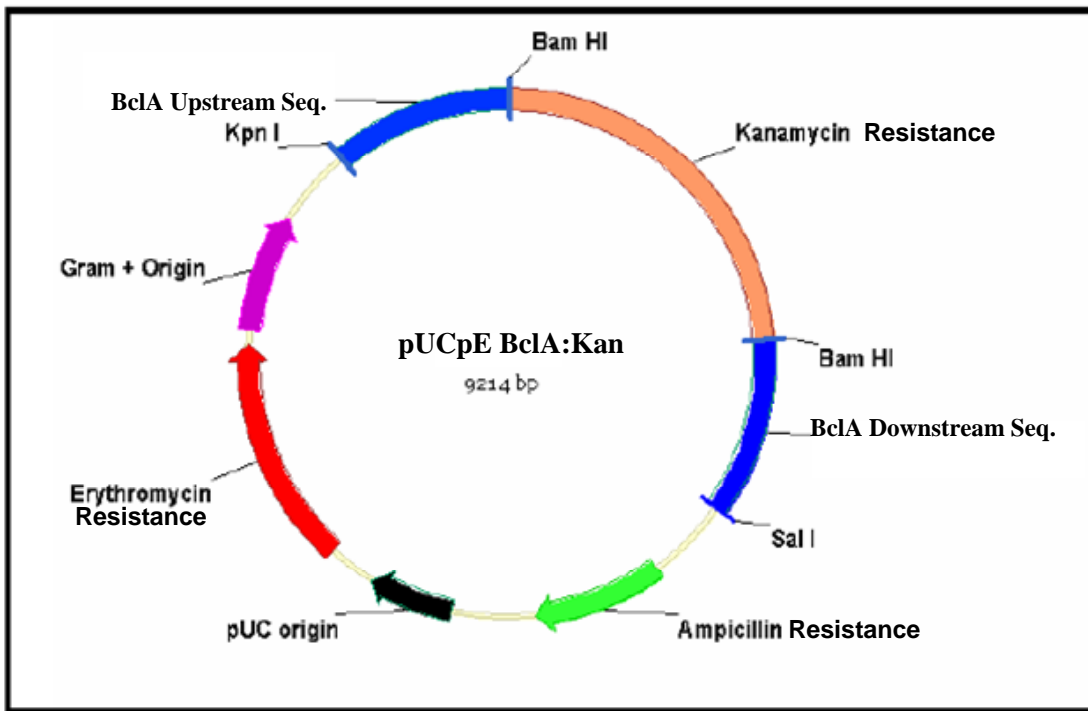


Fig. 23). pGS3630. the *bclA* knockout (KO) shuttle vector

This plasmid was electroporated into the Δ Sterne strain of *B. anthracis*, and passaged in the presence of kanamycin. After several passages, colonies were toothpicked onto Kan and Kan Ery plates. Loss of the EryR marker signifies double recombination, which was screened by PCR and by the loss of the plasmid. A representation of the KO is depicted in Figure 24. Correct clones were screened by PCR amplification using the same primers as in the CTL292 strain above.

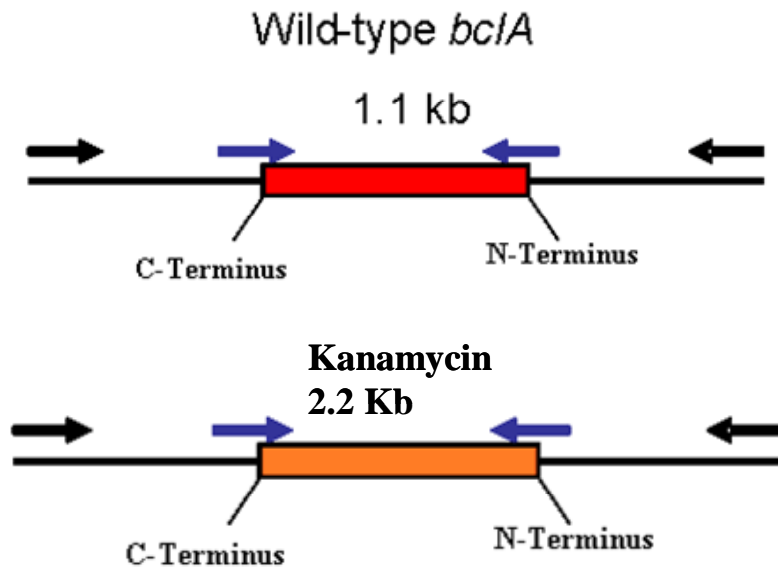


Fig. 24). Representation of the *bclA*::Kan construct. Blue arrows denote internal primer locations, Black, primers amplifying flanking regions

Deletion of the *bclA* determinant did not change the localization of the BclA NTD DsRed or the fusion containing the promoter of BclA with the BclB NTD DsRed when compared to the CTL292 strain (data not shown). Both of these data appear to support the notion that intact wild-type BclA is necessary for proper, stable incorporation of the fusions into the exosporium. It is unknown at this time whether the Full BclA ORF DsRed construct can complement the *bclA*::Kan strain. Failure to incorporate properly may be an artifact of the tetramerization of the BclA fusions, which in the absence of wild-type BclA to dilute the interactions, can not form a complete exosporium nap, and this incomplete exosporium nap is released into the mother cell upon spore release.

BclB mutant characterization

BclB wild-type protein is found in the exosporium, and likely internal to the nap as well (199). Figure 26 shows the surface localization of wild-type BclA and BclB in Δ Sterne. When the CTL292 partial BclA deletion or the complete *bclA::kan* strain is used, BclB localizes to one pole of the exosporium (199). The *bclB* mutant spores are also missing the exosporium at one pole, where it appears to have shed off a cap-like structure of exosporium. The *bclB* mutant also has a percent of spores without exosporium (199).

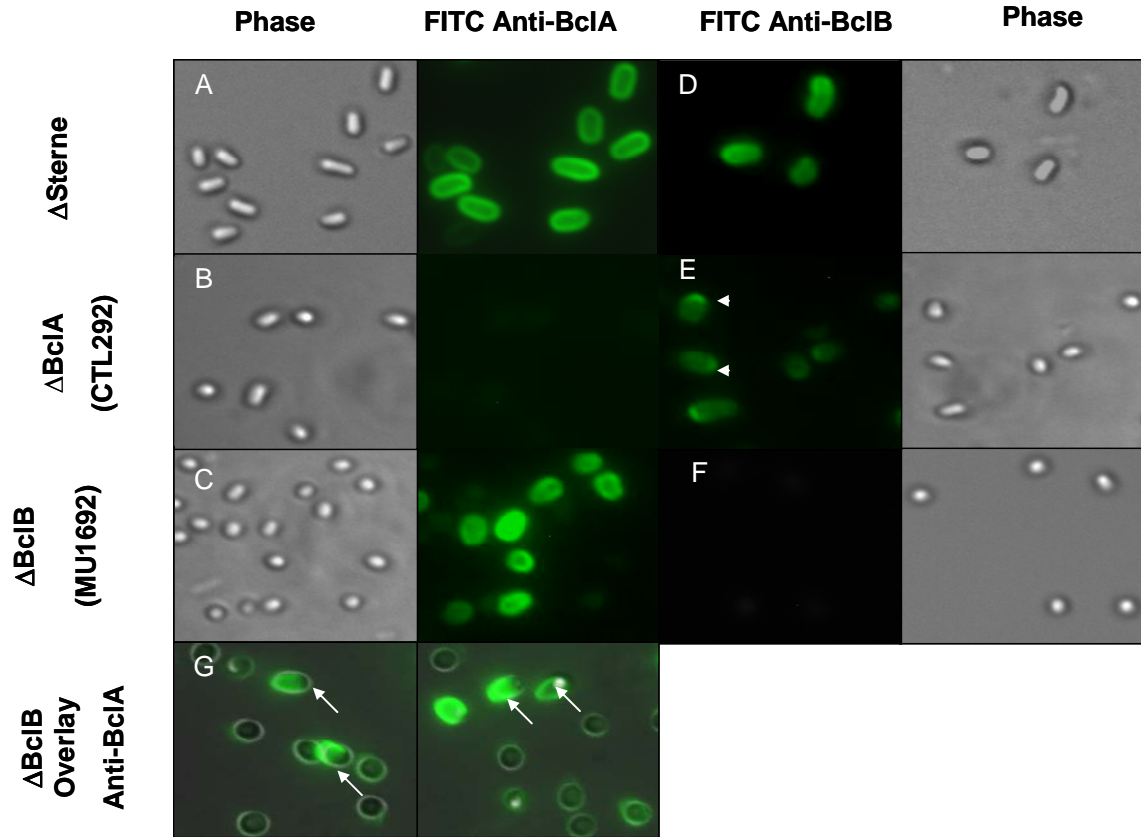


Fig. 25). BclB is surface exposed in *B. anthracis*. Purified spores were treated with anti-BclA antiserum (panels A-C, and G) or anti-BclB antiserum (panels D-F) followed by FITC-protein A. Phase contrast images are shown adjacent to the fluorescence images (panels A-F). Panel G contains two merged anti-BclA fluorescence and phase contrast images to more clearly show the loss of fluorescence at one pole of certain spores. Spores were from the Δ Sterne strain (panels A and D), the BclA mutant CTL292 (panels B and E) or the *bclB* mutant MUS1692 (panels C, F, and G). Image magnifications are 1000X. White arrowheads denote an increased concentration of the BclB protein at the pole of the spore. White arrows denote spores missing BclA at the cap or pole and sloughing of exosporium.

The BclB mutant phenotype can be observed by the use of the BclA NTD fluorescence constructs. The BclA NTD DsRed fusion in the *bclB*::Kan strain localizes to the exosporium, and the missing piece of exosporium at the pole of some spores can be seen (Fig. 26). When anti-spore antibodies are used to label the whole spore, it becomes clear that the BclA NTD DsRed fusion in the *bclB*::Kan spores accurately depicts the pattern of BclA incorporation into the mutated exosporium (Fig. 26.)

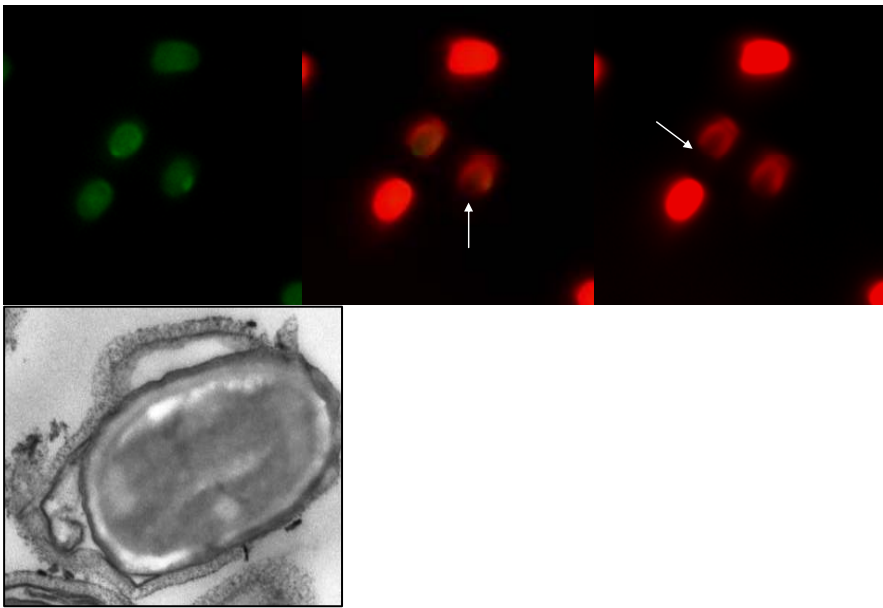


Fig. 26). Micrographs of the *bclB*::Kan strain expressing the BclA NTD DsRed fusion. Arrows denote missing exosporium in free spores. Far Left) *bclB*::Kan spores labeled with anti-spore antibodies, followed by FITC-ProteinA conjugate. Middle) Overlay of DsRed and FITC images, and DsRed images alone. Right) EM picture depicting the sloughing/missing exosporium on one pole, as seen in the epi-fluorescence pictures.

Localization of native BclB

When the BclA NTD DsRed fusion is counterstained using anti-BclB polyclonal rabbit antibodies followed by FITC-protein A, the BclA fusion and BclB are evenly distributed around the exterior of the exosporium (Fig. 27.) In the similar BclA NTD fusion that lacks the conserved motif region important in localization, the BclB distribution pattern changes dramatically. The native BclB localizes to the pole of the exosporium opposite of the poor incorporation of the fusion along the remaining 3/4s of the exosporium (Fig. 27).

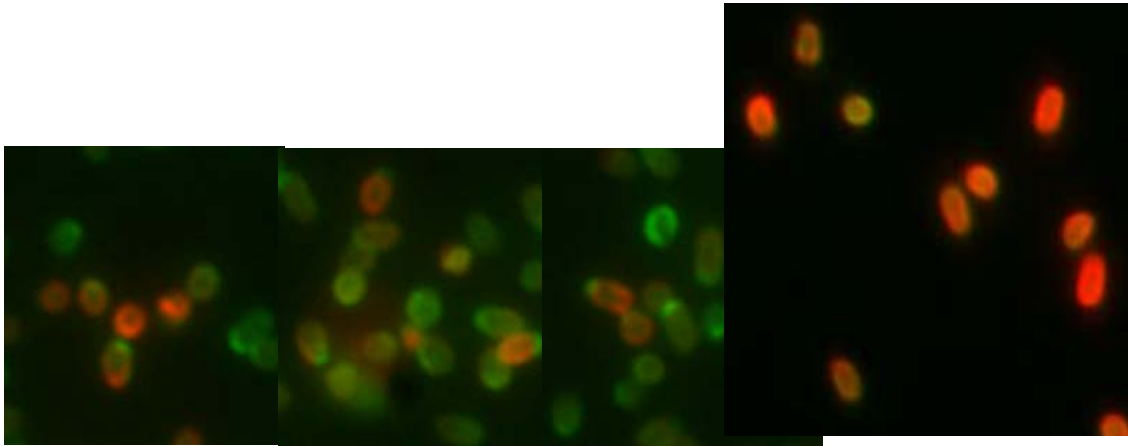


Fig. 27). Left) Micrographs of the BclA NTD without a motif after labeling using anti-rBclB rabbit polyclonal antibodies followed by FITC Protein A Conjugate. Note the polar localization. Right) The BclA NTD DsRed fusion with anti-BclB antibodies followed by FITC Protein A Conjugate.

This suggests the presence of the conserved motif in the incorporated fusions allows for the fusion to cover the entire exosporium, and the lack of the motif in the incorporated fusions allows for polar localization of wildtype BclB. As stated earlier in the Results

section, production of the BclB NTD DsRed construct under the control of the more active and later *bclA* promoter allows for incorporation into the exosporium instead of an intermediate stage of spore construction. The exosporium localization of the BclB NTD DsRed construct directly interferes with the ability of anti-BclA polyclonal rabbit antibodies to access BclA epitopes in the nap (Fig. 28, Top). Localization of the BclB NTD DsRed construct can be either polar like wildtype BclB in the CTL292 mutant, or cover $\frac{3}{4}$ of the spore as in the above experiments.

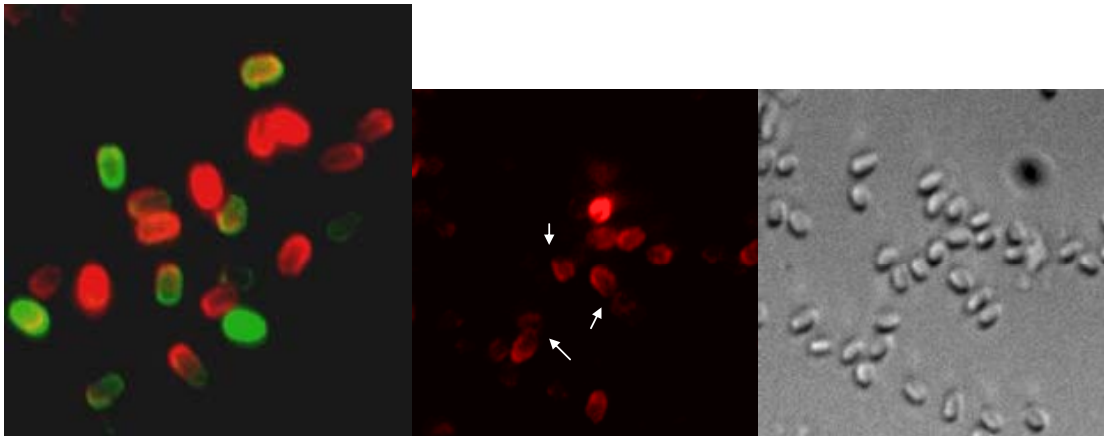


Fig. 28). Micrographs of the BclB NTD DsRed fusion under control of the *bclA* promoter. **Left)** Spores labeled with anti-rBclA polyclonal rabbit antibodies followed by FITC Protein A conjugate. **Right)** Fusion micrograph demonstrating the half moon pattern of BclB fusion distribution

cotE mutant analysis

The CotE protein is involved in late spore coat assembly and mutants lacking CotE do not have a proper outer spore coat or exosporium (87). The mutant spores create

a misattached exosporium in the mother cell. This can be seen by fluorescence using the BclA NTD EGFP fusion (Fig. 29). The curled up exosporium can be seen as glowing balls of fluorescence adjacent to the spores (darkened areas in the cells.) When the spores are released, they are riddled with tiny attached strips of exosporium. These can be imaged by EM microscopy, but also with fluorescence (Fig. 30). This same observation can be seen in CotE- spores with the BclA Full ORF Cherry fusion (data not shown).

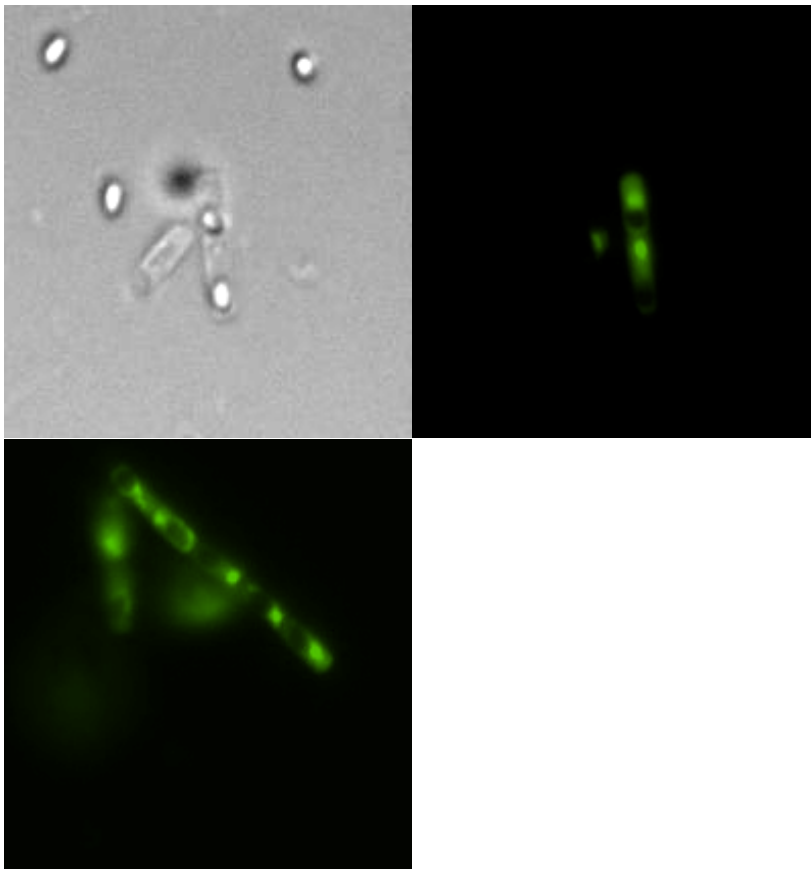


Fig. 29). Micrographs of *cotE::Kan* spores expressing the BclA NTD EGFP fusion. An arrow points to the darkened areas corresponding to a spore. Note the localization of the fusions adjacent to the emerging spore.

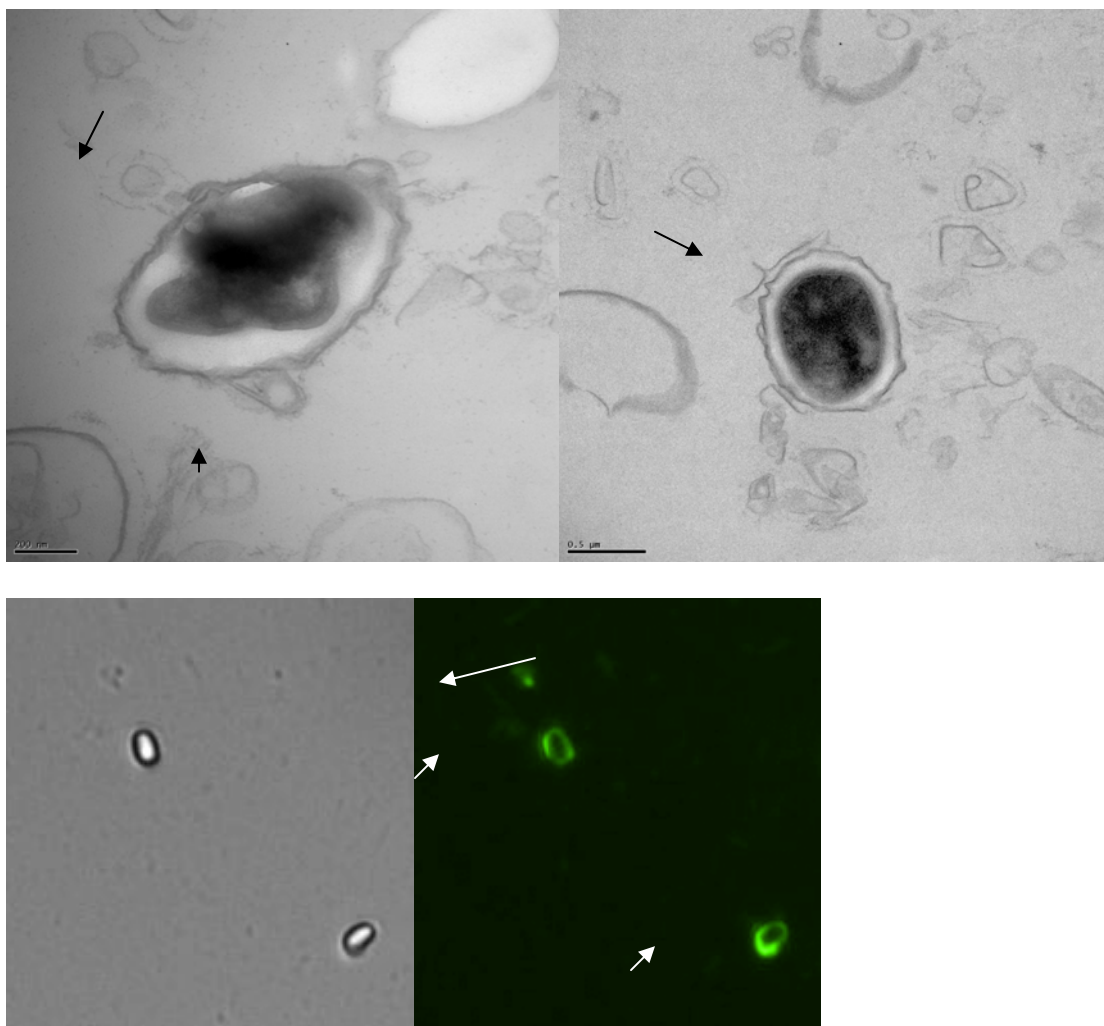


Fig. 30). **Top)** TEM micrographs of *cotE* mutant spores, with strips of exosporium denote with arrows. **Bottom)** Brightfield and epifluorescent images of *cotE* mutant spores expressing the BclA NTD EGFP fusion. Arrows denote strips of exosporium, long arrow denotes free floating strip of exosporium.

Localization of BclB NTD EGFP in *cotE* mutant cells differs than BclA fusions. The earlier production of BclB under its own native promoter allows for the BclB NTD EGFP fusions to localize to the spores, surrounding the newly constructed spores. This again is not the same ring structure that surrounds spores that is typically seen with BclA fusions. The BclB NTD EGFP does not seem to localize to the exosporium strips and is perhaps localizing to an internal still functioning part of the basal layer, the interspace region, or an outer spore coat layer (Fig. 31).

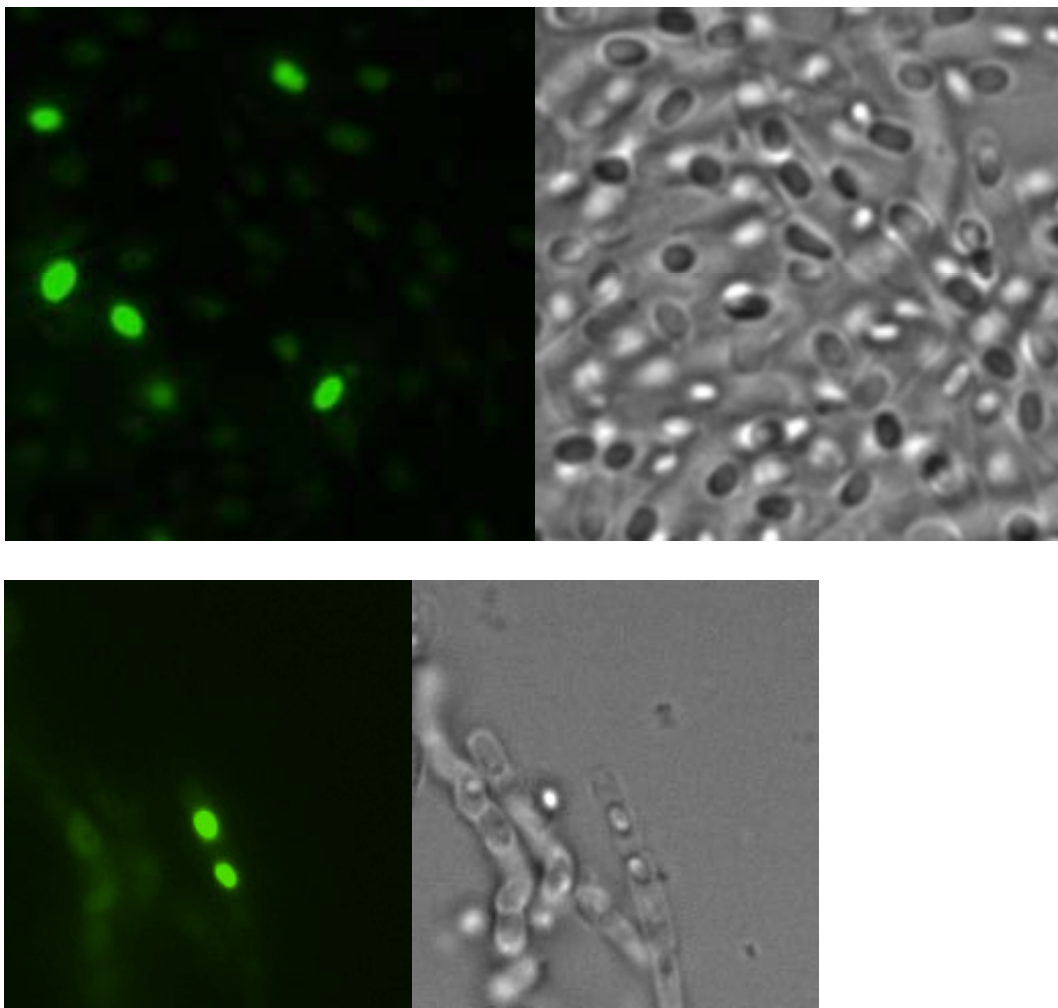


Fig. 31). Brightfield and epifluorescent images of *cotE* mutant spores expressing the BclB NTD EGFP fusion. Note the localization around the spores instead of the exosporium strips adjacent to the spores.

Maturation of the exosporium

This fluorescent reporter system can be utilized for analysis of exosporium maturation and assembly, as demonstrated in Figure 32.

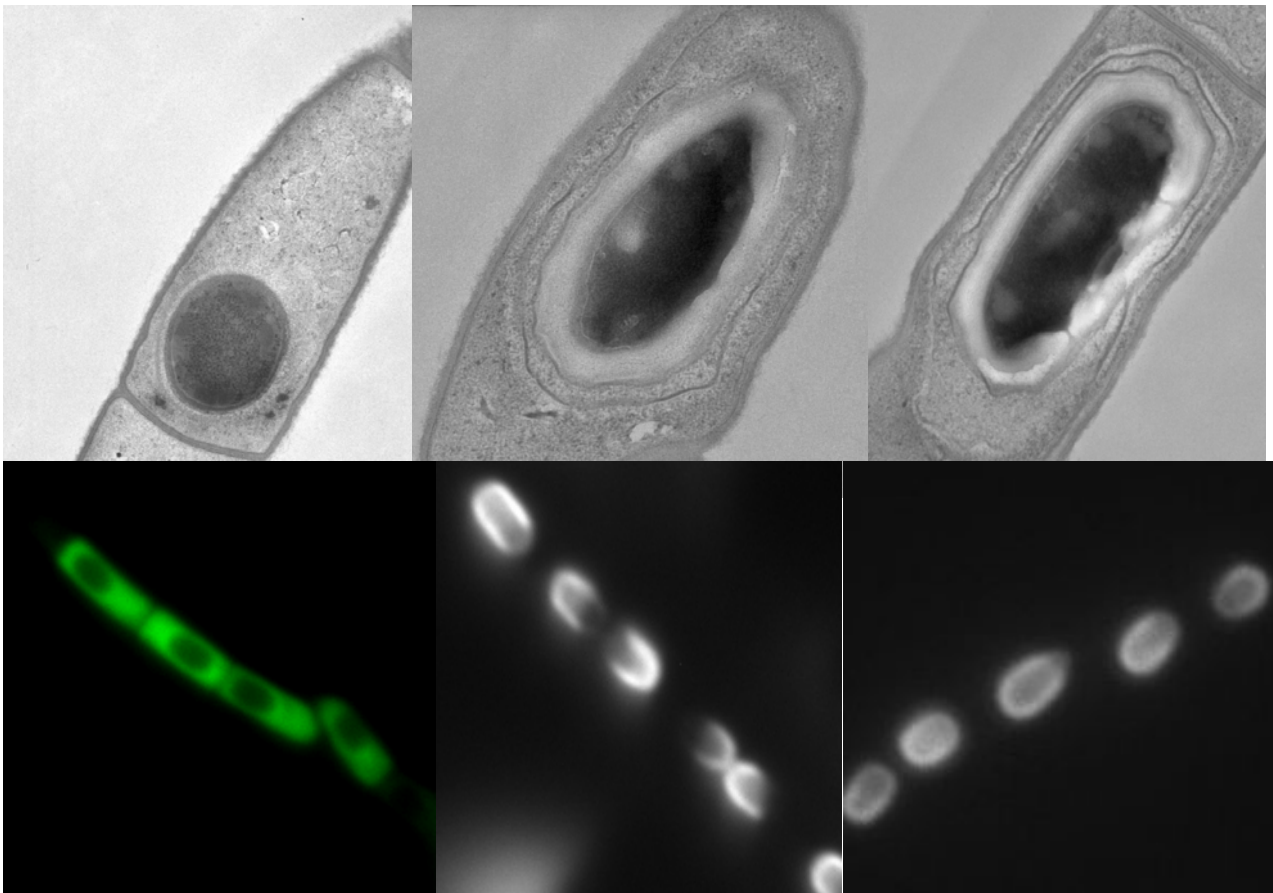


Fig. 32). Micrographs of developing spores in the mother cells. **Top)** TEM images of a newly-forming spore, cortex addition, exosporium basal layer assembly and beginning of nap formation, and completed exosporium, respectively. **Bottom)** Fluorescence images using the BclA NTD EGFP fusion corresponding to similar timepoints.

Defects in exosporium assembly can also be visualized using the fluorescent reporter system (Fig. 33). Concentrations of exosporium and spore coat proteins can be visualized in both EM and epi-fluorescence images in Fig. 33. Expression of the BclA NTD EGFP fusion can be observed in closely related species. Demonstration of expression in *B. thuringiensis kurstaki*, *B. thuringiensis israelensis*, and *B. cereus* ATCC 14579 is depicted in Fig. 34.

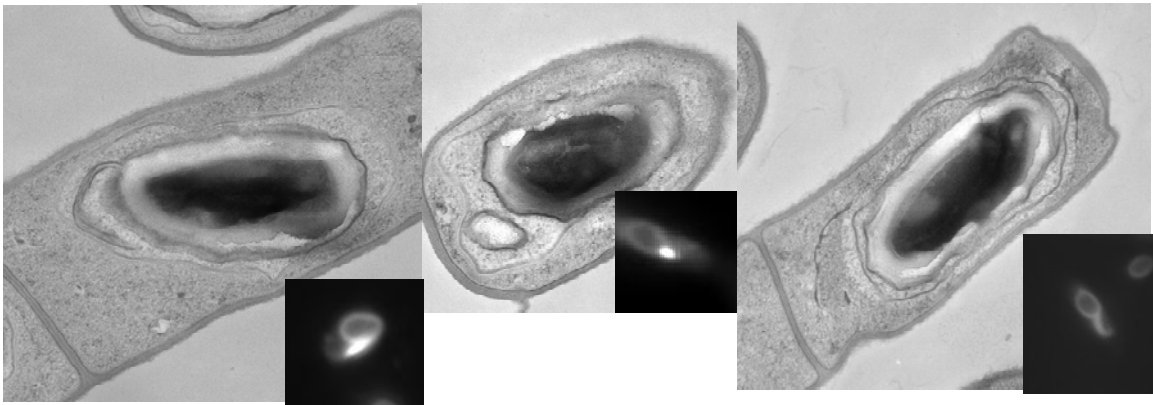


Fig. 33). EM pictures of wild-type exosporium and the comparative images visualized by usage of the fluorescent reporter system.

Verification of potential for localization of fusions in related bacteria

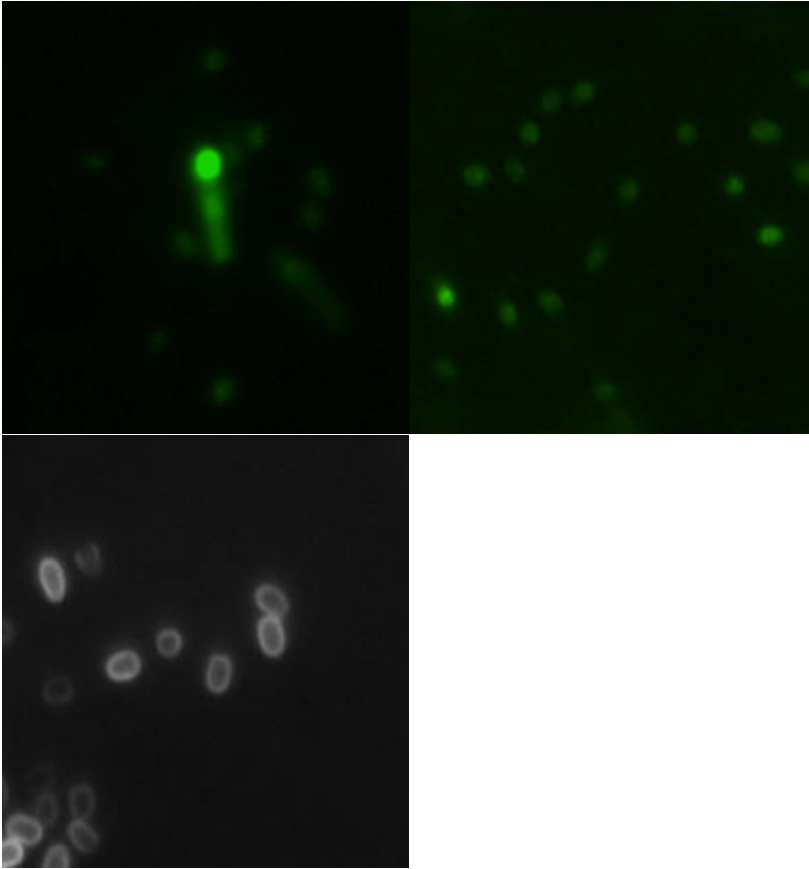


Fig. 34). Expression of the BclA NTD EGFP fusion in *B. thuringiensis kurstaki*, *B. thuringiensis israelensis*, and *B. cereus* ATCC 14579 respectively.

Discussion

Identification of protein domains important in protein incorporation into the exosporium

The N-terminal domains of BclA and BclB allow for the targeting and incorporation of these proteins into the exosporium of *B. anthracis*. The BclA N-terminal domain comprises an 11 amino acid conserved motif described herein and a 24 amino acid N-terminal region that contains a proteolytic cleavage site. This suggests the role of the conserved motif as a potential recognition site that leads to the positioning of the proteins to their appropriate target sites within the exosporium layer, but the attachment of proteins relies on more N-terminal sequences. Removal of the conserved motif (but retention of the N-terminal amino acid sequence) leads to poor incorporation of the fusion proteins into the exosporium. The low level of incorporation observed appears to result from reduced positioning of the proteins at their sites of incorporation (limited fluorescence targeted to the exosporium of developing spores) but those proteins that are properly aligned get incorporated.

Addition of only 5 additional amino acids plus a methionine to the conserved motif (amino acids 20-24) allows for efficient localization and attachment of proteins, suggesting a role for those 5 amino acids in the cleavage and attachment of BclA to the exosporium. This construct with the additional 6 amino acids mimics the final product after processing at the proteolytic cleavage site (with the exception of the methionine),

demonstrating incorporation likely can occur after proteolytic digestion. This casts doubt that the mechanism of cleavage is responsible primarily for removal of BclA from the exosporium, as these cleaved products could potentially be reincorporated into the exosporium.

The N-terminal domain of BclA is transported or localizes to the spore by action on the conserved motif region before cleavage occurs. After the N-terminal domain reaches the spore, it is proteolytically cleaved, releasing the distal N-terminal peptide into the mother cell cytoplasm, while the rest of the NTD remains stably attached to the exosporium. Whether cleavage and attachment are one reaction is still under investigation, but attachment can occur independently of the cleavage event in the fusion containing the “precleaved” product of the BclA NTD. An alternative explanation is the potential for the cleavage to still occur, chopping off the single methionine present in the “precleaved” BclA NTD fusion.

Incorporation of BclA appears to not be dependent on the glycosylation state, as the fusion proteins are incorporated efficiently and without noticeable flaws to the exosporium. The native triple helical conformation of BclA is also not necessary for glycoprotein incorporation into the exosporium, as the NTDs of the proteins are unable to form the helices. These targeting and attachment mechanisms appear to be indifferent to what is present following the targeting conserved motif. Stable incorporation into the exosporium is dependent on the presence of full length native BclA. The reason for this requirement is not known.

BclB is naturally produced earlier than BclA, despite the close timing of the transcription of their mRNAs (57). The timing of expression of BclB determines its localization pattern. BclB produced under control of its own promoter localizes internally to the final exosporium or BclA layer, whether this is an outer spore coat, interspace region, or internal exosporium layer has yet to be determined. When BclB was produced later, under the control of the *bclA* promoter, it incorporated into the exosporium. However, unlike the complete coverage seen with BclA, it incorporated modestly and in a mottled fashion across the exosporium surface. Overexpression of BclB early may lead to excess protein being incorporated into the exosporium.

The presence of the BclA conserved motif, in a fusion construct or otherwise, appears to allow for the even distribution of native BclB. Overproduction of a BclA fusion construct lacking the conserved motif or lack of native BclA resulted in a polar localization of BclB. Both BclA and BclB fusion targeting and incorporation are modified in *bclA* mutants.

The use of the BclA and BclB fusions allows for visualization of the complex exosporium assembly processes, and characterization of exosporium biosynthesis mutants without the primary use of transmission electron microscopy. The fusions can be exploited for use in identifying defective exosporia, characterizing the maturation process of the spore, screening for random mutations with exosporium-affected phenotypes, and identification of novel exosporium proteins.

Exploitation of the targeting domains as a *Bacillus* exosporium antigen delivery (BEAD) system

During the sporulation process in *Bacillus*, spores are assembled with the outermost spore layers deposited last (203; 204). The BclA glycoprotein is the predominant protein on the exosporium nap layer. This exosporium surface protein is expected to be among the last of the spore proteins to be incorporated into the spore. We have shown that the N-terminal domains of the BclA and BclB proteins are sufficient for localization to the exosporium surface and that efficient expression on the spore surface is also dependent on the timing or levels of expression during sporulation. Amino acid sequences distal to the first 35 amino acids of the BclA protein are not required for surface localization on spores and can be replaced with foreign protein sequences.

The use of this *Bacillus* exosporium targeting mechanism to incorporate tagged proteins into the exosporium enables high levels of expression of foreign proteins on the endospore of *B. anthracis* and other BclA-containing species. The amount of incorporation surpasses that of recombinant proteins expressed on *B. subtilis* spores using the CotB/C systems. The ability of *B. anthracis* spores to illicit an immune response has been well characterized, and combined with the inherent stability of the spores, provide a promising platform for the delivery of recombinant antigens (205, 28).

It has not escaped our notice that this targeting mechanism has implications for the development of potentially better and safer vaccines against anthrax and other biothreat agents. Important immunogens, such as *B. anthracis* protective antigen, could be

expressed on the surface of the anthrax spore. Spores derived from nontoxigenic strains, and perhaps genetically or physically inactivated, could be developed as a vaccine against human anthrax. This would provide the important protective antigen immunogen without the problems associated with residual toxicity and would have the additional advantage of providing spore-associated antigens that have been shown to provide enhanced protection against anthrax in animal models of the disease (3, 105). Furthermore, use of a spore as a vaccine platform provides adjuvant effects leading to both Th1 and Th2 immune responses, a feature not achieved with the current AVA vaccine (105, 206). Lastly, expression of additional proteins on the spore surface, for example; surface proteins from other biothreat agents, could lead to the development of multivalent vaccines against a variety of pathogens.

Bibliography

- 1. Gould GW.** History of Science – Spores. *J. Applied Microb.* (2006); **101**:507-523
- 2. Pickering AK, Osorio M, Lee GM, Grippe VK, Bray M, Merkel TJ.** Cytokine response to infection with *Bacillus anthracis* spores. *Infect. Immun.* (2004); **72**(11):6382-6389
- 3. Brossier F, Levy M, Mock M.** Anthrax spores make an essential contribution to vaccine efficiency. *Infect. Immun.* (2000);**68**(10):5731-5734.
- 4. Kiel JL, Parker JE, Alls JL, Kalns J, Holwitt EA, Stribling LJ, Morlaes PJ, Bruno JG.** Rapid recovery and identification of anthrax bacteria from the environment. *Ann. N. Y. Acad. Sci.* (2000);**916**:240-252
- 5. Mesnage S, Tosi-Couture E, Gounon P, Mock M, Fouet A.** The capsule and S-layer: two independent and yet compatible macromolecular structures in *Bacillus anthracis*. *J. Bacteriol.* (1998);**180**(1):52-58
- 6. Mignot T, Mock M, Fouet A.** Developmental switch of S-layer protein synthesis in *Bacillus anthracis*. *Mol. Microbiology.* (2002);**43**(6):1615-1628

7. Couture-Tosi E, Delcroix H, Mignot T, Mesnage S, Chami M, Fouet A, Mosser G.

Structural analysis and evidence for dynamic emergence of *Bacillus anthracis* S-layer networks. *J. Bacteriol.* (2002);**184**(23):6448-6456

8. Nessi C, Jedrzejewski MJ, Setlow P. Structure and mechanism of action of the protease that degrades small acid-soluble spore proteins during germination of spores of *Bacillus* species. *J. Bacteriol.* (1998);**180**(19):5077-5084

9. Moir A. Spore Germination. *Cell. Mol. Life Sci.* (2002);**59**:403-409

10. Setlow P. Spores of *Bacillus subtilis*: their resistance to and killing by radiation, heat, and chemicals. *J. Appl. Microb.* (2006);**101**(3):514-525

11. Moir A. How do spores germinate? *J. Appl. Microb.* (2006);**101**(3):526-530

12. Chada VG, Sansted EA, Wang R, Driks A. Morphogenesis of *Bacillus* spore surfaces. *J. Bacteriol.* (2003);**185**(21):6255-6261

13. Redmond C, Baillie LW, Hibbs S, Moir AJ, Moir A. Identification of proteins in the exosporium of *Bacillus anthracis*. *Microbiology.* (2004);**150**:355-363

14. Plomp M, Leighton TJ, Wheller KE, Malkin AJ. The high-resolution architecture and structural dynamics of *Bacillus* spores. *Biophys. J.* (2005);**88**(1):603-606

- 15. Steichen C, Chen P, Kearney JF, Turnbough CL.** Identification of the immunodominant protein and other proteins of the *Bacillus anthracis* exosporium. *J. Bacteriol.* (2003);**185**(6):1903-1910
- 16. Ireland JA, Hanna PC.** Amino acid- and purine ribonucleoside-induced germination of *Bacillus anthracis* Delta Sterne endospores: gerS mediated responses to aromatic ring structures. *J. Bacteriol.* (2002);**184**(5):1296-303
- 17. Cabrera-Martinez RM, Tovar-Rojo F, Vepachedu VR, Setlow P.** Effects of overexpression of nutrient receptors on germination of spores of *Bacillus subtilis*. *J. Bacteriol.* (2003);**185**(8):2457-2464
- 18. Charlton S, Moir AJ, Baillie L, Moir A.** Characterization of the exosporium of *Bacillus cereus*. *J. Appl. Micro.* (1999);**87**(2):241-245
- 19. Sylvestre P, Couture-Tosi E, Mock M.** A collagen-like surface glycoprotein is a structural component of the *Bacillus anthracis* exosporium. *Mol. Microbiol.* (2002);**45**(1):169-178
- 20. Welkos SL, Cote CK, Rea KM, Gibbs PH.** A microtiter fluorometric assay to detect the germination of *Bacillus anthracis* spores and the germination inhibitory effects of antibodies. *J. Microb. Methods.* (2004);**56**(2):253-65

- 21. Weiner MA, Read TD, Hanna PC.** Identification and characterization of the gerH operon of *Bacillus anthracis* endospores: a differential role for purine nucleosides in germination. *J.Bacteriol.* (2003);**185**(4):1462-1464
- 22. Weiner MA, Hanna PC.** Macrophage-mediated germination of *Bacillus anthracis* endospores requires the gerH operon. *J. Bacteriol.* (2003);**71**(7):3954-3959
- 23. Daubenspeck JM, Zeng H, Chen P, Dong S, Steichen CT, Krishna NR, Pritchard DG, Turnbough CL Jr.** Novel oligosaccharide side chains of the collagen-like region of BclA, the major glycoprotein of the *Bacillus anthracis* exosporium. *J. Biol. Chem.* (2004);**279**(30):30945-30953
- 24. Kim HS, Sherman D, Johnson F, Aronson AI.** Characterization of a major *Bacillus anthracis* spore coat protein and its role in spore inactivation. *J.Bacteriol.* (2004);**186**(8):2413-2417
- 25. Steichen CT, Kearney JF, Turnbough CL.** Characterization of the exosporium basal layer protein BxpB of *Bacillus anthracis*. *J. Bacteriol.* (2005);**187**(17):5868-5876
- 26. Acha P, Szyfres B.** Zoonoses and communicable diseases common to man and animals. 3rd Edition. (2003); *Renouf Publishing Co. Ltd*, Ogdensburg, NY 13669

- 27. Hasegawa M, Yang K, Hashimoto M, Park JH, Kim YG, Fujimoto Y, Nunez G, Fukase K, Inohara N.** Differential release and distribution of NOD1 and NOD2 immunostimulatory molecules among bacterial species and environments. *J. Biol. Chem.* (2004);**281**(39):29054-29063
- 28. Basu S, Kang TJ, Chen WH, Fenton MJ, Baillie L, Hibbs S, Cross AS.** Role of *Bacillus anthracis* spore structures in macrophage cytokine responses. *Infect. Immun.* (2007);**75**(5):2351-2358
- 29. Oncu S, Oncu S, Sakarya S.** Anthrax – an overview. *Med. Sci. Monit.* (2003);**9**(11):276-283
- 30. Mock M, Fouet A.** Anthrax. *Annu. Rev. Microbiol.* (2001);**55**:647-671
- 31. Baillie LWJ.** Past, imminent, and future human medical countermeasures for anthrax. *J. Appl. Microb.* (2006);**101**(3):594-606
- 32. Xu Q, Hessek ED, Zeng M.** Transcriptional stimulation of anthrax toxin receptors by anthrax edema toxin and *Bacillus anthracis* Sterne spores. *Microb. Pathog.* (2007);**43**(1):37-45

- 33. Zhong W, Shou Y, Yoshida TM, Marrone BL.** *Bacillus anthracis*, *B. cereus*, and *B. thuringiensis* differentiation using pulse field gel electrophoresis. *Appl. Env. Micro.* (2007);**73**(10):3446-3449
- 34. Russell B.H., Yasan R., Keene DR., Xu Y.** *Bacillus anthracis* internalization by human fibroblasts and epithelial cells. *Cell Microb.* (2007);(**5**):1262-1274.
- 35. Heffernan BJ, Thomason B, Herring-Palmer A, Hanna P.** *Bacillus anthracis* anthrolysin O and three phospholipases C are functionally redundant in a murine model of inhalational anthrax. *FEMS Microb. Lett.* (2007);(**1**):98-105
- 36. Heffernan BJ, Thomason B, herring-Palmer A, Shaughnessy L, McDonald R, Fisher N, Huffnagle GB, Hanna P.** *Bacillus anthracis* phospholipases C facilitate macrophage-associated growth and contribute to virulence in a murine model of inhalation anthrax. *Infect. Immun.* (2006);(**7**):3756-3764
- 37. Zink S, Burns DL.** Importance of SrtA and SrtB for growth of *Bacillus anthracis* in macrophages. *Infect. Immun.* (2005);**73**(8):5222-5228
- 38. Cendrowski S, MacArthur W, Hanna P.** *Bacillus anthracis* requires siderophore biosynthesis for growth in macrophages and mouse virulence. *Mol. Microb.* (2004);**51**(2):407-417

- 39. Dixon TC, Fadl AA, Koehler TM, Swanson JA, Hanna, PC.** Early *Bacillus anthracis*-macrophage interactions: intracellular survival and escape. *Cell. Microb.* (2000);**2**(6):453-463
- 40. Sirard JC, Guidi-Rontani C, Fouet A, Mock M.** Characterization of a plasmid region involved in *Bacillus anthracis* toxin production and pathogenesis. *Int. J. Med. Microb.* (2000);**290**(4-5)313-316.
- 41. Guidi-Rontani C, Weber-Levy M, Labruyere E, Mock M.** Germination of *Bacillus anthracis* spores within alveolar macrophages. *Mol. Microb.* (1999);**31**(1):9-17
- 42. Guidi-Rontani C, Levy M, Ohavon H, Mock M.** Fate of germinated *Bacillus anthracis* spores in primary murine macrophages. *Mol. Microb.* (2001);**42**(4):931-8
- 43. Cote CK, Rossi CA, Kang AS, Morrow PR, Lee JS, Welkos SL.** The detection of protective antigen (PA) associated with spores of *Bacillus anthracis* and the effects of anti-PA antibodies on spore germination and macrophages interactions. *Microb. Pathog.* (2005);**38**(5-6):209-225
- 44. Welkos S, Little S, Friedlander A, Fritz D, Fellows P.** The role of antibodies to *Bacillus anthracis* and anthrax toxin components in inhibiting the early stages of infection by anthrax spores. *Microbiology.* (2001);**147**(6):1677-1685

45. Guidi-Rontani C, Pereira Y, Ruffie S, Sirard JC, Weber-Levy M, Mock M.

Identification and characterization of a germination operon on the virulence plasmid pX01 of *Bacillus anthracis*. *Mol. Microb.* (1999);**33**(2):407-414

46. Lee JY, Janes BK, Passalacqua KD, Pfelger BF, Bergman NH, Liu H, Hakansson K, Somu RV, Aldrich CC, Cendrowski S, Hanna PC, Sherman DH.

Biosynthetic analysis of the petrobactin siderophore pathway from *Bacillus anthracis*. *J. Bacteriol.* (2007);**189**(5):1698-1710

47. Daniel R. Caldwell. *Microbial Physiology and Metabolism*. W.M. Brown Communications, Inc. 1995. Star Publishing Company (Belmont, CA)

48. Kozuka S, and Tochikubo K. Properties and origin of filamentous appendages on spores of *Bacillus cereus*. *Microbiol. Immunol.* (1985);**29**(1):21-37

49. Ruthel G, Ribot WJ, Bavari S, and Hoover, TA. Time-Lapse confocal imaging of development of *Bacillus anthracis* in macrophages. *J. Inf. Dis.* (2004);**189**:1313-1316

50. Qi Y, Patra G, Liang X, Williams LE, Rose S, Redkar RJ, DelVecchio VG.

Utilization of the *rpoB* gene as a specific chromosomal marker for real-time PCR detection of *Bacillus anthracis*. *Appl. Envi. Micro.* (2001);**67**(8):3720-3727

- 51. Helgason E, Okstad OA, Caugant DA, Johansen HA, Fouet A, Mock M, Hegna I, Kolsta AB.** *Bacillus anthracis*, *Bacillus cereus*, and *Bacillus thuringiensis* – one species on the basis of genetic evidence. *Appl. Environ. Microbiol.* (2000);**66**:2627-2630
- 52. Xu Y, Liang X, Chen Y, Koehler TM, Hook M.** Identification and biochemical characterization of two novel collagen binding MSCRAMMs of *Bacillus anthracis*. *J. Biol. Chem.* (2004);**279**(50)51760-51768
- 53. Hahn UK, Boehm R, and Beyer W.** DNA vaccination against anthrax in mice- combination of anti-spore and anti-toxin components. *Vaccine* (2005);**24**(21):4569-4571
- 54. Bergman NH, Anderson EC, Swenson EE, Niemeyer MM, Miyoshi AD, and Hanna, PC.** Transcriptional profiling of the *Bacillus anthracis* life cycle *in vitro* and an implied model for regulation of spore formation. *J. Bacteriol.* (2006);**188**(17)6092-6100.
- 55. Lai E, Phadke ND, Kachman MT, Giorno R, Vazquez S, Vazquez JA, Maddock JR, Driks A.** Proteomic analysis of the spore coats of *Bacillus subtilis* and *Bacillus anthracis*. *J. Bacteriol.* (2003);**185**(4):1443-1454
- 56. Firoved AM, Miller GF, Moayeri M, Kakkar R, Shen Y, Wiggins JF, McNally EM, Tang W, Leppla SH.** *Bacillus anthracis* edema toxin causes extensive tissue lesions and rapid lethality in mice. *Amer. J. Path.* (2005);**167**(5)1309-1320

- 57. Rampersad J, Khan A, and Ammons D.** A *Bacillus thuringiensis* isolate possessing a spore-associated filament. *Curr. Microbiol.* (2003);**47**(4):355-357
- 58. Setlow P.** Spores of *Bacillus subtilis*: their resistance to and killing by radiation, heat, and chemical. *J. Appl. Microbiol.* (2006);**101**:514-525
- 59. Hart SJ, Terray A, Leski TA, Arnold J, Stroud R.** Discovery of a significant optical chromatographic difference between spores of *Bacillus anthracis* and its closest relative, *Bacillus thuringiensis*. *Anal. Chem* (2006);**78**:3221-3225
- 60. Dai L, and Zimmerly S.** Compilation and analysis of group II intron insertions in bacterial genomes: evidence for retroelement behavior. *Nuc. Acids Res.* (2002);**30**(5)1091-1102
- 61. Chitlaru T, Ariel N, Zvi A, Lion M, Velan B, Shafferman A, Elhanany E.** Identification of chromosomally encoded membranal polypeptides of *Bacillus anthracis* by a proteomic analysis: Prevalence of proteins containing S-layer homology domains. *Proteomics* (2004);**6**(4):677-691
- 62. Klichko VI, Miller J, Wu A, Popov SG, and Alibek K.** Anaerobic induction of *Bacillus anthracis* hemolytic activity. *Bioch. Biophys. Res. Comm.* (2003);**303**:855-862

- 63. Agaisse H, Gominet M, Okstaf OA, Kolsto AM, Lereclus D.** PlcR is a pleiotrophic regulator of extracellular virulence factor gene expression in *Bacillus thuringiensis*. *Mol. Microb.* (1999);**32**:104310-104353
- 64. Mignot T, Mock M, Robichon D, Landier A, Lerechis D, Fouet A.** The incompatibility between PlcR- and AtxA-controlled regulons may have been selected a nonsense mutation in *Bacillus anthracis*. *Mol. Microb.* (2001);**42**:1189-1198
- 65. Pomerantsev AP, Kalnin KV, Osorio M, Leppla SH.** Phosphatidylcholine-specific phospholipase C and sphingomyelinase activities in bacteria of the *Bacillus cereus* group. *Infect. Immun.* (2003);**71**(11):6591-6606
- 66. Drysdale M, Bourgogne A, Koehler TM.** Transcriptional analysis of the *Bacillus anthracis* capsule regulators. *J. Bacteriol.* (2005);**187**(15):5108-5114
- 67. Bourgogne A, Drysdale M, Hilsenbeck SG, Peterson SN, Koehler TM.** Global effects of virulence gene regulators in a *Bacillus anthracis* strain with both virulence plasmids. *Infect. Immun.* (2003);**71**:2736-2743
- 68. Saile E, and Koehler T.** *Bacillus anthracis* multiplication, persistence, and genetic exchange in the rhizosphere of grass plants. *Appl. Env. Micro.* (2006);**72**:3168-3174
- 69. Rety S, Salameitou S, Garcia-verdugo I, Hulmes DJS, Le Hegerat F, Chaby R, Lewit-Bentley A.** The crystal structure of the *Bacillus anthracis* spore surface protein

BclA shows remarkable similarity to mammalian proteins. *J. Biol. Chem.*

(2005);**280**(52):43073-47078

70. Saksena R, Adamo R, and Kovac P. Synthesis of the tetrasaccharide side chain of the major glycoprotein of the *Bacillus anthracis* exosporium. *Bioorg. Med. Chem. Lett.*

(2006);**16**:615-617

71. Adamo R, Saksena R, Kovac P. Synthesis of the β -anomer of the spacer-equipped tetrasaccharide side chain of the major glycoprotein of the *Bacillus anthracis*

exosporium. *Carbohydrate Res.* (2005);**340**:2579-2582

72. Salamitou S, Rety S, Le Hegarat F, Leblon G, and Lewit-Bentley A. The use of high halide-ion concentrations and automated phasing procedures for the structural analysis of BclA, the major component of the exosporium of *Bacillus anthracis* spores.

Acta Cryst. (2005);**61**:344-349

73. Abachin E, Poyart C, Pellegrini E, Milhanic E, Fiedler F, Berche P, Cuot P.

Formation of D-alanyl-lipoteichoic acid is required for adhesion and virulence of *Listeria monocytogenes*. *Mol. Microb.* (2002);**43**:1-14

74. Daubenspeck JM, Zeng H, Chen P, Dong S, Steichen CT, Krishna NR, Pritchard DG, Turnbough CL. Novel oligosaccharide side chains of the collagen-like region of

BclA, the major glycoprotein of the *Bacillus anthracis* exosporium. *J. Biol. Chem.* (2004);**279**(30):30945-30953

75. Boydston JA, Chen P, Steichen CT, Turnbough CL. Orientation within the exosporium and structural stability of the collagen-like glycoprotein BclA of *Bacillus anthracis*. *J. Bacteriol.* (2005);**187**(15):5310-5317

76. Mehta AS, Saile E, Zhong W, Buskas T, Carlson R, Kannenberg E, Reed Y, Quinn CP, Boons G. Synthesis and antigenic analysis of the BclA glycoprotein oligosaccharide from the *Bacillus anthracis* exosporium. *Chemistry*. (2006);**12**(36):9136-9149

77. Bozue J, Cote CK, Moody KL, Welkos SL. Fully virulent *Bacillus anthracis* does not require the immunodominant protein BclA for pathogenesis. *Infect. Immun.* (2007);**75**(1):508-511

78. Koshikawa T, Yamazaki M, Yoshimi M, Ogawa S, Yamada A, Watabe K, Torii M. Surface hydrophobicity of spores of *Bacillus* spp. *J. Gen. Microbiol.* (1989);**135**(10):2717-2722.

79. Todd SJ, Moir AJG, Johnson MJ, and Moir A. Genes of *Bacillus cereus* and *Bacillus anthracis* encoding proteins of the exosporium. *J. Bacteriol.* (2003);**185**(11):3373-3378

- 80. Sylvestre P, Couture-Tosi E, and Mock M.** Contribution of ExsFA and ExsFB proteins to the localization of BclA on the spore surface and to the stability of the *Bacillus anthracis* exosporium. *J. Bacteriol.* (2005);**187**(15):5122-5128
- 81. Bailey-Smith K, Todd SJ, Southworth TW, Proctor H, and Moir A.** The ExsA protein of *Bacillus cereus* is required for assembly of coat and exosporium onto the spore surface. *J. Bacteriol.* (2005);**187**(11):3800-3806
- 82. Werz DB, and Seeberger PH.** Total synthesis of antigen *Bacillus anthracis* tetrasaccharide- creation of an anthrax vaccine candidate. *Angew. Chem. Int. Ed.* (2005);**44**:6315-6318
- 83. Sylvestre P, Couture-Tosi E, and Mock M.** Polymorphism in the collagen-like region of *Bacillus anthracis* BclA protein leads to variation in exosporium filament length. *J. Bacteriol* (2003);**185**(5):1555-1563
- 84. Swiecki MK, Lisanby MW, Shu F, Turnbough CL, and Kearney JF.** Monoclonal antibodies for *Bacillus anthracis* spore detection and functional analyses of spore germination and outgrowth. *J. Immun.* (2006);6076-6084
- 85. Boydston JA, Yue L, Kearney JF, and Turnbough CL.** The ExsY protein is required for complete formation of the exosporium of *Bacillus anthracis*. *J. Bacteriol.* (2006);**188**(21):7440-7448

- 86. Johnson MJ, Todd SJ, Ball DA, Shepard AM, Sylvestre P, Moir A.** ExsY and CotY are required for the correct assembly of the exosporium and spore coat of *Bacillus cereus*. *J. Bacteriol.* (2006);**188**(22):7905-7913
- 87. Giorno R, Bozue J, Cote C, Wenzel T, Moody KS, Mallozi M, Ryan M, Wang R, Zielke R, Maddock JR, Friedlander A, Welkos S, and Driks A.** Morphogenesis of the *Bacillus anthracis* spore. *J. Bacteriol.* (2007);**189**(3):691-705
- 88. Liu H, Bergman NH, Thomason B, Shallom S, Hazen A, Crossno J, Rasko DA, Ravel J, Read TD, Peterson SN, Yates III J, and Hanna, P.** Formation and composition of the *Bacillus anthracis* endospore. *J. Bacteriol.* (2004);**186**(1):164-178
- 89. Waller LN, Stump MJ, Fox KF, Harley WM, Fox A, Stewart GC, and Shahgholi M.** Identification of a second collagen-like glycoprotein produced by *Bacillus anthracis* and demonstration of associated spore-specific sugars. *J. Bacteriol.* (2005);**187**(13):4592-4597
- 90. Collins LV, Kristian SA, Weidenmaier C, Faigle M, Kessel KP, Strijp JA, Gotz F, Neumeister B, and Peschel A.** *Staphylococcus aureus* strains lacking D-alanine modification of teichoic acids are highly susceptible to human neutrophil killing and are virulence attenuated in mice. *J. Inf. Disease* (2002);**186**:214-219

- 91. Williams DD and Turnbough CL.** Surface layer protein EA1 is not a component of *Bacillus anthracis* spores but is a persistent contaminant in spore preparations. *J. Bacteriol.* (2004);**186**(2):566-569
- 92. Bozue JA, Parthasarathy N, Phillips LR, Cote CK, Fellows PF, Mendelson I, Shafferman A, Friedlander AM.** Construction of a rhamnase mutation in *Bacillus anthracis* affects adherence to macrophages but not virulence in guinea pigs. *Microb. Patho.* (2005);**38**:1-12
- 93. Fisher N, Sherton-Rama L, Herring-Palmer A, Heffernan B, Bergman N, and Hanna P.** The dltABCD operon of *Bacillus anthracis* Sterne is required for virulence and resistance to peptide, enzymatic, and cellular mediators of innate immunity. *J. Bacteriol.* (2006);**188**(4):1301-1309
- 94. Rasmussen M, Jacobsson M, and Bjorck L.** Genome-based identification and analysis of collagen-related structural motifs in bacterial and viral proteins. *J. Biol. Chem.* (2003);**278**(34):32313-32316
- 95. Karlstrom A, Jacobsson K, and Guss B.** SclC is a member of a novel family of collagen-like proteins in *Streptococcus equi* subspecies *equi* that are recognized by antibodies against SclC. *Vet. Microbiol.* (2006);**114**:72-81

- 96. Humtsoe JO, Kim JK, Xu Y, Keen DR, Hook M, Lukomski S, and Wary KK.** A streptococcus collagen-like protein interacts with the $\alpha 2\beta 1$ integrin and induces intracellular signaling. *J. Biol. Chem.* (2005);**289**(14):13848-13857
- 97. Steichen CT, Kearney JF, and Turnbough CL.** Non-uniform assembly of the *Bacillus anthracis* exosporium and a bottle cap model for spore germination and outgrowth. *Mol. Microb.* (2007);**64**(2):359-367
- 98. Williamson ED, Hodgson I, Walker NK, Topping AW, Duchars MG, Mott JM, Estep J, LeButt C, Flick-Smith HC, Jones HE, Li H, and Quinn CP.** Immunogenicity of recombinant protective antigen and efficacy against aerosol challenge with anthrax. *Infect. Immun.* (2005);**73**(9):5978-5987
- 99. Castanha ER, Swiger RR, Senior B, Fox A, Waller LN, Fox KF.** Strain discrimination among *B. anthracis* and related organisms by characterization of BclA polymorphisms using PCR coupled with agarose gel or microchannel fluidics electrophoresis. *J. Microb. Methods.* (2006);**64**(1):27-45
- 100. Mohamed N, Clagett M, Li J, Jones S, Pincus S, D'Alia G, Nardone L, Babin M, Spitalny G, and Casey L.** A High-affinity monoclonal antibody to anthrax protective antigen passively protects rabbits before and after aerosolized *Bacillus anthracis* spore challenge. *Infect. Immun.* (2005);**73**(2):795-802

- 101. Xie H, Gursel I, Ivins BE, Singh M, O'Hagan DT, Ulmer JB, and Klinman DM.** CpG oligodeoxynucleotides adsorbed onto polyactide-co-glycolide microparticles improve the immunogenicity and protective activity of the licensed anthrax vaccine. *Infect. Immun.* (2005);**73**(2):828-833
- 102. Lee JS, Hadjipanayis AG, and Welkos SL.** Venezuelan equine encephalitis virus-vectored vaccines protect mice against anthrax spore challenge. *Infect. Immun.* (2003);**71**(3):1491-1496
- 103. Schneerson R, Kubler-Kielb J, Liu T, Dai Z, Leppla SH, Yergey A, Backlund P, Shiloach J, Majadly F, and Robbins JB.** Poly(gamma-D-glutamic acid) protein conjugates induce IgG antibodies in mice to the capsule of *Bacillus anthracis*: A potential addition to the anthrax vaccine. *PNAS* (2003);**100**(15):8945-8950
- 104. Kudva IT, Griffin RW, Garren JM, Calderwood SB, and John M.** Identification of a protein subset of the anthrax spore immunome in humans immunized with the anthrax vaccine adsorbed preparation. *Infect. Immun.* (2005);**73**(9):5685-5696
- 105. Turnbull, PC.** Anthrax vaccines: past, present, and future. *Vaccine* (1991);**9**:533-539
- 106. Broster MG, and Hibbs SE.** Protective efficacy of anthrax vaccines against aerosol challenge. *Salisbury Med. Bull. Sp. Suppl.* (1990) **68**:91-92

- 107. Welkos SL, Keener TJ, and Gibbs PH.** Differences in susceptibility of inbred mice to *Bacillus anthracis*. *Infect. Immun.* (1986);**51**:795-800
- 108. Little SF, Knudson GB.** Comparative efficacy of *Bacillus anthracis* live spore vaccine and protective antigen vaccine against anthrax in the guinea pig. *Infect Immun.* (1986);**52**(2):509-512
- 109. Iber D, Clarkson J, Yudkin MD, and Campbell ID.** The mechanism of cell differentiation in *Bacillus subtilis*. *Nature Letters.* (2006);**441**:371-374
- 110. Haldenwang, WG.** The Sigma factors of *Bacillus subtilis*. *Microb. Reviews.* (1995);**59**(1):1-30
- 111. Hilbert DW, and Piggot PJ.** Compartmentalization of gene expression during *Bacillus subtilis* spore formation. *Microb. Mol. Biol. Rev.* (2004);**68**(2):234-262
- 112. Cui X, Li Y, Laird MW, Subramanian M, Moayeri M, Leppla SH, Fitz Y, Su J, Sherer K, and Eichacker PQ.** *Bacillus anthracis* edema and lethal toxin have different hemodynamic effects but function together to worsen shock and outcome in a rat model. *J. Inf. Dis.* (2007);**195**:572-579

- 113. Hadjifrangiskou M, Chen Y, and Koehler TM.** The alternative sigma factor SigH is required for toxin gene expression by *Bacillus anthracis*. *J. Bacteriol.* (2007);**189**(5):1874-1883
- 114. Tournier J, Quesnel-Hellmann A, Cleret A, and Vidal DR.** Contribution of toxins to the pathogenesis of inhalational anthrax. *Cell. Microb.* (2007);1-11
- 115. Brittingham KC, Ruthel G, Panchal RG, Fuller CL, Ribot WJ, Hoover TA, Young HA, Anderson AO, and Bavari S.** Dendritic cells endocytose *Bacillus anthracis* spores: implications for anthrax pathogenesis. *J. Immuno.* 5545-5552
- 116. Pickering AK, Osorio M, Lee GM, Grippe VK, Bray M, and Merkel TJ.** Cytokine response to infection with *Bacillus anthracis* spores. *Infect. Immun.* (2004);**72**(11):6382-6389
- 117. Cordoba-Rodriguez R, Fang H, Lankford CSR, and Frucht DM.** Anthrax lethal toxin rapidly activates caspase-1/ICE and induces extracellular release of interleukin IL-1B and IL-18. *J. Biol. Chem.* (2004);**279**(20):20563-20566
- 118. Bergman NH, Passalacqua KD, Gaspard R, Sherton-Rama LM, Quackenbush J, and Hanna PC.** Murine macrophage transcriptional responses to *Bacillus anthracis* infection and intoxication. *Infect. Immun.* (2005);**73**(2):1069-1080

- 119. Drysdale M, Heninger S, Hutt J, Chen Y, Lyons CR, and Koehler TM.** Capsule biosynthesis by *Bacillus anthracis* is required for dissemination in murine inhalational anthrax. *EMBO* (2005);**24**:221-227
- 120. Agrawal A, Lingappa J, Leppla SH, Agrawal S, Jabbar A, Quinn C, and Pulendran B.** Impairment of dendritic cells and adaptive immunity by anthrax lethal toxin. *Nature Letters*. (2003);**424**:329-334
- 121. Salles II, Tucker AM, Voth DE, and Ballard JD.** Toxin-induced resistance in *Bacillus anthracis* lethal toxin-treated macrophages. *PNAS* (2003);**100**(21):12426-12431
- 122. Welkos S, Friedlander A, Weeks S, Little S, and Mendelson I.** *In vitro* characterization of the phagocytosis and fate of anthrax spores in macrophages and the effects of anti-PA antibody. *J. Med. Microb.* (2002);**51**:821-831
- 123. Kirby, JE.** Anthrax lethal toxin induces human endothelial cell apoptosis. *Infect. Immun.* (2004);**72**(1):430-439
- 124. Cote CK, Rea KM, Norris SL, Van Rooijen N, and Welkos SL.** The use of *in vivo* macrophage depletion to study the role of macrophages during infection with *Bacillus anthracis* spores. *Microb. Patho.* (2004);**37**:169-175

- 125. Kaufmann, AF, Meltzer, MI, and Schmid, GP.** The economic impact of a bioterrorist attack: are prevention and postattack intervention programs justifiable? *Emerging Infectious diseases*, (1997);**3**(2): 83-94.
- 126. Hoffmaster AR, Ravel J, Rasko DA, Chapman GD, Chute MD, Marston CK, De BK, Sacchi CT, Fitzgerald C, Mayer LW, Maiden MCJ, Priest FG, Barker M, Jiang L, Cer RZ, Rilstone J, Peterson SN, Weyant RS, Galloway DR, Read TD, Popovic T, and Fraser CM.** Identification of anthrax toxin genes in a *Bacillus cereus* associated with an illness resembling inhalation anthrax. *PNAS*. (2004);**101**(22):8449-8454
- 127. Hoffmaster AR, and Koehler TM.** Control of virulence gene expression in *Bacillus anthracis*. *J. Appl. Microb.* (1999);**87**:279-281
- 128. Koehler TM, Dai Z, and Kaufman-Yarbray M.** Regulation of the *Bacillus anthracis* protective antigen gene: CO₂ and a trans-acting element activate transcription from one of two promoters. *J. Bacteriol.* (1994);**176**(3):586-595
- 129. Drysdale M, Bourgogne A, Hilsenbeck SG, and Koehler TM.** AtxA controls *Bacillus anthracis* capsule synthesis via *acpA* and a newly discovered regulator *acpB*. *J. Bacteriol.* (2004);**186**(2):307-315

- 130. Mignot T, Mock M, and Fouet A.** A plasmid-encoded regulator couples the synthesis of toxins and surface structures in *Bacillus anthracis*. *Mol. Microb.* (2003);**47**(4):917-927
- 131. Bourgogne A, Drysdale M, Hilsenbeck SG, Peterson SN, and Koehler TM.** Global effects of virulence gene regulators in a *Bacillus anthracis* strain with both virulence plasmids. *Infect. Immun.* (2003);**71**(5):2736-2743
- 132. Abrami L, Liu S, Cosson P, Leppla SH, and Van Der Goot FG.** Anthrax toxin triggers endocytosis of its receptor via a lipid raft-mediated clathrin-dependent process. *J. Cell Biol.* (2003);**160**(3):321-328
- 133. Kurzchalia T.** Anthrax toxin rafts into cells. *J. Cell. Biol.* (2003);**160**(3):295-296
- 134. Pellizzari R, Guidi-Rontani C, Vitale G, Mock M, and Montecucco C.** Anthrax lethal factor cleaves MKK3 in macrophages and inhibits the LPS/IFN-gamma release of NO and TNF alpha. *FEBS Letters* (1999);**462**:199-204
- 135. Park JM, Greten FR, Li Z, and Karin M.** Macrophage apoptosis by anthrax lethal factor through p38 MAP kinase inhibition. *Science* (2002);**297**:2048-2051

- 136. Moayeri M, Haines D, young HA, and Leppla SH.** *Bacillus anthracis* lethal toxin induces TNF-alpha-independent hypoxia-mediated toxicity in mice. *J. Clin. Invest.* (2003);**112**(5):670-682
- 137. Stranbacj MN and Collier RJ.** Anthrax delivers a lethal blow to host immunity. *Nature Med.* (2003);**9**(8):996-997
- 138. Wu AG, Alibek D, Li YL, Bradburne C, Bailey CL, and Alibek K.** Anthrax toxin induces hemolysis: an indirect effect through polymorphonuclear cells. *J. Inf. Disease* (2003);**188**:1138-1141
- 139. Gold JA, Hoshino Y, Hoshino S, Jones MB, Nolan A, and Weiden MD.** Exogenous gamma and alpha/beta interferon rescues human macrophages from cell death induced by *Bacillus anthracis*. *Infect. Immun.* (2004);**72**(3):1291-1297
- 140. Ramarao N and Lereclus D.** The InhA1 metalloprotease allows spores of the *B. cereus* group to escape macrophages. *Cell. Microb.* (2005);**7**(9):1357-1364
- 141. Raines KW, Kang TJ, Hibbs S, Cao G, Weaver J, Tsai P, Baillie LW, Cross AS, and Rowen GM.** Importance of nitric oxide synthase in the control of infection of *Bacillus anthracis*. *Infect. Immun.* (2006);**74**(4):2268-2276

- 142. Beaman TC, Pankratz HS, and Gerhardt P.** Paracrystalline sheets reaggregated from solubilized exosporium of *Bacillus cereus*. *J. Bacteriol.* (1971);**107**(1):320-324
- 143. Beaman TC, Pankratz HS, and Gerhardt P.** Ultrastructure of the exosporium and underlying inclusions in spores of *Bacillus megaterium* strains. *J. Bacteriol* (1972);**109**(3):1198-1209
- 144. Hachisuka Y, Kojima K, and Sato T.** Fine filaments on the outside of the exosporium of *Bacillus anthracis* spores. *J. Bacteriol* (1966);**91**(6):2382-2385
- 145. Martinex-Pomares L, wienke D, Stillino R, McKenzie EJ, Anronl JN, Harris J, McGreal E, Sim RB, Isacke CM, and Gordon S.** Carbohydrate-independent recognition of collagens by the macrophage mannose receptor. *Eur. J. Immun.* (2006);**36**:1074-1082
- 146. Jedrzejewski MJ and Huang WJM.** *Bacillus* species proteins involved in spore formation and degradation: from identification in the genome, to sequence analysis, and determination of function and structure. *Crit. Rev. Bioch. Mol. Biol.* (2003);**38**(3):173-198
- 147. Priest FG, Barker M, Baillie LWJ, Holmes EC, and Maiden MCJ.** Population structure and evolution of the *Bacillus cereus* group. *J. Bacteriol.* (2004);**186**(23):7959-7970

- 148. Mosser Em and Rest RF.** The *Bacillus anthracis* cholesterol-dependent cytolysin, anthrolysin O, kills human neutrophils, monocytes, and macrophages. *BMC Microb.* (2006);**56**(6):
- 149. Birnboim HC and Doly J.** A rapid alkaline extraction procedure for screening of recombinant plasmid DNA. *Nuc. Acid Res.* (1979);**7**(6):1513-1523
- 150. Ho, S. N., H. D. Hunt, R. M. Horton, J. K. Pullen, and L. R. Pease.** Site-directed mutagenesis by overlapping extension using the polymerase chain reaction. *Gene* (1989)**77**:51-59.
- 151. Horton, R. M., H. D. Hunt, S. N. Ho, J. K. Pullen, and L. R. Pease.** Engineering hybrid genes without the use of restriction enzymes: gene splicing by overlap extension. *Gene* (1989);**77**:61-68.
- 152. Perez-Casal, J., M. G. Caparon, and J. R. Scott.** Mry, a *trans*-acting positive regulator of the M protein gene of *Streptococcus pyogenes* with similarity to the receptor proteins of two-component regulatory systems. *J. Bacteriol.* (1991);**173**:2617–2624.
- 153. Chen, Y., F.C. Tenover, and T.M. Koehler.** β -lactamase gene expression in a penicillin-resistant *Bacillus anthracis* strain. *Antimicrob. Ag. Chemother.* (2004);**48**:4873-4877.

154. Green, B. D., L. Battisti, T. M. Koehler, C. B. Thorne, and B. E. Ivins.

Demonstration of a capsule plasmid in *Bacillus anthracis*. *Infect. Immun.* (1985);**49**:291-297

155. Saile E., and T. M. Koehler. Control of anthrax toxin gene expression by the transition state regulator *abrB*. *J Bacteriol* (2002);**184**:370–380

156. Waller L., K. F. Fox, A. Fox, and R. L. Price. Ruthenium red staining for ultra-structural visualization of a glycoprotein layer surrounding the spore of *Bacillus anthracis* and *B. subtilis*. *J. Microbiol. Meth.* (2004);**58**:23-30.

157. Zolock, R. A., Li, G, Bleckman, C, Burggraf, L, and Fuller, D. Atomic force microscopy of *Bacillus* spore surface morphology. *Micron* (2006);**37**:363-369

158. Riesenman, P. J. and W. L. Nicholson. Role of the spore coat layers in *Bacillus subtilis* spore resistance to hydrogen peroxide, artificial UV-C, UV-B and solar UV radiation. *Appl. Env. Micro.* (2000);**66**:620-626.

159. Gerhardt P. Cytology of *Bacillus anthracis*. *Fed. Proc.* (1967);**26**(5):1504-1517

160. Hart CA and Beeching NJ. A spotlight on anthrax. *Clin. Dermat.* (2002);**20**(4):365-375

- 161. Cieslak TJ and Eitzen EM Jr.** Clinical and epidemiological principles of anthrax. *Emerg. Inf. Dis.* (1999);**5**(4):552-555
- 162. Bradley KA, Mogridge J, Mourez M, Collier RJ, Young JA.** Identification of the cellular receptor for anthrax toxin. *Nature.* (2001);**414**(6860):225-229.
- 163. Hanna P.** Lethal toxin actions and their consequences. *J. Appl. Microbiol.* (1999);**87**(2):285-287.
- 164. Leppla SH.** Purification and characterization of adenylyl cyclase from *Bacillus anthracis*. *Methods Enzymol.* (1991);**195**:153-168.
- 165. O'Brien J, Friedlander A, Dreier T, Ezzell J, Leppla S.** Effects of anthrax toxin components on human neutrophils. *Infect. Immun.* (1985);**47**(1):306-310.
- 166. Wright GG, Mandell GL.** Anthrax toxin blocks priming of neutrophils by lipopolysaccharide and by muramyl dipeptide. *J.Exp. Med.* (1986);**164**(5):1700-1709
- 167. Vancurik J.** Causes of the failure of antibiotic prophylaxis of inhalation anthrax and clearance of the spores from the lungs. *Folia Microbiol (Praha).* (1966);**11**(6):459-464.

- 168. Bradaric N, Punda-Polic V.** Cutaneous anthrax due to penicillin-resistant *Bacillus anthracis* transmitted by an insect bite. *Lancet*. (1992);**340**(8814):306-307.
- 169. Lalitha MK, Thomas MK.** Penicillin resistance in *Bacillus anthracis*. *Lancet*. (1997);**349**(9064):1522.
- 170. Friedlander AM, Welkos SL, Pitt ML, Ezzell JW, Worsham PL, Rose KJ, Ivins BE, Lowe JR, Howe GB, Mikesell P.** Postexposure prophylaxis against experimental inhalation anthrax. *J. Infect. Dis.* (1993);**167**(5):1239-1243.
- 171. Hu H, Sa Q, Koehler TM, Aronson AI, Zhou D.** Inactivation of *Bacillus anthracis* spores in murine primary macrophages. *Cell Microbiol.* (2006);**8**(10):1634-1642.
- 172. Alileche A, Serfass ER, Muehlbauer SM, Porcelli SA, Brojatsch J.** Anthrax lethal toxin-mediated killing of human and murine dendritic cells impairs the adaptive immune response. *PLoS Pathog.* (2005);**1**(2):19.
- 173. Gimenez AP, Wu YZ, Paya M, Delclaux C, Touqui L, Goossens PL.** High bactericidal efficiency of type iia phospholipase A2 against *Bacillus anthracis* and inhibition of its secretion by the lethal toxin. *J. Immunol.* (2004);**173**(1):521-530.

- 174. Batty S, Chow EM, Kassam A, Der SD, Mogridge J.** Inhibition of mitogen-activated protein kinase signalling by *Bacillus anthracis* lethal toxin causes destabilization of interleukin-8 mRNA. *Cell Microbiol.* (2006);**8**(1):130-138.
- 175. Kassam A, Der SD, Mogridge J.** Differentiation of human monocytic cell lines confers susceptibility to *Bacillus anthracis* lethal toxin. *Cell Microbiol.* (2005);**7**(2):281-292.
- 176. Fang H, Xu L, Chen TY, Cyr JM, Frucht DM.** Anthrax lethal toxin has direct and potent inhibitory effects on B cell proliferation and immunoglobulin production. *J. Immunol.* (2006);**176**(10):6155-6161.
- 177. Fang H, Cordoba-Rodriguez R, Lankford CS, Frucht DM.** Anthrax lethal toxin blocks MAPK kinase-dependent IL-2 production in CD4+ T cells. *J. Immunol.* (2005);**174**(8):4966-4971.
- 178. Paccani SR, Tonello F, Ghittoni R, Natale M, Muraro L, D'Elia MM, Tang WJ, Montecucco C, Baldari CT.** Anthrax toxins suppress T lymphocyte activation by disrupting antigen receptor signaling. *J. Exp. Med.* (2005);**201**(3):325-331.
- 179. Duverger A, Jackson RJ, van Ginkel FW, Fischer R, Tafaro A, Leppla SH, Fujihashi K, Kiyono H, McGhee JR, Boyaka PN.** *Bacillus anthracis* edema toxin acts

as an adjuvant for mucosal immune responses to nasally administered vaccine antigens. *J. Immunol.* (2006);**176**(3):1776-1783.

180. Warfel JM, Steele AD, D'Agnillo F. Anthrax lethal toxin induces endothelial barrier dysfunction. *Am. J. Pathol.* (2005);**166**(6):1871-1881.

181. Gozes Y, Moayeri M, Wiggins JF, Leppla SH. Anthrax lethal toxin induces ketotifen-sensitive intradermal vascular leakage in certain inbred mice. *Infect. Immun.* (2006);**74**(2):1266-1272.

182. Kau JH, Sun DS, Tsai WJ, Shyu HF, Huang HH, Lin HC, Chang HH. Antiplatelet activities of anthrax lethal toxin are associated with suppressed p42/44 and p38 mitogen-activated protein kinase pathways in the platelets. *J. Infect. Dis.* (2005);**192**(8):1465-1474.

183. Alam S, Gupta M, Bhatnagar R. Inhibition of platelet aggregation by anthrax edema toxin. *Biochem. Biophys. Res. Commun.* (2006);**339**(1):107-114.

184. Stewart GS, Eaton MW, Johnstone K, Barrett MD, Ellar DJ. An investigation of membrane fluidity changes during sporulation and germination of *Bacillus megaterium* K.M. measured by electron spin and nuclear magnetic resonance spectroscopy. *Biochem. Biophys. Acta.* (1980);**600**(2):270-290

- 185. Cowan AE, Olivastro EM, Koppel DE, Loshon CA, Setlow B, Setlow P.** Lipids in the inner membrane of dormant spores of *Bacillus* species are largely immobile. *Proc. Natl. Acad. Sci. U S A.* (2004);**101**(20):7733-7738.
- 186. Clements MO, Moir A.** Role of the gerI operon of *Bacillus cereus* 569 in the response of spores to germinants. *J Bacteriol.* (1998);**180**(24):6729-6735
- 187. Titball RW, Manchee RJ.** Factors affecting the germination of spores of *Bacillus anthracis*. *J. Appl. Bacteriol.* (1987);**62**(3):269-273
- 188. Chen Y, Fukuoka S, Makino S.** A novel spore peptidoglycan hydrolase of *Bacillus cereus*: biochemical characterization and nucleotide sequence of the corresponding gene, *sleL*. *J. Bacteriol.* (2000);**182**(6):1499-1506.
- 189. Cohen S, Mendelson I, Altboum Z, Kobiler D, Elhanany E, Bino T, Leitner M, Inbar I, Rosenberg H, Gozes Y, Barak R, Fisher M, Kronman C, Velan B, Shafferman A.** Attenuated nontoxigenic and nonencapsulated recombinant *Bacillus anthracis* spore vaccines protect against anthrax. *Infect. Immun.* (2000);**68**(8):4549-58.
- 190. Matz LL, Beaman TC, Gerhardt P.** Chemical composition of exosporium from spores of *Bacillus cereus*. *J. Bacteriol.* (1970);**101**(1):196-201
- 191. DesRosier JP, Lara JC.** Isolation and properties of pili from spores of *Bacillus cereus*. *J. Bacteriol.* (1981);**145**(1):613-619

- 192. Hunter ME, DeLamater ED.** Observations on the nuclear cytology of spore germination in *Bacillus megaterium*. *J. Bacteriol.* (1952);**63**(1):23-31
- 193. Cole HB, Ezzell JW Jr, Keller KF, Doyle RJ.** Differentiation of *Bacillus anthracis* and other *Bacillus* species by lectins. *J. Clin. Microbiol.* (1984);**19**(1):48-53.
- 194. Timpl R, Beil W, Furthmayr H, Meigel W, Pontz B.** Characterization of conformation independent antigenic determinants in the triple-helical part of calf and rat collagen. *Immunology.* (1971);**21**(6):1017-1030.
- 195. Mann K, Mechling DE, Bachinger HP, Eckerskorn C, Gaill F, Timpl R.** Glycosylated threonine but not 4-hydroxyproline dominates the triple helix stabilizing positions in the sequence of a hydrothermal vent worm cuticle collagen. *J. Mol. Biol.* (1996);**261**(2):255-66.
- 196. Chopra AP, Boone SA, Liang X, Duesbery NS.** Anthrax lethal factor proteolysis and inactivation of MAPK kinase. *J. Biol. Chem.* (2003);**278**(11):9402-6
- 197. Glomski IJ, Corre JP, Mock M, Goossens PL.** Cutting Edge: IFN-gamma-producing CD4 T lymphocytes mediate spore-induced immunity to capsulated *Bacillus anthracis*. *J Immunol.* (2007);**178**(5):2646-50

- 198. Kubler-Kielb J, Vinogradov E, Hu H, Leppla SH, Robbins JB, Schneerson R.** Saccharides cross-reactive with *Bacillus anthracis* spore glycoprotein as an anthrax vaccine component. *Proc. Natl. Acad. Sci. U S A.* (2008).
- 199. Thompson BM, Waller LN, Fox KF, Fox A, Stewart GC.** The BclB glycoprotein of *Bacillus anthracis* is involved in exosporium integrity. *J Bacteriol.* (2007);**189**(18):6704-13
- 200. Sullivan, M.A., Yasbin R.E., and Young, F.E.** New shuttle vectors for *Bacillus subtilis* and *Escherichia coli* which allow rapid detection of inserted fragments. *Gene* **29**:21-26.
- 201. Yang, F., Moss, L.G., and Phillips, G.N. Jr.** The molecular structure of green fluorescent protein. *Nature Biotech.* (1996);**14**:1246-1251.
- 202. Baird, G.S., Zacharias, D.A., and Tsien, R.Y.** Biochemistry, mutagenesis, and oligomerization of DsRed, a red fluorescent protein from coral. *Proc.Natl. Acad. Sci USA* (2000);**97**:11984-11989.
- 203. Hilbert, D.W., and Piggot, P.J.** Compartmentalization of gene expression during *Bacillus subtilis* spore formation. *Microbiol Mol. Biol. Rev.* (2004);**68**:234-262.

- 204. Henriques, A.O., and Moran, C.P. Jr.** Structure, assembly, and function of the spore surface layers. *Ann. Rev. Microbiol.* (2007);**61**:555-588.
- 205. Chakrabarty, K., Wu, W., Booth, J.L., Duggan, E.S., Coggeshall, K.M., and Metcalf, J.P.** *Bacillus anthracis* spores stimulate cytokine and chemokine innate immune responses in human alveolar macrophages through multiple mitogen-activated protein kinase pathways. *Infect. Immun.* (2006);**74**:4430-4438.
- 206. Barnes, A.G., Cerovic, V., Hobson, P.S., and Klavinskis, L.S.** *Bacillus subtilis* spores: a novel microparticle adjuvant which can instruct a balanced Th1 and Th2 immune response to specific antigen. *Eur. J. Immunol.* (2007);**37**:1538-1547